

# A STUDY ON THE EFFECTIVENESS OF CATHODIC PROTECTION FOR STEEL BARS IN CONCRETE STRUCTURES

アクバル チャロニ, ムハマド

<https://doi.org/10.15017/1543954>

---

出版情報：九州大学, 2015, 博士（工学）, 課程博士  
バージョン：  
権利関係：全文ファイル公表済

# **A STUDY ON THE EFFECTIVENESS OF CATHODIC PROTECTION FOR STEEL BARS IN CONCRETE STRUCTURES**



A DISSERTATION

Submitted to  
Kyushu University  
in partial fulfillment of the requirements  
for the degree of  
**Doctor of Engineering**

by

**MUHAMMAD AKBAR CARONGE**

DEPARTMENT OF CIVIL AND STRUCTURAL ENGINEERING  
GRADUATE SCHOOL OF ENGINEERING  
**KYUSHU UNIVERSITY**

Fukuoka, Japan

July, 2015

## ACKNOWLEDGMENTS

I would like to express the deepest appreciation and thanks to my supervisor Prof. Hidenori HAMADA, who has given me invaluable guidance, knowledge, suggestion and encouragement during doctoral program. Without his supervision and constant help this dissertation would not have been possible. Also, I would like to thank him for discussion how to grow as a research scientist.

My sincere thanks also address to other members of my Advisory Committee, Prof. Shinichi HINO and Prof. Koji TAKEWAKA for their in valuable suggestions and insightful comments with regard to this research work.

I would like to thank the contributions of Assoc. Prof. Yasutaka SAGAWA for his guidance and advice during my research and writing of this dissertation. Also, I am thankful to Mr. Daisuke YAMAMOTO for tremendous help and precious friendship during my study.

I acknowledge my gratitude to the Ministry of Education, Culture, Sports, Science and Technology (MEXT) Japan for financial support during my study in Japan. I also wish to thank the Nakabohtec Corrosion Protection Co., Ltd and Denki Kagaku Kogyo Kabushiki Kaisha (DENKA) for their support by preparing materials in this research.

I would like to express my very sincere thanks to Dr. Hiroyuki KOBAYASHI and Dr. Shunsuke OTANI from Nakabohtec Corrosion Protection Co., Ltd for the guidance, advice, discussion and support in this work.

I also want to thanks to Prof. M. Wihardi TJARONGE and Dr. Eng. Rita IRMAWATY for their support and guidance from start to finish this program. In addition, I thank my fellow lab mates in Concrete Engineering Laboratory for their help and cooperation.

Finally, I take this opportunity to express the profound gratitude from my deep heart to my beloved parents (Drs. Anwar CARONGE and Nur ASIA, S.Pd), my brothers and sister for their love, patience and continuous support both spiritually and materially during my study in Japan.

## ABSTRACT

Deterioration of reinforced concrete (RC) structures is commonly caused due to corrosion of steel bars. Exposure to de-icing salts, seawater and chloride containing set accelerators play an important role in the corrosion process. Long term exposure to carbon dioxide is also cited as a main factor to the corrosion of steel in concrete as well. The initial corrosion deposits of iron oxides and hydroxides in the restricted space between concrete and steel bar would set up expansive force which leads to the crack and spall of the concrete cover, followed by further contamination and deterioration.

Cathodic protection (CP) system has been introduced as an effective technique of corrosion protection of steel for both new constructions and repair of concrete member in severe environments. Although CP system has been used successfully for corrosion mitigation, there is still debate regarding the CP design for reinforced concrete structures. In addition, only a few experimental studies have been carried out to verify the actual effectiveness of CP design for RC structures. Based on the reason, this study evaluated the effectiveness of cathodic protection for reinforced concrete structures. This dissertation consists mainly of the eight chapters.

In **Chapter 1**, the research background, research objectives and dissertation arrangement in this study are explained. Two types of CP system were evaluated namely Sacrificial Anode Cathodic Protection (SACP) and Impressed Current Cathodic Protection (ICCP). SACP system was applied in chloride contaminated concrete, repaired concrete and cracked concrete. While, ICCP system was performed in chloride contaminated concrete exposed to the atmospheric condition. Also, an appropriate CP design for RC structures was proposed.

In **Chapter 2**, previous study relates to the corrosion and corrosion protections of steel bar in concrete and issues addressed in this study are described. Experimental works which have been conducted to examine the CP criteria are reviewed. Corrosion rate of steel bar are affected by a number of variables such as chloride content, quality of concrete, concrete cover and environmental condition. The 100 mV decay potential has been shown to be an accurate criterion to measure the effectiveness of CP systems for steel in concrete. For cases of severe corrosion (i.e. very high chloride concentration), at least 150 – 200 mV is necessary to stop the corrosion. In addition, the -850 mV vs CSE criteria has been found to result in very high current requirement in structures where much steel is in passive state and dissolved oxygen is enough.

In **Chapter 3**, the effectiveness of commercially available sacrificial point anode for corrosion prevention of steel in concrete structure is presented. In this study, three types of concrete

specimens with sacrificial point anode were prepared: (1) chloride contaminated concrete; (2) repaired concrete; and (3) cracked concrete. Specimens were exposed to three conditions namely air curing (T:  $20\pm 2^\circ\text{C}$ , RH: 60%), immersion in 3% NaCl solution and dry/wet cycles. Electrochemical tests include the potential, protective current, polarization behavior of sacrificial point anode, anodic-cathodic polarization curve, polarization resistance and visual observation. The test results conclude that sacrificial point anode is effective to prevent microcell and macrocell corrosion of steel bar and it becomes much remarkable in high moisture condition. In addition, the specimen with gap between steel bar and sacrificial point anode provide a stable protective current than without gap.

In **Chapter 4**, the environment improvement of the steel surface as a secondary effect of CP was studied. Nine levels of constant current densities were applied on the steel bar embedded in concrete specimens in the size of 120 mm x 120 mm x 200 mm with water to cement ratio (W/C) of 55% and chloride ion of  $2\text{ kg/m}^3$ ,  $5\text{ kg/m}^3$  and  $10\text{ kg/m}^3$ . Prior to CP tests, accelerated corrosion test were performed to generate initial corrosion on the surface of steel bar. The instant-off potential ( $E_{i0}$ ), depolarization test, anodic-cathodic polarization curve, corrosion rate and visual observation were evaluated. From test results, it was found that the 100 mV decay potential was achieved even with small protective current after certain periods in all chloride contents due to the “Environment Improvement” effects. It means that the protection of steel bar is not instantaneous but gradual process to achieve. In the concrete with  $10\text{ kg/m}^3$  of chloride, the decay potential slightly decreased at 230 days due to the diffusion of dissolved oxygen (DO). Also, a small protective current has improved the passivity film of steel bars. In addition, the corrosion rate of steel under protection is approximately 20, 16 and 100 times lower than the open-circuit corrosion rate for current densities of 10, 20 and  $100\text{ mA/m}^2$  respectively.

In **Chapter 5**, three levels of depolarization value of 25 mV, 50 mV and 100 mV were examined in concrete specimen with different chloride content. All the materials, concrete composition, dimension of specimens and CP arrangement are identical as in **Chapter 4**. The protective films of steel bar were removed before being embedded in the concrete specimen and then subjected to the accelerated corrosion test. From the test results, it is concluded that the depolarization level of 25 mV and 50 mV is adequate to polarize the steel bar in concrete, with chloride lower than  $5\text{ kg/m}^3$ . However, the depolarization level higher than 100 mV is necessary when the chloride content in concrete is more than  $5\text{ kg/m}^3$ . In addition, the protective current may be reduced under the CP of stable condition after a certain period.

In **Chapter 6**, two CP methods were used: (1) constant current density and (2) constant potential shift from its natural potential of steel bar 24 hours after the switch off. Both CP methods were examined in the concrete specimens with corrosive steel bar and high chloride concentration. Concrete with water to cement ratio (W/C) of 60% with initial chloride content of  $10 \text{ kg/m}^3$  were prepared. The initial corrosion of steel bars were formed by dry/wet cycles of 3% NaCl solution spray (1W:1D) about two weeks before concrete casting. In the case of constant current density, additional accelerated corrosion tests were performed for 15 days prior to CP tests. Protection levels of 25 mV, 50 mV and 100 mV were maintained. The results showed that a larger protective current was not required at early time to satisfy the 100 mV, which leads to the earlier deterioration of anode. Therefore, reduction of current density is necessary after achieving the 100 mV criterion to reduce the negative effects of large CP current. Although the protective current decreased, the depolarization value of steel bar is kept higher than 100 mV (constant potential shift of 100 mV). This would indicate that the steel bar is polarized even the current density is decreased after the 100 mV depolarization value is achieved. The test results also showed that corrosion rate under protection are lower than the open-circuit condition due to the presence of protective current at the surface of steel bar. CP current ensures that supply of electrons at all point of steel inhibits the loss of electrons due to corrosion of the steel surface.

In **Chapter 7**, an appropriate CP design for reinforced concrete structures exposed to the atmospheric zone is discussed. By considering the amount of chloride content in concrete, 50 – 100 mV depolarization value is enough to polarize of steel bar in concrete at chloride lower than  $5 \text{ kg/m}^3$ . However, depolarization value more than 100 mV should be applied if chloride content is large than that value. CP design of decreasing the protective current after achievement specific protection level is recommended for reinforced concrete structures. In addition, an adjustment of the protection level of steel bar in concrete depends on the chloride concentration, corrosion degree and the environmental condition. In the implementation of cathodic protection, many factors are found in adjusting the protection level, such us actual chloride content, corrosion degree of steel bar and non-homogenous environmental condition of structures. An accurate analysis data relates to these factors is needed before installing a CP system.

In **Chapter 8**, conclusions and recommendations for future work is presented.

# TABLE OF CONTENTS

ACKNOWLEDGEMENT		i
ABSTRACT		ii
TABLE OF CONTENTS		v
LIST OF TABLES		ix
LIST OF FIGURES		x
CHAPTER		
<b>1. GENERAL INTRODUCTION</b>		<b>1</b>
1.1	Research Background	1
1.2	Research Objectives	1
1.3	Dissertation Arrangement	2
	References	4
<b>2. LITERATURE REVIEW</b>		<b>6</b>
2.1	Introduction	6
2.2	Corrosion of Steel Embedded in Concrete	6
	2.2.1 Corrosion mechanism	7
	2.2.2 Microcell and macrocell corrosion	9
	2.2.3 Chloride induced corrosion of steel in concrete	10
	2.2.4 Effect of concrete cracking on corrosion	13
2.3	Cathodic Protection of Steel in Concrete	14
	2.3.1 Impressed Current Cathodic Protection (ICCP)	14
	2.3.2 Sacrificial Anode Cathodic Protection (SACP)	15
	2.3.3 Effect of cathodic protection in concrete	17
	2.3.4 Cathodic protection criteria in concrete	17
2.4	Cathodic Prevention of Steel in Concrete	19
2.5	Issues Addressed in this Study	21
	References	23
<b>3. EFFECTIVENESS OF SACRIFICIAL POINT ANODES FOR CORROSION PREVENTION OF STEEL BARS IN CONCRETE</b>		<b>27</b>
3.1	Introduction	27

3.2	Preparation of Specimens	28
	3.2.1 Chloride Contaminated Chloride	28
	3.2.2 Repaired Concrete	30
	3.2.3 Cracked Concrete	31
3.3	Electrochemical Tests	33
3.4	Chloride Contaminated Concrete	37
	3.4.1 Half-cell potential and instant-off potential of steel bars	37
	3.4.2 Instant-off potential of sacrificial point anode	38
	3.4.3 Protective current of the sacrificial anode	39
	3.4.4 Depolarization tests	40
	3.4.5 Anodic polarization behavior of the sacrificial anode	40
	3.4.6 Polarization resistance and corrosion current density	41
3.5	Repaired Concrete	42
	3.5.1 Half-cell potential and on-potential of steel bars	42
	3.5.2 Depolarization tests	46
	3.5.3 Polarization behavior of sacrificial anode	47
	3.5.4 Anodic-cathodic polarization curve of steel bars	48
	3.5.5 Visual observation	48
3.6	Cracked Concrete	49
	3.6.1 Half-cell potential and on potential of steel bars	49
	3.6.2 Depolarization tests	52
	3.6.3 Polarization behavior of the sacrificial anode	53
	3.6.4 Anodic-cathodic polarization curve	54
	3.6.5 Visual observation and corrosion area	54
3.7	Conclusions	57
	References	59

<b>4.</b>	<b>DEVELOPMENT OF STEEL PASSIVITY IN CONCRETE BY CATHODIC PROTECTION WITH ENVIRONMENT IMPROVEMENT EFFECTS</b>	<b>60</b>
4.1	Introduction	60
4.2	Preparation of Specimens	61
	4.2.1 Mix proportion	61
	4.2.2 Specimens design	61
	4.2.3 Accelerated corrosion test	62



4.3	Method of Investigation	63
	4.3.1 Cathodic protection (CP) instrumentation	63
	4.3.2 Measurement Method	64
4.4	Results and Discussion	67
	4.4.1 Initial potential shift versus current density	67
	4.4.2 Instant-off potential ( $E_{io}$ )	67
	4.4.3 Depolarization tests	68
	4.4.4 Rest potential of steel bar ( $E_{off}$ )	71
	4.4.5 Anodic-cathodic polarization curve	72
	4.4.6 Corrosion rate of steel bars	75
	4.4.7 Visual observation	76
4.5	Conclusions	79
	References	81
<b>5.</b>	<b>EVALUATION OF THE CATHODIC PROTECTION CRITERIA LESS THAN 100 mV FOR STEEL IN CHLORIDE-CONTAMINATED CONCRETE</b>	<b>82</b>
5.1	Introduction	82
5.2	Preparation of Specimens	82
5.3	Method of Investigation	84
5.4	Results and Discussion	85
	5.4.1 Accelerated corrosion test	85
	5.4.2 Protective current	86
	5.4.3 Instant-off potential ( $E_{io}$ )	88
	5.4.4 Rest potential of steel bars ( $E_{off}$ )	89
	5.4.5 Polarization resistance ( $R_p$ )	91
	5.4.6 Corrosion rate of steel bars	91
	5.4.7 Corrosion appearances and weight loss corrosion	93
5.5	Conclusions	96
	References	97
<b>6.</b>	<b>EVALUATING THE EFFECTIVENESS OF CATHODIC PROTECTION METHOD FOR STEEL IN CONCRETE</b>	<b>98</b>
6.1	Introduction	98

6.2	Constant CP Current	98
	6.2.1 Preparation of specimens	98
	6.2.2 Cathodic protection (CP) instrumentation	100
	6.2.3 Electrochemical tests	101
	6.2.4 Results and Discussion	102
6.3	Constant Potential Shift	108
	6.3.1 Method of evaluation	108
	6.3.2 Results and discussion	109
6.4	Summary and Conclusions	113
	References	115
<b>7.</b>	<b>AN APPROPRIATE CATHODIC PROTECTION (CP) DESIGN FOR REINFORCED CONCRETE STRUCTURES</b>	<b>116</b>
7.1	Introduction	116
7.2	Review of CP Design in Marine Exposure Zones	116
7.3	Discussions and Recommendations	118
	7.3.1 Effective CP design for reinforced concrete structures	118
	7.3.2 Impact of surface steel condition on corrosion rate	119
7.4	Conclusions	121
	References	122
<b>8.</b>	<b>CONCLUSION AND FUTURE WORK</b>	<b>123</b>
8.1	Conclusions	123
8.2	Future Work	125

## LIST OF TABLES

<b>Table No</b>		<b>Page</b>
Table 2.1	Definition of deterioration stages due to chloride attack	10
Table 2.2	Practical CP current density requirements for varying steel conditions	19
Table 2.3	Comparison of corrosion mitigation strategies	20
Table 3.1	Physical property of concrete materials	28
Table 3.2	Mix proportion of concrete (chloride contaminated concrete)	28
Table 3.3	Summary of specimens (chloride contaminated concrete)	29
Table 3.4	Mix proportion of concrete (repaired concrete)	30
Table 3.5	Summary of specimens (repaired concrete)	31
Table 3.6	Table 3.6 Mix proportion of concrete (cracked concrete)	32
Table 3.7	List of test specimen (cracked concrete)	33
Table 3.8	Summary of electrochemical tests and visual observation each specimen	34
Table 3.9	Corrosion probability	34
Table 3.10	Grade of passivated film associated with anodic polarization curve	36
Table 3.11	Typical polarization resistance for steel in concrete	37
Table 3.12	Polarization resistance and corrosion rate of steel bars at 400 days	42
Table 3.13	The rest potential and depolarization values	46
Table 3.14	The rest potential and depolarization value of PSCP at the end of test	52
Table 4.1	Mix design of concrete	61
Table 4.2	Summary of specimens	63
Table 4.3a	Corrosion appearance and weight loss of steel bars with 2 kg/m <sup>3</sup> of chloride	77
Table 4.3b	Corrosion appearance and weight loss of steel bars with 5 kg/m <sup>3</sup> of chloride	78
Table 4.3c	Corrosion appearance and weight loss of steel bars with 10 kg/m <sup>3</sup> of chloride	79
Table 5.1	List of specimens in testing	84
Table 5.2	Corrosion weight loss of steel bars after accelerated corrosion test	86
Table 6.1	Mix proportion of concrete	98
Table 6.2	Summary of the specimen tests (constant CP current)	101
Table 6.3	Summary of specimen tests (constant potential shift)	109
Table 7.1	Summary of the depolarization level requires under various chloride concentration	118

## LIST OF FIGURES

<b>Figure No</b>		<b>Page</b>
Fig. 1.1	Flowchart of dissertation arrangement	4
Fig. 2.1	Cracking, spalling and loss of bond between steel and concrete due to corrosion	7
Fig. 2.2	Deterioration mechanism for corrosion of steel in concrete	7
Fig. 2.3	Microcell and macrocell corrosion of steel in concrete	9
Fig. 2.4	Progress of deterioration due to chloride attack	11
Fig. 2.5	CEB-FIP Critical chloride ions content for corrosion (FIP, 2000 in Robert M., et al)	12
Fig. 2.6	Schematic illustration of the anodic behavior of steel in the presence of chloride	12
Fig. 2.7	Cracking accelerates onset of corrosion, but over time corrosion is similar in cracked and uncracked concrete	13
Fig. 2.8	Typical ICCP system setup	15
Fig. 2.9	Typical commercially available of the sacrificial anode	16
Fig. 2.10	Schematic illustration of steel behaviour in concrete for different potentials and chloride contents	20
Fig. 3.1	Sacrificial point anodes	27
Fig. 3.2	Detail of specimens chloride contaminated concrete (unit: mm)	29
Fig. 3.3	Detail of specimen repaired concrete (unit: mm)	31
Fig. 3.4	Detail of specimen cracked concrete (unit: mm)	32
Fig. 3.5	(a) Bending loading for cracking; (b) crack width measurement	32
Fig. 3.6	Immersion in 3% NaCl solution	33
Fig. 3.7	Setup for polarization resistance measurement	36
Fig. 3.8	Half-cell potential of the steel bar without sacrificial point anode (PS)	37
Fig. 3.9	Instant-off potential of the steel bars with sacrificial point anode (PSCP)	38
Fig. 3.10	Instant-off potential of the sacrificial point anode	39
Fig. 3.11	Protective current of the sacrificial point anode	39
Fig. 3.12	Depolarization values of steel bars in chloride contaminated concrete	40
Fig. 3.13	Anodic polarization behaviors of the point anode: 0 day, 148 days (air curing); 320 days, 400 days (dry/wet cycles)	41
Fig. 3.14	Half-cell potential of PS with time	43

<b>Figure No</b>		<b>Page</b>
Fig. 3.15	On-potential of PSCP with time	44
Fig. 3.16	Half-cell potential of PSE with time	45
Fig. 3.17	Rest potential of the steel bars and the sacrificial point anodes at the end of tests	47
Fig. 3.18	Polarization behavior of the sacrificial point anodes	47
Fig. 3.19	Anodic-cathodic polarization curve of PS and PSCP	48
Fig. 3.20	Visual observation of the steel bars (repaired concrete)	49
Fig. 3.21	Half-cell potential of PS at cracked area: (a) air curing; (b) immersed in 3% NaCl solution; (c) dry/wet cycles.	50
Fig. 3.22	On-potential of PSCP at cracked area: (a) air curing; (b) immersed in 3% NaCl solution; (c) dry/wet cycles	51
Fig. 2.23	The rest potential of steel bars and sacrificial point anodes (crack width: 0.31mm, 0.32mm, and 0.34mm)	52
Fig. 2.24	Anodic polarization behavior of the sacrificial point anode and cathodic polarization curve of steel bar	53
Fig. 3.25	Anodic-cathodic polarization curve (crack width: 0.31mm, 0.32mm, 0.34mm) at 530 days	54
Fig. 3.26	Corrosion and leaching products at the cracked area: (a) dry/wet cycles; (b) immersed in 3% NaCl solution.	55
Fig. 3.27	Corrosion appearances of steel bars	55
Fig. 3.28	Condition of the sacrificial point anode after removing from concrete specimen: (a) air curing; (b) immersed in 3% NaCl solution; (c) dry/wet cycles	56
Fig. 3.29	Total corroded area of the steel bars (crack width: 0.31 mm, 0.32 mm, 0.34 mm)	57
Fig. 4.1	Detail of specimen (unit: mm)	62
Fig. 4.2	Setup for accelerated corrosion tests	62
Fig. 4.3	The schematic of CP tests.	63
Fig. 4.4	The schematic measurement of the $E_{i0}$	64
Fig. 4.5	Depolarization test and measurement of the $E_{off}$	64
Fig. 4.6	Anodic-cathodic polarization curve test	65
Fig. 4.7	Estimation of corrosion rate of steel bar	66
Fig. 4.8	Steel bars condition before and after cutting then cleaning	66

<b>Figure No</b>		<b>Page</b>
Fig. 4.9	The relationship between initial potential shift and current density	67
Fig. 4.10	The instant-off potential ( $E_{io}$ ) of steel bars	68
Fig. 4.11	Depolarization values of steel bars after 24 hours disconnecting	69
Fig. 4.12a	Time dependence of depolarized steel potential with 2 kg/m <sup>3</sup> of chloride	70
Fig. 4.12b	Time dependence of depolarized steel potential with 5 kg/m <sup>3</sup> of chloride	70
Fig. 4.12c	Time dependence of depolarized steel potential with 10 kg/m <sup>3</sup> of chloride	71
Fig. 4.13	Rest potential ( $E_{off}$ ) of steel bars	72
Fig. 4.14a	Anodic-cathodic polarization curve with 2 kg/m <sup>3</sup> of chloride	73
Fig. 4.14b	Anodic-cathodic polarization curve with 5 kg/m <sup>3</sup> of chloride	74
Fig. 4.14b	Anodic-cathodic polarization curve with 10 kg/m <sup>3</sup> of chloride	74
Fig. 4.15	Reduction of the open-circuit corrosion rate of steel bars	75
Fig. 4.16	Corrosion rate of steel bars under protection and the open-circuit condition in 10 kg/m <sup>3</sup> of chloride at 230 days	76
Fig. 5.1	Steel bar before and after removing the protective film	83
Fig. 5.2	Detail of specimen design (unit: mm)	83
Fig. 5.3	Fig. 5.3 Polarization resistance ( $R_p$ ) measurement by using contact method	85
Fig. 5.4	Severity corrosion of steel bars in each chloride contents	86
Fig. 5.5	Protective current of steel bars versus time	87
Fig. 5.6	The instant-off potential ( $E_{io}$ ) of steel bars	88
Fig. 5.7	Rest potential ( $E_{off}$ ) of steel bars	90
Fig. 5.8	Polarization resistance ( $R_p$ ) of steel bar at the end of testing (250 days)	91
Fig. 5.9	Reduction in the open-circuit corrosion rate of steel bars with time	92
Fig. 5.10	Corrosion rate of steel bars under protection at 250 days	93
Fig. 5.11a	Corrosion appearance of steel in concrete with 2 kg/m <sup>3</sup> of chloride	94
Fig. 5.11b	Corrosion appearance of steel in concrete with 5 kg/m <sup>3</sup> of chloride	94
Fig. 5.11c	Corrosion appearance of steel in concrete with 10 kg/m <sup>3</sup> of chloride	95
Fig. 5.12	Corrosion weight loss of steel bars after CP test	95
Fig. 6.1	Steel bars preparation: (a). before; (b). after dry/wet cycles sprayed	99
Fig. 6.2	Detail of specimen design (unit: millimeter)	99
Fig. 6.3	Reduction of current supply during accelerated corrosion test	100
Fig. 6.4	Setup of accelerated corrosion test (anode was used as counter electrode)	100
Fig. 6.5	Schematic of CP test	101

<b>Figure No</b>		<b>Page</b>
Fig. 6.6	Temperature and humidity conditions during CP tests	102
Fig. 6.7	Instant-off potential ( $E_{io}$ ) of steel bars versus exposure time	102
Fig. 6.8	Instant-off potential ( $E_{io}$ ) of anode	103
Fig. 6.9	Depolarization value of steel bars ( $E_{off} - E_{io}$ )	104
Fig. 6.10	Time dependence of depolarized of steel bars	104
Fig. 6.11	Rest potential ( $E_{off}$ ) of steel bars	105
Fig. 6.12	Natural potential ( $E_{corr}$ ) of steel bar without CP	105
Fig. 6.13	Rest potential of anode with time	106
Fig. 6.14	Relationship between potential of MMO anode and pH	106
Fig. 6.15	Polarization curve and estimation of corrosion rate (No.1_21mA/m <sup>2</sup> )	107
Fig. 6.16	Corrosion rate of steel bar with time	107
Fig. 6.17	Corrosion rate of steel bar without CP	108
Fig. 6.18	CP method with constant potential shift	109
Fig. 6.19	The instant-off potential ( $E_{io}$ ) of steel bars versus time	110
Fig. 6.20	Protective current (I) of steel bars with time	110
Fig. 6.21	Depolarization value of steel bars versus time	111
Fig. 6.22	Rest potential ( $E_{off}$ ) of steel bars with time	111
Fig. 6.23	Corrosion rate of steel bars both open-circuit and under protection condition	112
Fig. 6.24	Polarization resistance ( $R_p$ ) of steel bars respect with time	113
Fig. 7.1	Corrosion regions of concrete structure in marine environments	117
Fig. 7.2	Surface condition of steel bar prior CP tests	120
Fig. 7.3	Corrosion rate under protection in concrete with 10 kg/m <sup>3</sup> of chloride at the end of tests	120





## **CHAPTER 1. GENERAL INTRODUCTION**

### **1.1 Research Background**

Corrosion of steel bars is recognized as the main factor cause of the deterioration of steel reinforced concrete structures. Chloride ions, moisture and oxygen play a significant role to accelerate the corrosion initiation of steel in concrete. From there, a series of events cause progressive deterioration of concrete such as cracking, spalling and delamination of concrete. To prevent continuing deterioration, repaired technique can be applied. However, application of fresh repair materials caused new corrosion risk in the surrounding areas because they are often in electrical contact, which promote an electromotive force between steel in original concrete and repair material <sup>(1.1), (1.2)</sup>.

Cathodic protection (CP) system has been introduced as an effective technique of corrosion protection of steel for both new constructions and repair concrete member in severe environments <sup>(1.3)</sup>. The CP system is aimed to shift the potential of the steel to the least probable range for corrosion. Although CP system has been used successfully for corrosion mitigation, there is still debate regarding the CP criteria that effective to apply in reinforced concrete structures.

Several CP criteria have been proposed include potential shift, potential decay and current-potential relationship (E-Log I). However, only few experimental studies have been carried out to verify the actual effectiveness of these criteria.

### **1.2 Research Objectives**

The purpose of this study is to evaluate the effectiveness of CP criteria for steel bar in concrete structures. Two types of the CP system that commonly used in practical CP installation on reinforced concrete structure namely ICCP and SACP were examined. The main objective of this study is firstly to investigate the effectiveness of sacrificial anode cathodic protection (SACP) for prevention of the steel corrosion under various exposure conditions.

Secondly, to investigate the development of steel passivity in concrete exposed to the atmosphere by CP considering “Environment Improvement” effects. Thirdly, to examine the effectiveness of the steel decay potential criterion less than 100 mV in chloride-contaminated concrete. Finally, based on the experimental results, an appropriate CP design for reinforced concrete structures is proposed.

### 1.3 Dissertation Arrangement

**Fig. 1.1** illustrated the dissertation arrangement which is composed of eight chapters as follows:

**Chapter 1** describes the background and objectives of the present study.

**Chapter 2** literature review related to corrosion and corrosion protection methods of steel in concrete structures at the current situation and the issues to be addressed in this study.

**Chapter 3**, this chapter describes the effectiveness of sacrificial point anode for corrosion prevention of steel bars embedded in concrete under various applications. There were three parts of investigation conducted and discussed. The first part was the fundamental study on the effectiveness of sacrificial point anode for corrosion prevention of steel bars in chloride contaminated concrete. The second part was focused on the effectiveness of sacrificial point anode for controlling macrocell corrosion in repaired concrete member. Then, the third part was investigated the possibility of sacrificial point anode for prevention of steel corrosion in cracked concrete. Also some factors affecting the effectiveness of the sacrificial point anode are discussed.

**Chapter 4** investigates the effect of environmental change on the surface of steel bar due to even small protective current. In this case, the protection of steel bar can be achieved after certain periods. Nine levels of constant current densities were applied on the steel bar embedded in concrete specimens with chloride ion of  $2 \text{ kg/m}^3$ ,  $5 \text{ kg/m}^3$  and  $10 \text{ kg/m}^3$ .

**Chapter 5** evaluates the effectiveness of cathodic protection (CP) criteria of steel bar less than 100 mV for reinforced concrete structures. Protection levels of 25 mV, 50 mV and 100 mV were kept constant after disconnecting the steel bar from anode for 24 hours (depolarization test). Protective current was adjusted after depolarization test to achieve these protection levels. Evaluation was carried out in concrete specimens with water to cement ratio (W/C) of 55% and contained chloride of  $2 \text{ kg/m}^3$ ,  $5 \text{ kg/m}^3$  and  $10 \text{ kg/m}^3$ .

**Chapter 6** evaluates the effectiveness of two CP methods namely (1) constant current density and (2) constant potential shift from its natural potential of steel bar 24 hours after switch off. Both CP methods were examined in the concrete specimens with corrosive steel bar

and high chloride concentration. Concrete with water to cement ratio (W/C) of 60% with initial chloride content of  $10 \text{ kg/m}^3$  were prepared. The initial corrosion of steel bars were formed by dry/wet cycles 3% NaCl solution spray (1W:1D) about two weeks before concrete casting. In the case of constant current density, additional accelerated corrosion tests were performed for 15 days prior to CP tests. Protection levels of 25 mV, 50 mV and 100 mV were maintained.

**Chapter 7** provides discussions and recommendations an appropriate CP design for reinforced concrete structures exposed to the atmospheric zone.

**Chapter 8** concludes the result obtained from **Chapter 3** to **Chapter 7**. From these conclusions, future works are recommended.

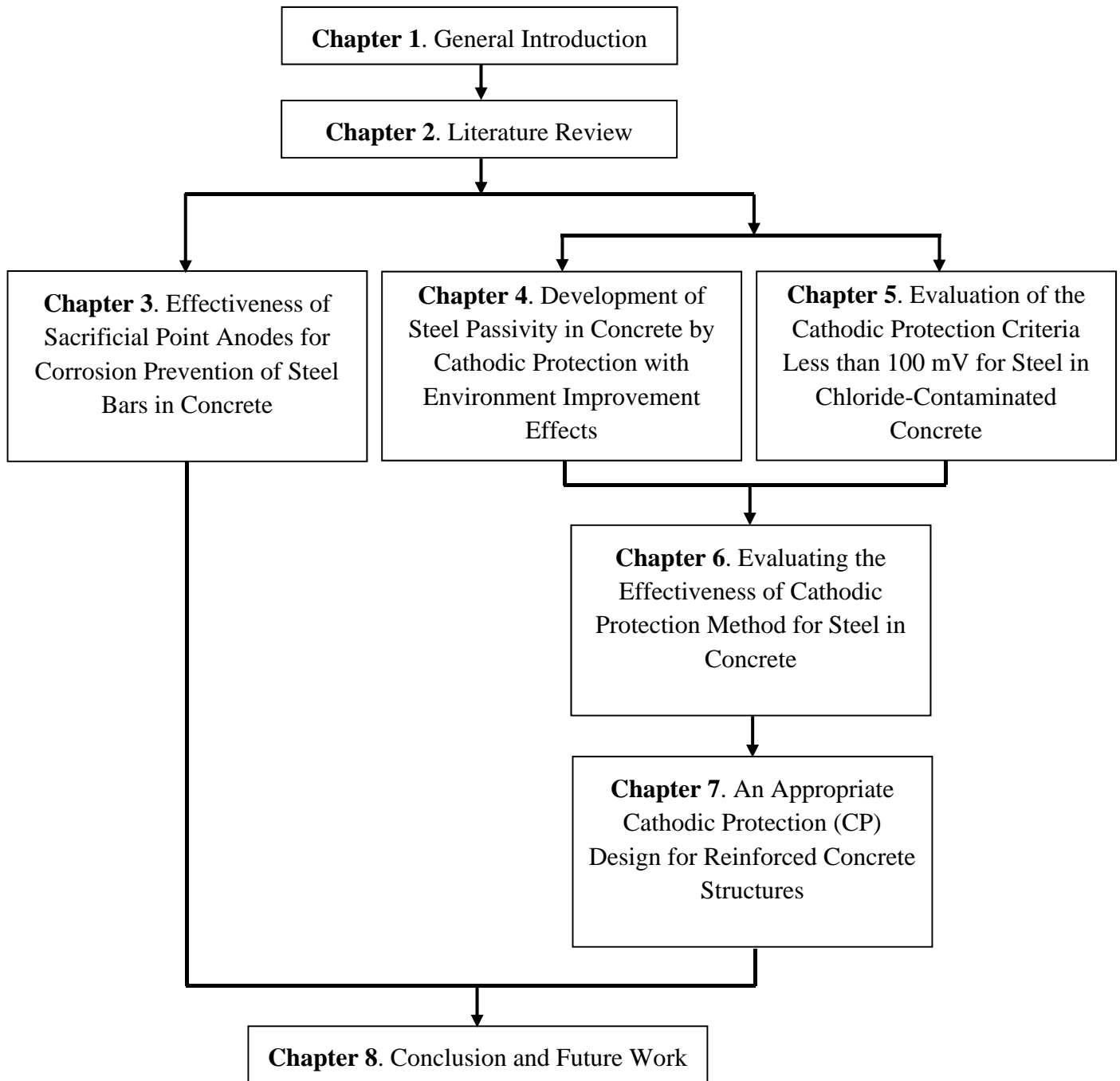


Fig. 1.1 Flowchart of dissertation arrangement

## References

- 1.1 Qian, S., et al, "Theoretical and Experimental Study of Microcell and Macrocell corrosion in Patch Repairs of Concrete Structures." *Cement and Concrete Composites*, 28, 2006, pp. 685-695.

- 1.2 Pruckner, F. and Gjrv, E., "Patch Repair and Macrocell activity in Concrete Structure," ACI Materials Journal, Vol. 99, 2, 2002, pp. 143-148.
- 1.3 Takewaka, K., "Cathodic Protection for Reinforced Concrete and Prestressed Concrete Structures," Corrosion Science, Vol. 35, 1993, pp. 1617-1626.

## CHAPTER 2. LITERATURE REVIEW

### 2.1 Introduction

Corrosion of steel caused by chloride becomes a primary problem in reinforced concrete structure worldwide. The presence of chloride ions on the steel surface causes the passive film is destroyed and leads corrosion initiation. After the initiation of the corrosion process, the accumulation of corrosion product leads to internal stresses that result in cracking and spalling of the concrete cover, thus, decrease the service life of the structure. Cathodic protection (CP) has demonstrated to be an effective technique to control corrosion of steel bars. CP system is aimed to shift the potential of the steel to least probable range for corrosion. A review of corrosion of steel embedded in concrete and prevention methods are presented in this chapter.

### 2.2 Corrosion of Steel Embedded in Concrete

In recent years, the long-term durability of reinforced concrete structures has become an issue of concern, commonly because of the corrosion of steel bars. The steel in concrete normally has a high degree of corrosion resistance due to the protection of passive film formation. However, chloride ions derived from admixture that are added during mixing and also from aggregates/mixing water (internal chloride), or transported into the concrete during exposure to aggressive environment (external chloride), may initiate pitting corrosion on the surface of steel <sup>(2.1)</sup>. From there, a series of events cause progressive deterioration of concrete such as cracking, spalling and loss of bond between steel and concrete as shown in **Fig. 2.1**.

Corrosion is an electrochemical process that requires a flow of electric current and several chemical reactions (i.e. an anode, a cathode and an electrolyte) which is affected by a particular environment, resulting in a measurable loss of metal. **Figure 2.2** illustrates the deleterious effects of corrosion in reinforced concrete structure. The corrosion of steel means that iron is being removed from the steel. The liberated ferrous ions are then free to complex

with hydroxyl ions to form various corrosion products depending on the availability of oxygen (2.2).



Fig. 2.1 Cracking, spalling and loss of bond between steel and concrete due to corrosion

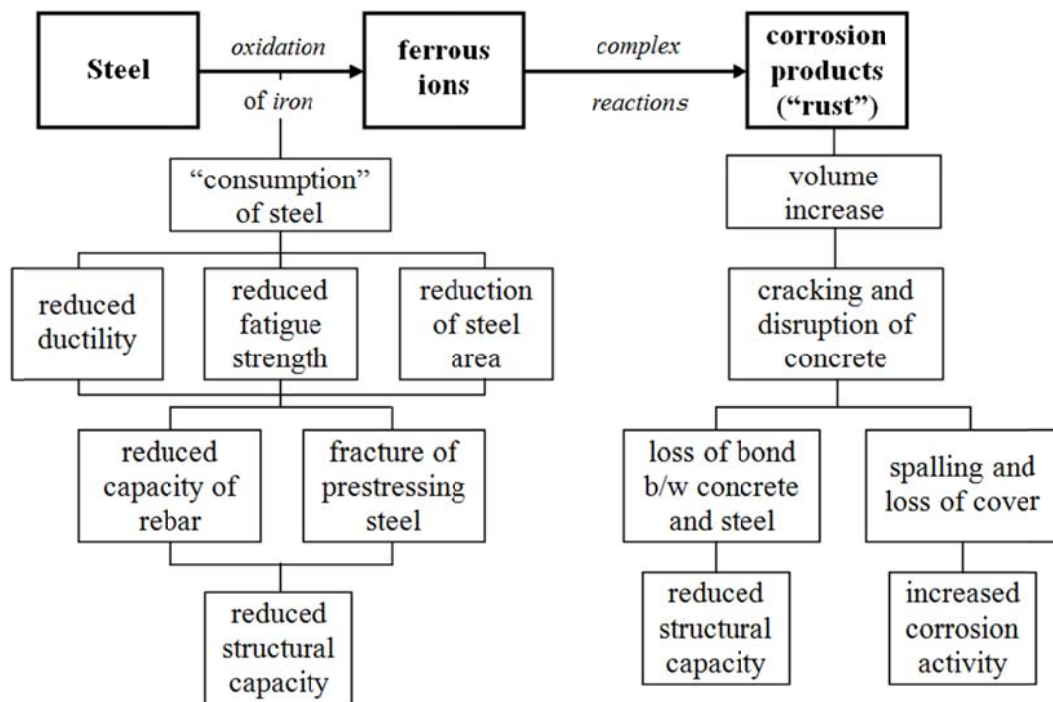


Fig. 2.2 Deterioration mechanism for corrosion of steel in concrete (2.2)

### 2.2.1 Corrosion mechanism

Corrosion of steel in concrete is an electrochemical process with cathodic and anodic reactions. In the absence of chloride ions and a good quality concrete, the anodic reaction leads to the formation of iron cations as shown in Eq. (2.1) (2.3):

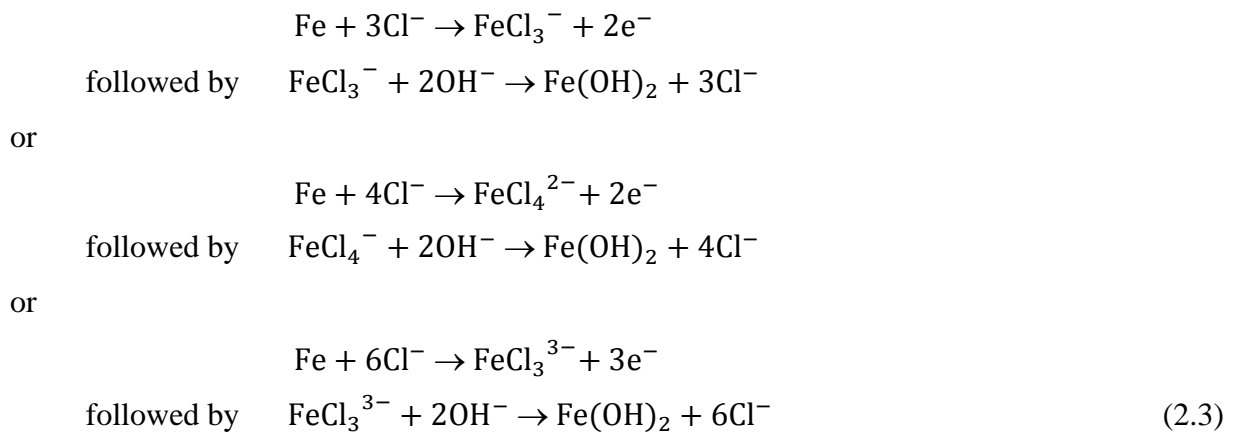


This reaction is balanced by the cathodic reduction of oxygen, which produces hydroxyl anions according to **Eq. (2.2)**.

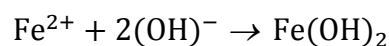


The reaction products between anodic and cathodic combine together to build the stability of the passive film on the steel. The stability of this passive film depends on the oxygen availability and the pH value in the interface of steel/concrete <sup>(2.4)</sup>. Corrosion start to initiate when the passive film is destroyed due to the presence of chloride ions at the steel-concrete interface.

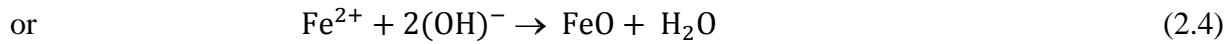
In the presence of chloride ions, oxygen and water in concrete, they may act as a catalyst by introducing additional anodic reactions are represented in **Eq. (2.3)** <sup>(2.5), (2.6)</sup>.



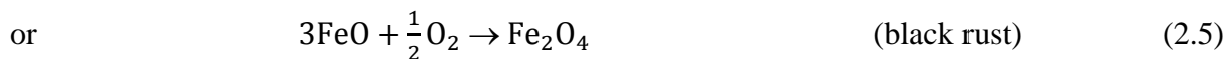
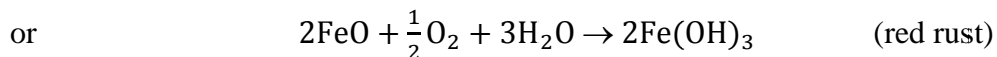
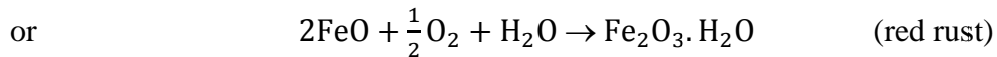
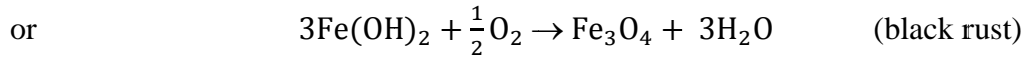
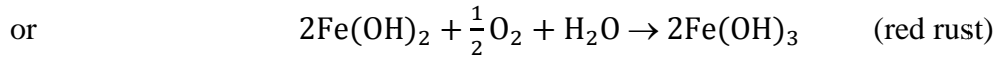
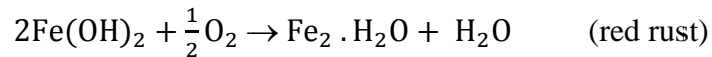
These reactions remove ferrous or ferric ions from the steel by forming complex ions with the chlorides then deposited near the anode where they join with hydroxyl ions to form various corrosion products. The chloride ions are released to repeat the process. Secondary reactions may occur due to the expansive products of corrosion. Although the  $\text{Fe}^{2+}$  and  $\text{OH}^{-}$  ions both diffuse into the concrete (from anode to cathode, respectively), the corrosion products form near the anode because the  $\text{OH}^{-}$  ions are smaller and more diffuse through the concrete more readily <sup>(2.2)</sup>. If the supply of oxygen is restricted, ferrous oxides and hydroxides form (**Eq. (2.4)**):







If the oxygen is available, ferric oxides and hydroxides form (**Eq. (2.5)**)<sup>(2.2), (2.5)</sup>:



### 2.2.2 Microcell and macrocell corrosion

The corrosion cell may exist as a macrocell or a micro cell<sup>(2.5)</sup>. The corrosion microcell consists of tiny anodes and cathodes separated by a distance of as small as a micron. The corrosion macrocell consists of anodic and cathodic regions separated by a finite distance of millimeter or meters, as briefly illustrated in **Fig. 2.3**<sup>(2.7)</sup>.

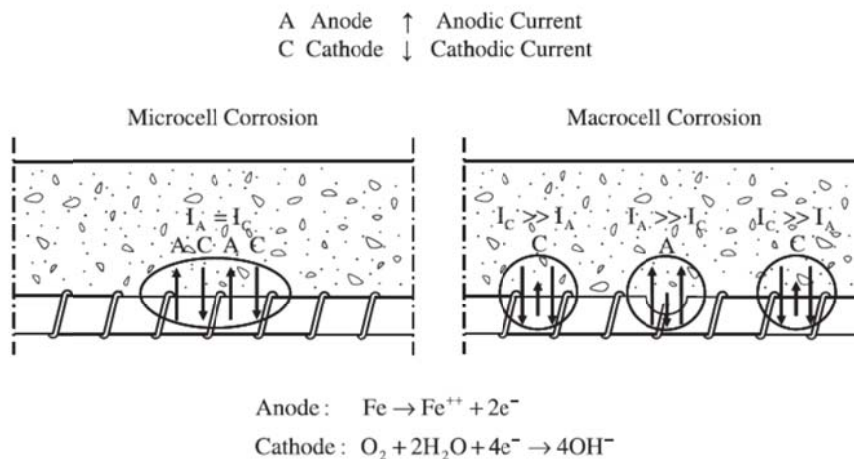


Fig. 2.3 Microcell and macrocell corrosion of steel in concrete<sup>(2.7)</sup>

Macrocell corrosion occurs when an electric current runs through an active and a passive area of steel. It can also occur following a patch repair of reinforced concrete member, when there is a significant difference in chloride concentration between the new patch (chloride free) and its surrounding substrate (chloride contaminated). The corrosion rate may be very

high because the passive steel surface in the patched area often shows very positive potentials the effect of which will be a very large driving force <sup>(2.8)</sup>. It means the larger the difference in corrosion potential is between these areas the larger the macrocell current becomes. One reason why macrocell corrosion is more severe is that negative ions like  $\text{Cl}^-$  may migrate to the anode in higher amounts than in microcell corrosion, because of the high positive potential in this area and the high current. This means that the chlorides can move to the corroded area, and the corrosion may then be accelerated. At the same time the positively charged and dissolved  $\text{Fe}^{2+}$ , migrate to the cathode zone with less volume expanding corrosion products as a consequence <sup>(2.9)</sup>.

### 2.2.3 Chloride-induced corrosion of steel in concrete

As described in the previous section, corrosion of steel mainly affected by chloride ions, oxygen and water at the interface of steel and concrete. Chloride ions may be derived from internal and external of concrete. Marine structures, especially substructures are susceptible to severe corrosion due to chloride ingress <sup>(2.10)</sup>. Chloride ions firstly attack ferrous oxide layer ( $\text{Fe}_2\text{O}_3$ ) of steel and caused the loss of the passivation layer. When the passive layer is loss, only water, oxygen and a conductive medium is needed to maintain the corrosion reactions <sup>(2.11)</sup>. In this condition, corrosion tends to be localized, and chloride-induced corrosion initiation in concrete follows the model of pitting corrosion <sup>(2.12)</sup>.

After initiation of corrosion process, the volume corrosion products can occupy up to six time larger than the volume of iron leads to tensile stress in the hardened cement paste that result in cracking, spalling, eventual loss of concrete and reduced capacity of structure <sup>(2.13), (2.14)</sup>.

Table 2.1 Defenition of deterioration stages due to chloride attack <sup>(2.15)</sup>

Stage of deterioration	Defenition	Stage determined by
Initiation stage	Until the chloride ion concentration on the surface of steel reaches the marginal concentration for the occurrence of corrosion (standard value is $1.2 \text{ kg/m}^3$ ).	Diffusion of chloride ions Initially contained chloride ion concentration.
Propagation stage	From the initiation of steel corrosion until cracking due to corrosion.	Rate of steel corrosion.
Acceleration stage	Stage in which steel corrodes at a high rate due to cracking due to corrosion.	Rate of corrosion of steel with cracks.
Deterioration stage	Stage in which load bearing capacity is reduced considerably due to the increase of corrosion amount.	

Standard Specification for Concrete Structures-JSCE (Part: Maintenance)<sup>(2.15)</sup> is defined the performance of degradation of structures due to chloride attack as shown in **Table 2.1**. Also presents the relationship between performance degradation of the structural member and deterioration due to chloride attack (**Fig. 2.4**).

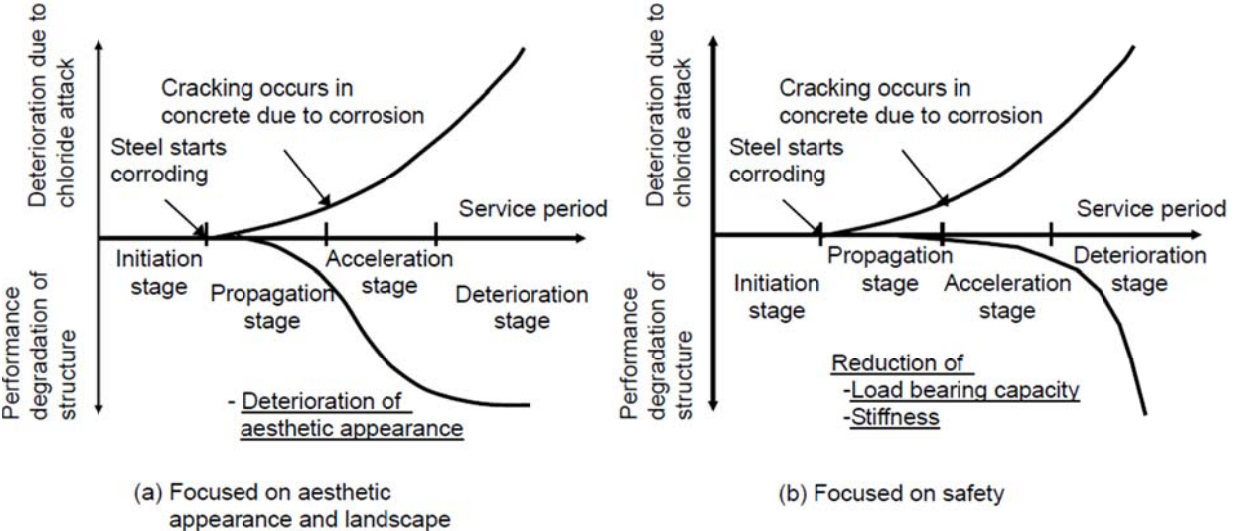


Fig. 2.4 Progress of deterioration due to chloride attack <sup>(2.15)</sup>

The risk of corrosion increases when the concentration of chlorides in the concrete increases. Chloride threshold value is the chloride concentration at the steel-concrete interface that causes a significant corrosion rate <sup>(2.16)</sup>. Many factors are affecting the chloride threshold such as pH, water cement ratio, cement type, mineral admixture, pore, and capillary structure, curing period and environment <sup>(2.3)</sup>. Because of the high number of factors affecting the chloride threshold level, CEB (Comite' Euro-International du Beton)<sup>(2.17)</sup> is given the chloride threshold level based on the interrelation of these factors as shown in **Fig. 2.5**. The Federal Highway Administration (FHWA) has stated that chloride ion concentration of 0.15% by weight of cement can be tolerated but that 0.3% is considered dangerous <sup>(2.19)</sup>. Another study also reported that the threshold value in the range of 0.17 to 2.5 by weight of cement <sup>(2.20)</sup>. In addition, Raupach (1996)<sup>(2.8)</sup> indicates that the critical value for chloride content varies between 0.5 and 1% by weight of cement for ordinary Portland cement and between 0.5 and 2% for blast furnace slag and fly ash cement depending on permeability, cover of concrete and cement type.

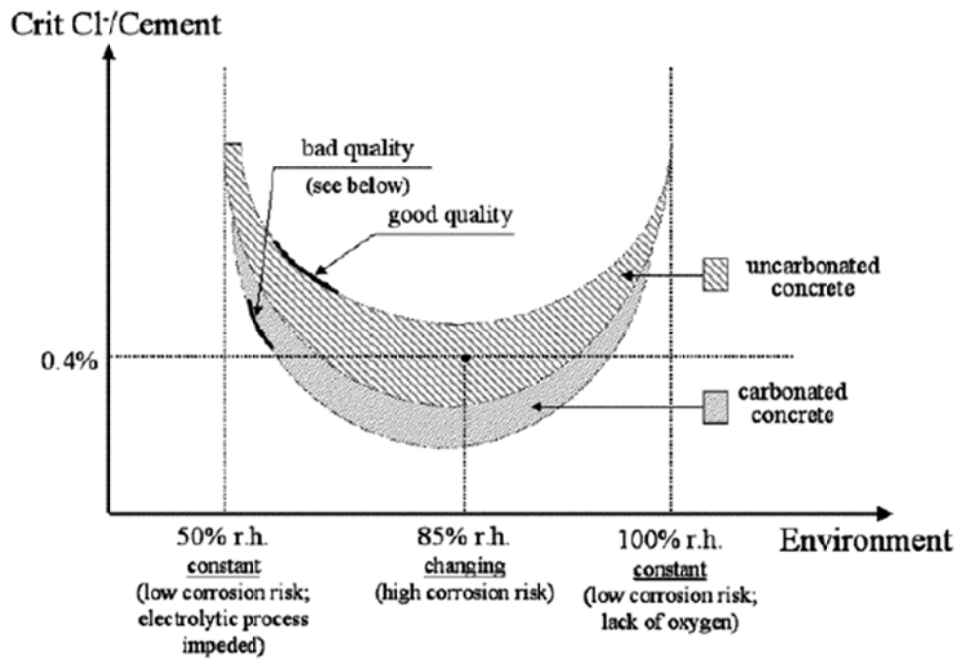


Fig. 2.5 CEB-FIP Critical chloride ions content for corrosion  
(FIP, 2000 in Robert M., et al)<sup>(2.18)</sup>

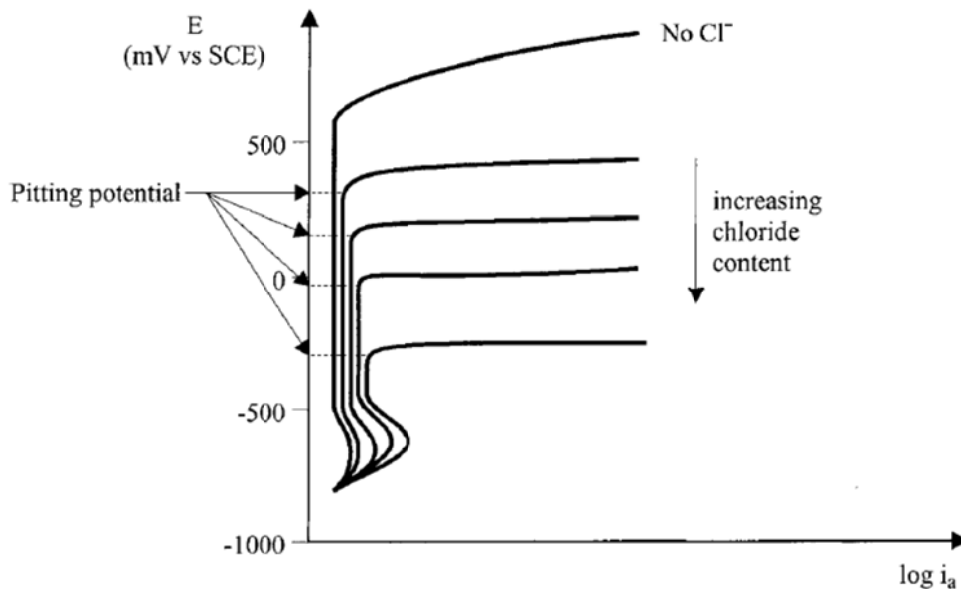


Fig. 2.6 Schematic illustration of the anodic behavior of steel in the presence of chloride<sup>(2.21)</sup>

Chloride content also play the important role the range of potentials in which the steel is passive. The upper potential of this range called the pitting potential ( $E_{pit}$ ), diminishes typically from +500 to -400 mV passing from sound very heavily chloride contaminated concrete (Fig. 2.6). For the structure exposed in atmospheric zone, the usual corrosion potentials around 0 V vs. SCE the critical content is in the range 0.4-1% of cement weight<sup>(2.21)</sup>.

In addition, corrosion initiation may be prevented if the concrete too dry than in very wet environments. One of the effects of a dry environment may be to prevent moisture entering the entrapped air voids in the steel <sup>(2.12)</sup>.

**2.2.4 Effect of concrete cracking on corrosion**

Reserachers have been debated the relationship between crack width and corrosion rate of steel in concrete since long ago. Several researchers have suggested the influence of crack width on the corrosion rate of steel <sup>(2.22), (2.23), (2.24)</sup>. Nevertheless, several researcher reported that little relationship between crack width and corrosion rate <sup>(2.25), (2.26), (2.27)</sup>. Both opinions indicate that the presence of crack will accelerate the onset of corrosion <sup>(2.2)</sup>. The first opinion suggests that the accelerated onset of corrosion will lead to more corrosion damage in a shorter periods, and thus reduce the service life of the structure. The second opinion suggests that the corrosion rate in uncracked concrete will reach the corrosion rate at the crack location after some duration. It is implied that the length of time between corrosion initiation at a crack ( $t_i$ ) and corrosion initiation in uncracked concrete ( $t_{icr}$ ) is not significant as illustrated in **Fig. 2.7**.

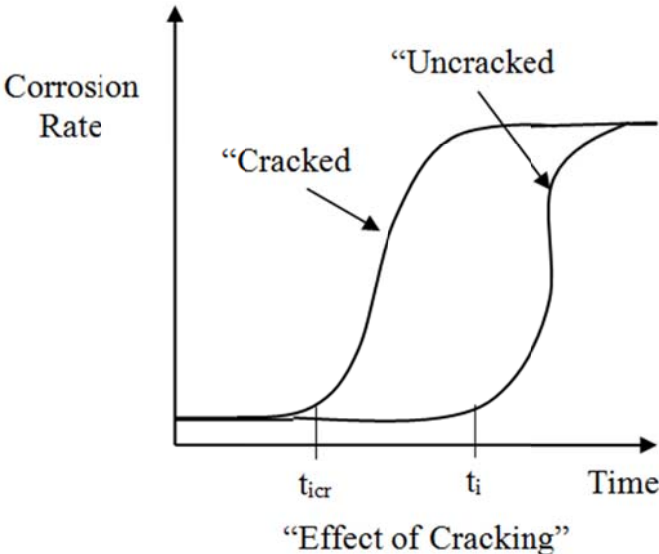


Fig. 2.7 Cracking accelerates onset of corrosion, but over time corrosion is similar in cracked and uncracked concrete <sup>(2.2)</sup>

In order to reduce the influence of crack width on the corrosion rate of steel in concrete, most codes specify the maximum crack widths from the durability point of view. BS 8110 (BSI 1985)<sup>(2.28)</sup> and IS 456 (BIS 2005)<sup>(2.29)</sup> recommended that for appearance and corrosion, the maximum surface width of the crack should not exceed 0.3 mm. According to ACI 224.1 R-07

(2009)<sup>(2.30)</sup> and ACI 318-09 (2009)<sup>(2.31)</sup> limit crack widths to 0.4 mm, although it is recognized that corrosion is not correlated with surface crack widths. In addition, JSCE standard for concrete structures is given more strict maximum crack width of 0.21 mm <sup>(2.32)</sup>. The JSCE surface crack width requirements are specified in terms of the amount of concrete cover. Because the JSCE requires larger cover for severe exposure, the allowable surface crack width is larger than for mild conditions <sup>(2.2)</sup>.

## 2.3 Cathodic Protection of Steel in Concrete

Cathodic protection (CP) has been demonstrated to be an effective technique to control corrosion of steel in chloride contaminated concrete. Cathodic protection works by the passing of a small electrical current from the anode to the corroding steel thereby protecting it from further deterioration by increasing the hydroxyl ions locally <sup>(2.33)</sup>. At first, CP was used commonly to prevent further deterioration due to corrosion after repair of damaged structures. However, recently, CP has been incorporated in new construction in an effort to avoid corrosion from starting (cathodic prevention) <sup>(2.34)</sup>.

There are two types CP system commonly use for reinforced concrete structure namely the impressed current cathodic protection (ICCP) and the sacrificial anode cathodic protection (SACP). The decision on which of the two CP systems to use is usually also influenced by a number of factors including but not limited to the condition of the structure, the client's budget, the anticipated life expectancy of the structure, appearance of structure after completion and maintenance and monitoring requirements for the system <sup>(2.33), (2.35)</sup>.

### 2.3.1 Impressed Current Cathodic Protection (ICCP)

ICCP system is usually more appropriate for atmospherically exposed concrete than SACP system. The main components of ICCP system include the anode system, steel bar, electrolyte, cabling, monitoring device, e.g. reference electrodes and a direct current (DC) power supply. In this system, CP is attained by applying a small amount of direct current through the concrete. An anode is usually laid on the concrete surface connected to the positive terminal, and the steel acts as the cathode is connected to the negative terminal of DC power supply. Concrete contains enough pore water to serve as the electrolyte so that when DC is applied, current can flow from the anode to the cathode. **Figure 2.8** shows the basic setup for a typical ICCP system in concrete.

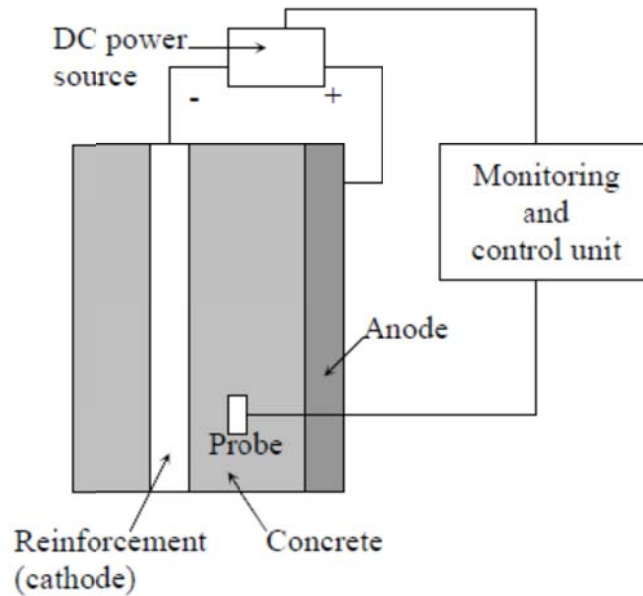


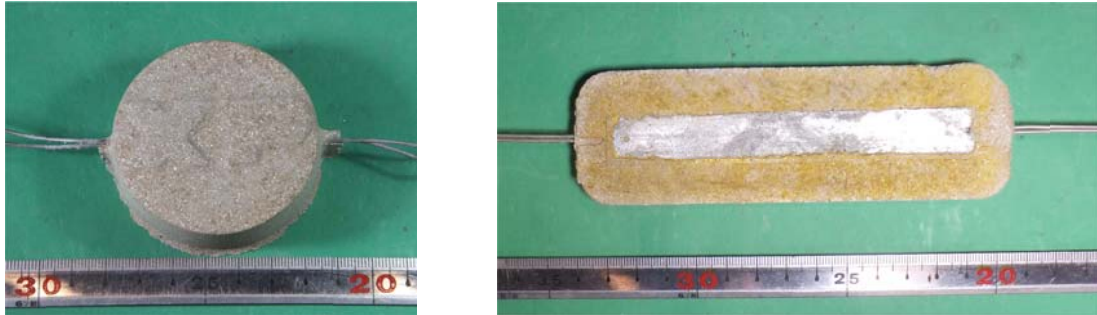
Fig. 2.8 Typical ICCP system setup <sup>(2.36)</sup>

The primary benefit of ICCP system is its flexibility and durability <sup>(2.33)</sup>. The current output of the power supply can be adjusted to optimise the protection delivered. Also, ICCP system can be controlled to accommodate variations in exposure conditions and future chloride contamination. The performance of ICCP system is widely determined by the material composition, shape, type and orientation of the anode <sup>(2.36)</sup>. There are a number of different types of anode that are used in ICCP system for reinforced concrete structure. These include conductive coating, titanium-based mesh in cementitious overlay, conductive overlay incorporating carbon fibres, flame-sprayed zinc and various discrete anode systems. The selection of the anode system must considered environmental conditions, anode zoning, accessibility, maintenance requirements, performance requirements and operating characteristics, life expectancy, weight restriction, track record and costs <sup>(2.33)</sup>.

### 2.3.2 Sacrificial Anode Cathodic Protection (SACP)

When the Sacrificial Anode Cathodic Protection (SACP) system is selected, the service life is expected to be shorter than an ICCP system because the anode must consume (sacrificed) to produce the protective current. Therefore, if a concrete structure has a relative long life remaining, the SACP may need replacement during the remaining service life of the structure. In general, the life expectancy of a sacrificial anode may be 5-20 years (or longer), and is dependent on the type of material used and the environmental condition <sup>(2.35)</sup>. Aluminium (Al), zinc (Zn) and magnesium (Mg) are the type of metals that is commonly used for SACP.

These metals are also covered with a highly alkaline mortar to improve the long-term performance and dissolution characteristics. **Figure 2.9** shows typical commercially available of the sacrificial anode.



(a). Sacrificial anode Galvashield XP

(b). Sacrificial anode Galvashield F

Fig. 2.9 Typical commercially available of the sacrificial anode

For reinforced concrete application, zinc has become the most common SACP used presently because several advantages <sup>(2.11)</sup>:

- a. Zinc has high corrosion efficiency i.e. high percentages of the electrons that are discharged when the zinc corrodes are available to protect the steel.
- b. As the zinc corrodes, it has a relative low rate of expansion compared to other metals including steel. This makes zinc anodes particularly suitable for application where the anodes are embedded into the concrete structure.
- c. Zinc anodes are suitable for use with prestressed and/or post-tensioned concrete because their native potential is not sufficient to generate atoms or cause hydrogen embrittlement in a concrete environment.

The primary benefit of SACP is its simplicity and the fact that minimal or no maintenance is required. In SACP system, an external power source is not required to maintain the protective current because directly electrically connected to the steel. This significantly reduces the start-up costs as no provision has to be made to connect to a power supply <sup>(2.35)</sup>. Also, SACP usually operates below the threshold for hydrogen embrittlement ( $\sim -900$  mV vs. CSE) <sup>(2.37)</sup>.

The main disadvantages of SACP system are the uncertain lifespan of the anodes, and it is dependent on the average current output of the anodes. The amount of current that is generated by SACP is significantly influenced by environmental factors, such as temperature, oxygen content, humidity and also chloride content. In addition, the resistivity of the concrete



must be taken into account as the lower driving voltage of the anodes means they may not be effective in high resistivity of concrete <sup>(2.35)</sup>.

### **2.3.3 Effect of cathodic protection in concrete**

CP current circulation between an anode and a cathode causes steel to polarize to a negative potential, increase the alkalinity of concrete and reduce the chloride content at the cathodic area by electrochemical reactions inside the electrolyte.

The negative potential shift can reduce the driving force for the anodic process (thermodynamic effect) and increase or maintain the resistance of the anodic process (kinetic effect) <sup>(2.38)</sup>. The cathodic reactions reduce oxygen content and generate alkalinity on the steel surface, which prevents corrosion because they widen the passive region and depolarize the cathodic process. In the case of passive steel, they hinder local acidification and also interfere with pitting initiation <sup>(2.38)</sup>. In addition, CP current also reduces the chloride concentration on the steel surface by electrophoresis.

The use of CP current in reinforced concrete gives not only beneficial effects but also negative effects such as concrete degradation, bond loss and hydrogen embrittlement. These are caused by ion migration of sodium ( $\text{Na}^+$ ) and potassium ( $\text{K}^+$ ) towards the concrete-steel interface <sup>(2.39), (2.40)</sup>. Application of a greater CP current can promote hydrogen activity at the concrete-steel interface and the consumption of electrons from the corrosion process <sup>(2.41)</sup>. In addition, hydrogen evolution can occur only at potentials more negative than about -950 mV vs. SCE in the case of alkaline environments ( $\text{pH} > 12$ ) <sup>(2.38)</sup>. For these reasons, it is necessary to determine suitable CP criteria for reinforced concrete structures.

### **2.3.4 Cathodic protection criteria in concrete**

The technique of CP has introduced to be an effective method to mitigate corrosion of steel in reinforced concrete structures. However, there is still a difference of opinion about the appropriate criteria for CP system. A variety of CP criteria have been proposed including using electrode operating potential, potential shift, potential decay, current-potential relationship (E-log I), macrocell probes, chloride concentration and a statistical treatment of static potentials <sup>(2.42)</sup>. Many of these criteria are complex and difficult to apply, and few experimental studies have been conducted to determine the actual effectiveness of the various criteria.

### **100 mV depolarization criterion**

The 100 mV depolarization criterion is the most popular criterion currently used for CP system and has been adopted by several codes. This criterion was investigated empirically by Bennett and Mitchell in 1989<sup>(2.43)</sup>. In their investigation, the procedure for measuring the instant-off potential (current interruption) and duration of the test is proposed. Also, the effect of temperature, static potential, and steel density was investigated by the test. They recommended that if the chloride concentration is not known, the 100 mV depolarization criterion is reasonable. Although 150 mV should be required if conditions are known to be very corrosive.

Several researchers have been investigated to determine the effectiveness of this criterion on the corrosion rate of steel in concrete. Funahashi and Young (1992)<sup>(2.44)</sup> studied the total depolarization needed for complete protection for macrocell and microcell currents under various environments. They found that the 100 mV depolarization criterion does not adequately eliminate both macrocell and microcell corrosion. Takewaka (1993)<sup>(2.45)</sup> investigated the relationship between corrosion weight loss and depolarization value on the 18 concrete blocks with 0.5% chloride by weight of concrete under a dry and wet cycle. Current density levels from 0 to nearly 500 mV were used to polarize the steel for eight months. The test results concluded that 100 mV criterion may not be sufficient and that 150-200 mV is necessary to protect the steel under these conditions. Another study was reported by Bennett et al. (1993)<sup>(2.46)</sup>, the amount of polarization needed to control corrosion to an acceptable level was found to be a complex function of many variables. 100 mV of polarization was adequate if chloride concentration was less than 0.26% by weight of concrete. However, at higher chloride concentrations, polarizations up to 150 mV were needed.

### **E-log I criterion**

Several investigations have been carried out to understand the effectiveness of the E-log I criterion<sup>(2.47), (2.48)</sup>. Although these investigations describe the experimental procedure in detail and the effects of variables such as concrete cover, temperature, and moisture content, there is no documentation of the actual effectiveness of this criterion. Bennett and Mitchell (1993)<sup>(2.46)</sup> observed the current density established by the E-log I criterion. They found that the current density required is higher than that required to achieve 100 mV of polarization. It might be that the current density determined by E-log I criterion is sufficient to control corrosion even if data are not available to support this conclusion.

## **Other criteria**

The -850 mV vs. CSE “instant-off” potential criteria has been suggested in practical CP installation on reinforced concrete structures. However, in structures where much of steel is in a passive state and availability of dissolved oxygen, the application of such criteria has been found to result in very high unneeded current requirement<sup>(2.42)</sup>. This might be cause premature deterioration of the anode, hydrogen evolution and the loss bond between concrete and steel.

Corrosion rate are affected by a number of variables such as chloride content, quality of concrete, concrete cover, moisture and oxygen availability. Therefore, there is no fixed value for the protective current or potential value that a CP system must supply. Protection will increase over time as chloride ions are forced away from, and hydroxide ions are generated at the steel. The increase in hydroxyl ions and decrease in chloride ions around the steel surface reduce the risk of corrosion, so the CP current can be reduced<sup>(2.49)</sup>.

It is important to determine the amount of protective current or potential difference that required for CP system apply to reinforced concrete structures and to make sure that the anode can provide that current uniformly across the structure. Cathodic (1998)<sup>(2.36)</sup> estimated practical current density requirements for CP system in various material and environmental conditions are listed in **Table 2.2**.

Table 2.2 Practical CP current density requirements for varying steel conditions<sup>(2.36)</sup>

<b>Environmental surrounding steel reinforcement</b>	<b>Current density (mA/m<sup>2</sup>)</b>
Alkaline, no corrosion occurring, a little oxygen resupply	0.1
Alkaline, no corrosion occurring, exposed structure	1 - 3
Alkaline, chloride present, dry, good quality concrete, high cover, light corrosion observed on the steel	3 - 7
Chloride present, wet, poor quality concrete, medium-low cover, widespread pitting and general corrosion on steel	8 - 20
High chloride levels, wet fluctuating environment, high oxygen level, hot, severe corrosion on steel and low cover	30 - 50

## **2.4 Cathodic Prevention of Steel in Concrete**

Application of CP system not only to stop on-going corrosion activity in chloride contaminated concrete, but also to increase the corrosion resistance of the steel in new structure. Once the new concrete is placed, the anodes begin to provide corrosion protection to the steel. This technique called ‘cathodic prevention’, is based on the strong influence of the potential on

the critical chloride content <sup>(2.21)</sup>. The objective of a cathodic prevention strategy is to provide sufficient current to the steel to prevent the initiation of the corrosion sites. The current density required ranges from 0.2 to 2 mA/m<sup>2</sup> <sup>(2.37), (2.38)</sup>. **Table 2.3** shows the comparison between cathodic protection and the cathodic prevention mitigation strategies <sup>(2.50)</sup>.

Table 2.3 Comparison of corrosion mitigation strategies <sup>(2.50)</sup>

	Cathodic prevention	Cathodic protection
Objective	Preventing corrosion from initiating in contaminated areas	Stopping on-going corrosion activity
Current required per m <sup>2</sup> of steel surface	0.2 to 2 mA/m <sup>2</sup>	2 to 20 mA/m <sup>2</sup>
Polarization	< 100 mV	≥ 100 mV

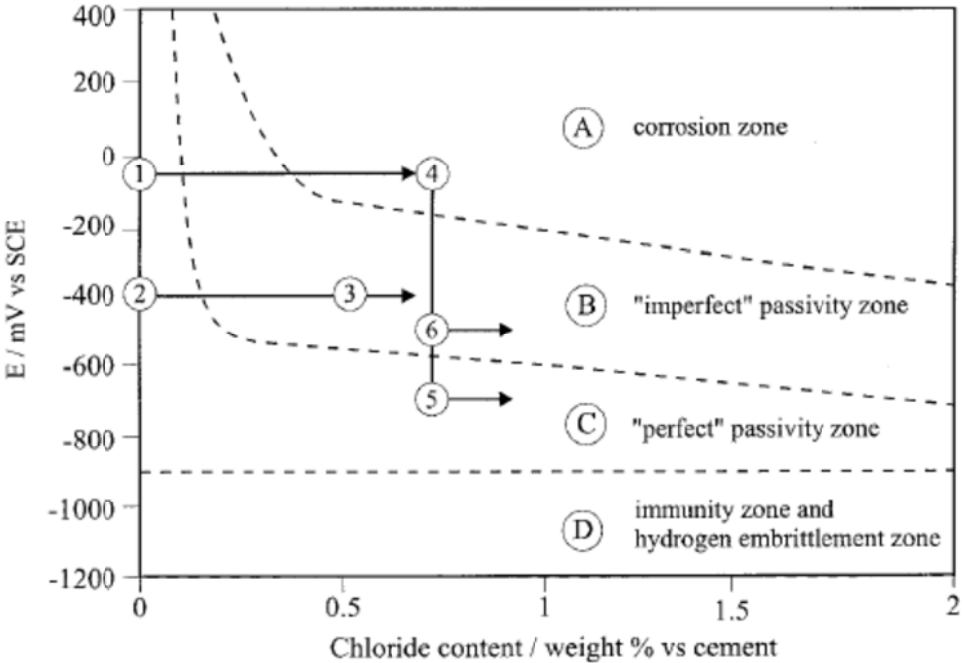


Fig. 2.10 Schematic illustration of steel behaviour in concrete for different potentials and chloride contents <sup>(2.21)</sup>

Bertolini et al. (1998)<sup>(2.21)</sup> proposed the typical evolution path (in terms of potential and chloride content) of the cathodic prevention as illustrated in **Fig. 2.10**. Path (1→2→3→) for cathodic prevention; CP restoring passivity (4→5→); CP reducing corrosion rate (4→6→). Cathodic prevention is applied from the beginning and CP only after corrosion has initiated. At usual current density for cathodic prevention in the range 1 to 2 mA/m<sup>2</sup>, a decrease in potential

of at least 100-200 mV is produced, leading to an increase in the critical chloride content higher than one order magnitude.

Although the cathodic prevention system have a similar operation as the traditional CP system in concrete, its different aims, features, operating condition, effects and side effects. In particular, cathodic prevention has a different consequence as far as hydrogen evolution is concerned, and this makes it even possible to apply it to prestressed structures without risk of embrittlement <sup>(2,38)</sup>. In addition, preventing corrosion from initiating is useful in the case of patch repair of chloride contaminated concrete to mitigate the formation of secondary corrosion sites after completed repairs, and also use in the areas that corrosion is likely to occur in new construction such as tidal and splash zone.

## 2.5 Issues Addressed in this Study

As was stated in the literature review, the corrosion rate of steel in concrete mainly affect by chloride content and oxygen availability especially in the atmospherically exposure zone. The only one method that used to prevent or stop the corrosion of steel in concrete is cathodic protection system both ICCP and SACP. Although CP system has been introduced to control corrosion of steel in concrete effectively, there are still debate regarding the CP design for reinforced concrete structures. In this study, a laboratory test was carried out to examine the effectiveness of CP and the results obtain are used to provide information the reliable CP design for reinforced concrete structure.

Two types of CP system will be evaluated, namely ICCP and SACP. In **Chapter 3**, the fundamental study and application of SACP system as corrosion prevention of steel will be presented. The test focused on the effectiveness of SACP system to prevent corrosion initiation of steel in concrete structure.

Meanwhile, **Chapter 4, 5** and **6** described of the ICCP system. The CP method by improvement in the local environment of the steel surface will be discussed in **Chapter 4**. For this, a various constant current density was applied to the steel in concrete specimen with different chloride content. In this case, the protection of steel is not instantaneous, but a gradual process that may take several time to achieve (i.e., decay potential  $\geq 100$  mV). In **Chapter 5**, the actual effect of CP criteria for steel in concrete will be presented. The protection level (depolarization value) of 25 mV, 50 mV, and 100 mV were kept constant during test periods. The protective current was adjusted after depolarization test to achieve the protection level value. In **Chapter 6**, the effectiveness of two CP methods namely (1) constant current density

and (2) constant potential shift from its natural potential of steel bar 24 hours after switch off will be discussed. Both CP methods were examined in the concrete specimens with corrosive steel bar and high chloride concentration. In addition, an appropriate CP design for reinforced concrete structures will be presented in **Chapter 7**.

## References

- 2.1 Suryavanshi, A. K., et al, “Corrosion of Reinforcement Steel Embedded in High Water-cement Ratio Concrete Contaminated with Chloride”, *Cement and Concrete Composites*, Vol. 20, 1998, pp. 263-381.
- 2.2 West, J. S., et al, “State of the Art Report about Durability of Post-tensioned Bridge Substructures”, Research Report 1405-1, Center for Transportation Research, Texas Univ., 1999.
- 2.3 Montemor, M. F., et al, “Chloride-Induced Corrosion on Reinforcing Steel: from the Fundamental to the Monitoring Techniques”, *Cement and Concrete Composites*, Vol. 25, 2003, pp. 491-502.
- 2.4 Pourbaix, M., “Atlas of Electrochemical Equilibria in Aqueous Solution”, Oxford: Pergamon Press, 1996.
- 2.5 Hime, W. and Erlin, B., “Some Chemical and Physical Aspects of Phenomena Associated with Chloride-Induced Corrosion”, ACI SP-02, Corrosion, Concrete and Chlorides – Steel Corrosion in Concrete: Causes and Restraints, F.W. Gibson, Editor, American Concrete Institute, Detroit, MI, 1987, pp. 1-12.
- 2.6 Fraczek, J., “A Review of Electrochemical Principles as Applied to Corrosion of Steel in a Concrete or Grout Environment,” ACI SP-02, Corrosion, Concrete and Chlorides – Steel Corrosion in Concrete: Causes and Restraints, F.W. Gibson, Editor, American Concrete Institute, Detroit, MI, 1987, pp. 13-24.
- 2.7 Cheung, Moe M. S. and Cao C., “Application of Cathodic Protection for Controlling Macrocell corrosion in Chloride Contaminated RC Structures”, *Construction and Building Materials*, Vol. 45, 2013, pp. 199-207.
- 2.8 Raupach, M., “Chloride-Induced Macrocell corrosion of Steel in Concrete – Theoretical Background and Practical Consequence”, *Construction and Building Materials*, Vol. 10, 1996, pp. 329-338.
- 2.9 Skoglund, P., et al, “Chloride Redistribution and Reinforcement Corrosion in the Interfacial Region between Substrate and Repair Concrete – A laboratory Study”, *Materials and Structures*, 41, 2008, pp. 1001-1014.
- 2.10 Sagues, A. A., “Corrosion of Epoxy Coated Rebar in Florida Bridges”, WPI No. 0510603, 1994, University of South Florida, Tampa, FL.
- 2.11 Rajendran, V and Murugesan, R., “Study on Performance of Self Regulating Sacrificial Galvanic Anodes with and without Preconditioning Against Control

- Specimen and Using Accelerated Corrosion”, Asian Journal of Civil Engineering (BHRC), Vol. 14, 2013, pp. 181-199.
- 2.12 Glass, G. K. and Buenfeld, N. R., “Chloride-Induced Corrosion of Steel in Concrete”, Prog. Struct. Engng Mater, 2, 2000, pp. 448-458.
- 2.13 Mansfeld, F., “Recording and Analysis of AC Impedance Data for Corrosion Studies”, Corrosion, 37(5), 1981, pp. 301-307.
- 2.14 Tuutti, K., “Corrosion of Steel in Concrete”, Report 4-82, Swedish Cement and Concrete Research Institute, Stockholm, Sweden, 1982, pp. 469.
- 2.15 JSCE Guidelines for Concrete No. 17, “Standard Specifications for Concrete Structure- JSCE (Part: Maintenance)”, 2007.
- 2.16 Schiessl, P. and Raupach, M., “Influence of Concrete Composition and Microclimate on the Critical Chloride Content in Concrete”, Corrosion of Reinforcement in Concrete, Wishaw, Warwickshire, UK, 49-58.
- 2.17 CEB, “Guide to Durable Concrete Structures”, 1992, Comite’ Euro-International du Beton, Lausanne, Switzerland.
- 2.18 Robert, M, et al, “Durability of Precast Prestressed Concrete Piles in Marine Environment: Reinforcement Corrosion and Mitigation-Part 1”, Final Report, June 2011, pp. 2-32.
- 2.19 Hansson, C. M. and Sorensen, B., “Corrosion Rates of Steel in Concrete”, p. 3, ASTM STP 1065, 1990.
- 2.20 Glass, G. K. and Buenfeld, N. R., “The Presentation of the Chloride Threshold Level for Corrosion of Steel in Concrete”, Corrosion Science, 39(5), pp. 1001-1013.
- 2.21 Bertolini, L, et al, “Cathodic Protection and Cathodic Prevention in Concrete: Principles and Applications”, Journal of Applied Electrochemistry, 28, 1998, pp. 1321-1331.
- 2.22 Okada, K. and Miyagawa, T., “Chloride Corrosion of Reinforcing Steel in Cracked Concrete”, Performance of Concrete in Marine Environment, V. M. Malhotra, ed., SP-65, ACI, pp. 237-254.
- 2.23 Francois, R. and Maso, J. C., “Effect of Damage in Reinforced Concrete on Carbonation and or Chloride Penetration”, Cement and Concrete Research, 18, 1988, pp. 961-670.
- 2.24 Ohno, Y., et al, “Influence of Cracking and Water to Cement Ratio on Macrocell Corrosion of Steel in Concrete”, Corrosion of Reinforcement in Concrete Construction,



- C. L. Page, P. B. Bamforth and J. W. Figg, eds., The Royal Society of Chemistry, pp. 88-104.
- 2.25 Schießl, P., “Corrosion of Steel in Concrete”, RILEM Report, Chapman & Hall, London.
- 2.26 Arya, C. and Ofori-Darko, F. K., “Influence of Crack Frequency on Reinforcement Corrosion in Concrete”, Cement and Concrete Research, 26(3), 1996, pp. 345-353.
- 2.27 Schießl, P. and Raupach, M., “Laboratory Studies and Calculations on the Influence of Crack Width on Chloride-Induced Corrosion of steel in Concrete”, ACI Materials Journal, 94(1), 1997, pp. 56-62.
- 2.28 British Standard Institution (BSI), “Structural Use of Concrete – Part 2: Code of Practice for Special Circumstances”, BS 8110-2, London, 1985.
- 2.29 Bureau of Indian Standard (BSI), “Code of Practice for Plain and Reinforced Concrete”, IS 456:2000 (reaffirmed), New Delhi, 2005.
- 2.30 American Concrete Institute (ACI), “Control of Cracking in Concrete Structures”, ACI 224.1 R-07, Detroit, 2009.
- 2.31 American Concrete Institute (ACI), “Building Code Requirements for Structural Concrete and Commentary”, ACI 318-09, Detroit, 2009.
- 2.32 Standard Specification for Design and Construction of Concrete Structures – Part 1 (Design), Japan Society of Civil Engineers (JSCE), Tokyo, Japan, 1986.
- 2.33 Ngala, V., et al, “The Selection and Use of Cathodic Protection Systems for the Repair of Reinforced Concrete Structures”, Construction and Building Materials, 39, 2013, pp. 19-25.
- 2.34 Polder, Rob B., “Cathodic Protection of Reinforced Concrete Structures in the Netherland – Experience and Developments” HERON, Vol. 43, No. 1, pp. 3-14.
- 2.35 Callon, R., et al, “Selection Guidelines for Using Cathodic Protection Systems on Reinforced and Prestressed Concrete Structures”, Corrpro Technical Library, Medina.
- 2.36 “Cathodic Protection of Steel in Concrete”, Ed. P. M. Chess, E and FN Spon, New York, NY, 1998, pp. 187.
- 2.37 EN 12696, “Cathodic Protection of Steel in Concrete”, European Standard, 2000.
- 2.38 Pedferri, P., “Cathodic Protection and Cathodic Prevention”, Construction and Building Materials, Vol. 10, No. 5, 1996, pp. 391-402.
- 2.39 Chang, J.J., “A Study of the Bond Degradation of Rebar due to Cathodic Protection Current”, Cement and Concrete Research, 32(4), 2002, pp. 657-663.

- 2.40 Rasheeduzzafar, M. G. A. and Alsulaimani, G. j., “Degradation of Bond Between Reinforcing Steel and Concrete due to Cathodic Protection Current”, *ACI Materials Journal*, 90(1), 1993, pp. 8-15.
- 2.41 Garcia, J., et al, “Effect of Cathodic Protection on Steel – Concrete Bond Strength using Ion Migration Measurements”, *Cement & Concrete Research*, 34, 2012, pp. 242-247.
- 2.42 Bennett, J. and Broomfield, J. P., “An Analysis of Studies Conducted on Criteria for the Cathodic Protection of Steel in Concrete”, *NACE CORROSION/97*, Paper No. 251, 1997.
- 2.43 Bennett, J. E. and Mitchell, T. A., “Depolarization of Cathodically Protected Reinforcing Steel in Concrete”, *NACE CORROSION/89*, Paper No. 373, 1989.
- 2.44 Funahashi, M. and Young, W. T., “Investigation of 100 mV Shift Criterion for Reinforcing Steel in Concrete”, *NACE CORROSION/92*, Paper No. 193, 1992.
- 2.45 Takewaka, K., “Cathodic Protection for Reinforced Concrete and Prestressed Concrete Structures”, *Corrosion Science*, Vol. 35, 1993, pp. 1617-1626.
- 2.46 Bennett, J. E., “Cathodic Protection Criteria Related Studies Under SHRP Contract”, Paper No. 323, *NACE CORROSION/93*, 1993.
- 2.47 Bushman, J. B. and Swiat, W. J., “Corrosion Control Performance and Criteria Used to Adjust and Evaluate Cathodic Protection of Steel Reinforced Concrete Bridge Components”, Paper No. 343, *NACE CORROSION/93*, 1993.
- 2.48 Funahashi, M. and Young, W. T., “Investigation of E-Log I Tests and Cathodically Polarized Steel in Concrete”, *NACE CORROSION/94*, Paper No. 301, 1994.
- 2.49 Kepler, J. L., et al, “Evaluation of Corrosion Protection Methods for Reinforced Concrete Highway Structures”, University of Kansas Center for Research, Inc., Lawrence, Kansas, 2000.
- 2.50 Liao, H., “Concrete Corrosion Protection with Various Galvanic Systems”, *NACE East Asia Pacific Conference*, Kyoto, Japan, 2013.

## CHAPTER 3. EFFECTIVENESS OF SACRIFICIAL POINT ANODES FOR CORROSION PREVENTION OF STEEL BARS IN CONCRETE

### 3.1 Introduction

Usually, the steel embedded in concrete is protected because a high alkalinity resulting from hydration cement in concrete. However, corrosion will take place by the presence of chloride ions and carbonation. The corrosion product (iron oxides and hydroxides) can lead to concrete cracking, spalling and delamination of concrete. In order to prevent continuing deterioration, repair technique needs to be undertaken <sup>(3.1)</sup>. Unfortunately, many patch repairs exhibited the new corrosion damage only after a few months to a year <sup>(3.2)</sup>. To reduce the need for repairs, several protection techniques have been developed to prevent the corrosion initiation for both newly constructed structures and to repair concrete structures in aggressive environmental <sup>(3.3)</sup>.

Cathodic protection (CP) has been introduced to be an effective technique to stop the corrosion of embedded steel bar in concrete. One of many different kinds of CP methods is the sacrificial point anode method (galvanic anode). Sacrificial point anode system is aimed to shift the potential of steel to the least probable range for corrosion.



Fig 3.1 Sacrificial point anodes

Nowadays, sacrificial point anode is commercially available. These are typically made from zinc nucleus covered by a highly alkaline cement mortar with lithium hydroxide (LiOH)

to maintain zinc corrosion activation. The type and sizes of this sacrificial point anode are variable, depending on the fabricating and distributing company. The anode used in this study is commercially available with sizes of 60 mm in diameter and 30 mm in thickness as shown in **Fig. 3.1**.

This study describes the effectiveness of sacrificial point anodes to prevent corrosion of steel bar under various application namely chloride contaminated concrete, repaired concrete and cracked concrete. Also, factor affecting the effectiveness of the sacrificial point anodes was evaluated.

### 3.2 Preparation of Specimens

Three different types of specimens were prepared in this investigation, namely chloride contaminated concrete, repaired concrete and cracked concrete. In addition, all potentials value is converted to the reference copper/copper sulfate electrode (CSE). The details of the investigation are describes as follows:

#### 3.2.1 Chloride Contaminated Concrete

Ordinary Portland Cement (OPC), crushed river stone and sea sand were used. The physical properties of concrete materials are presented in **Table 3.1**. Concrete with water to cement ratio (W/C) of 47% was used for all specimens. Initial chloride content was set as 4 kg/m<sup>3</sup> or 10 kg/m<sup>3</sup> or without chloride (0 kg/m<sup>3</sup>). The mix proportion of concrete is described in **Table 3.2**.

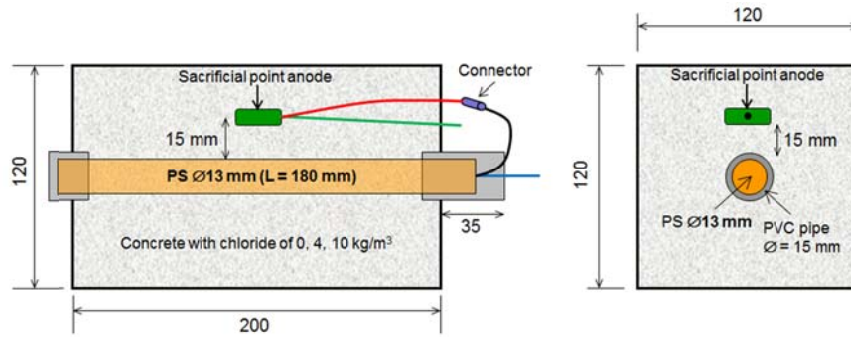
Table 3.1 Physical property of concrete materials

Material	Description
Cement	Ordinary Portland Cement (OPC), Density = 3.16 g/cm <sup>3</sup> , SSA = 3390 cm <sup>2</sup> /g
Sand	Sea sand, SSD density = 2.58 g/cm <sup>3</sup> , F.M = 2.77
Gravel	Crushed stone, SSD density = 2.85 g/cm <sup>3</sup> , MSA = 20 mm

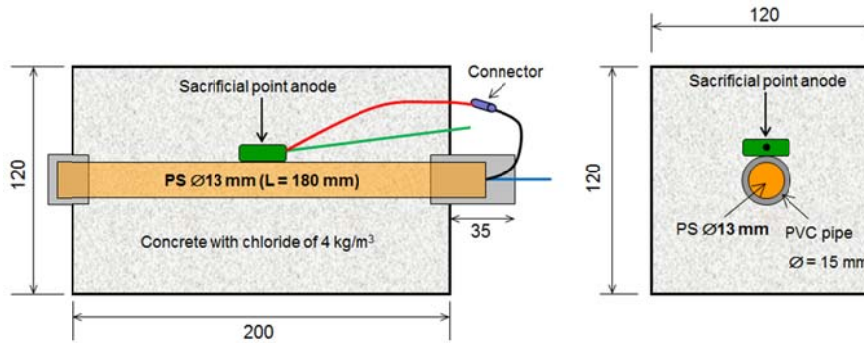
SSD: Saturated Surface Dry; F.M: Fineness Modulus; MSA: Maximum Size of Aggregates; SSA: Specific Surface Area.

Table 3.2 Mix proportion of concrete (chloride contaminated concrete)

W/C (%)	Concrete (kg/m <sup>3</sup> )				
	Water	Cement	Sand	Gravel	Chloride
47	164	350	844	953	0, 4, 10



(a) With gap between sacrificial point anode and steel bar



(b) Without gap between sacrificial point anode and steel bar

Fig. 3.2 Detail of specimen chloride contaminated concrete (unit: mm).

Table 3.3 Summary of specimens (chloride contaminated concrete)

W/C (%)	Series	Chloride (kg/m <sup>3</sup> )	Gap (mm)	Remarks
47	PSCP-0-G15	0	15	With sacrificial point anode
	PS-0		-	Without sacrificial point anode
	PSCP-4-G15	4	15	With sacrificial point anode
	PSCP-4-G0		0	With sacrificial point anode
	PS-4		-	Without sacrificial point anode
	PSCP-10-G15	10	15	With sacrificial point anode
PS-10	-		Without sacrificial point anode	

Notation:

PSCP : Plain steel bar with sacrificial point anode.

PS : Plain steel bar without sacrificial point anode.

G15 : Gap between steel bar and sacrificial point anode is 15 mm.

Specimens were casted in the form of reinforced concrete prisms with dimensions of 120 mm x 120 mm x 200 mm. A plain steel bar (PS) of 13 mm in diameter and 180 mm in length with surface area of 73.48 cm<sup>2</sup> were placed in the center of the specimen. Both ends of exposed steel bar was covered by PVC pipe with resin to avoid penetration of chloride ions and

oxygen during exposure. Sacrificial point anode and steel bar were set with a gap of 15 mm. One specimen was prepared without gap between steel bar and sacrificial point anode for concrete with 4 kg/m<sup>3</sup> of chloride. Detail of specimen design is shown in **Fig. 3.2**.

At 24 hours after casting, specimens were demoulded and cured with a wet towel for 28 days in the room with constant temperature of 20±2°C (relative humidity: 60%). Seven test prisms were prepared as summarized in **Table 3.3**. At the age of 28 days, steel bar and sacrificial point anode were connected and exposed in the following conditions. Firstly, all specimens were exposed in the air condition (20±2°C, RH: 60%) around 150 days. After that, specimens were moved to the dry/wet cycles (2 days immersion in 3% NaCl solution and 5 days drying) up to 250 days. In total, exposure period was around 400 days.

### 3.2.2 Repaired Concrete

All materials were used similar in the chloride contaminated concrete. Additionally, Blast Furnace Slag (BFS) was added as a replacement of cement. Mix proportions of concrete were divided in two categories; existing concrete (EC) and repairing concrete (RPC). For EC, concrete with water to cement ratio (W/C) of 53.5% and 40% was prepared, namely N53.5, N40 and BB40 respectively. Both concrete contained 4 kg/m<sup>3</sup> or 10 kg/m<sup>3</sup> of chloride. For BB40, OPC were replaced by 50% BFS. Meanwhile, for repairing concrete RPC, concrete with 47% of W/C ratio without chloride was placed. All mix proportions are presented in **Table 3.4**.

Table 3.4 Mix proportions of concrete (repaired concrete)

Material	EC			RPC
	N53.5	N40	BB40	
W/C, %	53.5	40	40	47
Water, kg/m <sup>3</sup>	166	161	161	164
Cement, kg/m <sup>3</sup>	310	403	201	350
BFS, kg/m <sup>3</sup>	0	0	201	0
Sand, kg/m <sup>3</sup>	719	680	680	844
Gravel, kg/m <sup>3</sup>	1141	1102	1102	953
Chloride, kg/m <sup>3</sup>	4, 10	4, 10	4, 10	0

The specimen was fabricated in the form of concrete prism with dimensions of 150 mm x 150 mm x 500 mm and cover thickness of 30 mm. Each specimen consist of plain steel bar (PS), plain steel bar with the point anodes (PSCP) and epoxy coated steel bar (PSE). Reinforced concrete prisms specimen was casted in two layers. EC containing chloride of 4 kg/m<sup>3</sup> or 10 kg/m<sup>3</sup> was cast at first. Specimen was demoulded after 24 hours and cured by wet

towel until 14 days. After curing for 14 days, the point anodes were fixed in steel bars. Before placing RPC, surface of existing concrete were layered with the epoxy resin and silica sand, but some of the specimens without epoxy materials. Then, RPC was placed and demoulded after 24 hours and cured again by wet towel until 28 days. Detail of specimen design is shown in **Fig. 3.3**. Twelve test prisms were prepared as summarized in **Table 3.5**. In addition, specimens were kept in air curing ( $20\pm 2^{\circ}\text{C}$ , RH: 60%) during test periods. Exposure period was around 12 months.

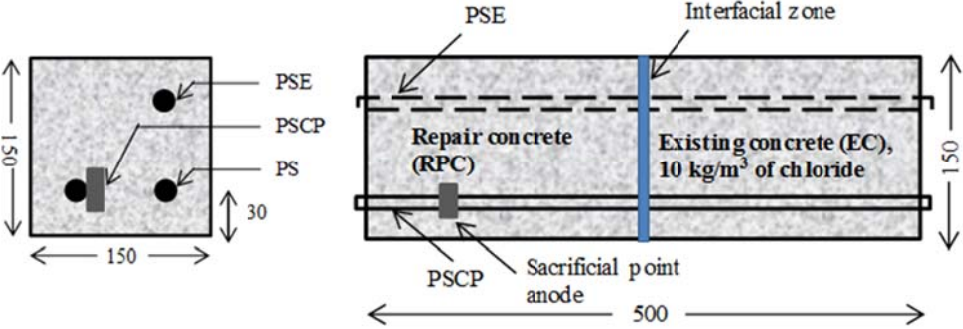


Fig. 3.3 Detail of specimen repaired concrete (unit: mm)

Table 3.5 Summary of specimen (repaired concrete)

Type	Specimen Series	Chloride (kg/m <sup>3</sup> )	*Epoxy Materials
N53.5	N53.5-N-4	4	N
	N53.5-Y-4	4	Y
	N53.5-N-10	10	N
	N53.5-Y-10	10	Y
N40	N40-N-4	4	N
	N40-Y-4	4	Y
	N40-N-10	10	N
	N40-Y-10	10	Y
BB40	BB40-N-4	4	N
	BB40-Y-4	4	Y
	BB40-N-10	10	N
	BB40-Y-10	10	Y

Notation:

\*Epoxy materials : Epoxy resin and silica sand.

N : Specimen without epoxy materials.

Y : Specimen with epoxy materials.

### 3.2.3 Cracked Concrete

The mix proportion of concrete is shown in **Table 3.6**. Concrete mix with water to cement (W/C) ratio of 40% was used throughout all specimens without chloride. Specimens were casted in the form of reinforced concrete prism of 150 mm x 150 mm x 500 mm in

dimensions. The specimen had a plain steel bar of 13 mm diameter placed at the cover depth of 30 mm. Each concrete specimen contained plain steel bar (PS) and a plain steel bar with the sacrificial point anode (PSCP). Detail of specimen design is shown in **Fig. 3.4**. Before placing concrete in molds, sacrificial point anode was installed on the steel bar and checked the maximum resistance of  $0.3 \Omega$  by using ampere meter, then concrete was placed and demolded after 24 hours. The specimens were cured under sealed conditions in a wet towel for 28 days in constant room temperature of  $20 \pm 2^\circ\text{C}$ . To determine the compressive strength of concrete,  $\Phi 100 \times 200$  mm concrete cylinders were fabricated and tested after 28 days of curing in water.

Table 3.6 Mix proportion of concrete (cracked concrete)

W/C (%)	Concrete (kg/m <sup>3</sup> )			
	Water	Cement	Sand	Gravel
40	161	403	680	1108

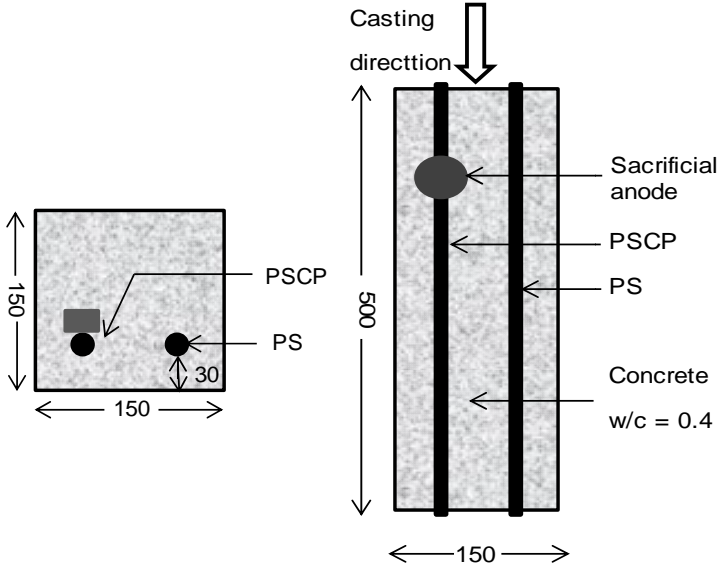


Fig. 3.4 Detail of specimen cracked concrete (unit: mm)

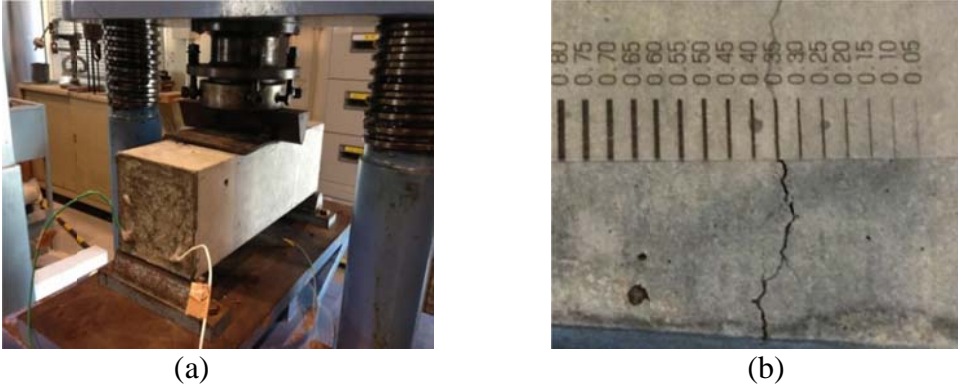


Fig. 3.5 (a) Bending loading for cracking; (b) crack width measurement.



At 28 days moisture curing, all specimens were cracked under one point flexural loading (**Fig. 3.5a**). One set of displacement transducer ( $\pm 2$  mm) was fixed at the bottom side of the specimen in order to check the crack width. Ten data were measured immediately after loading for each side (bottom and lateral) of the specimen in order to calculate an average crack width (**Fig. 3.5b**). In addition, twelve test prism specimens were prepared in this investigation.

After cracking, both ends of specimens were sealed with epoxy resin. Then, specimens were exposed in air curing (T:  $20\pm 2^\circ\text{C}$ , RH: 60%), immersed in 3% NaCl solution and dry/wet cycle as listed in **Table 3.7**. For specimen exposed in 3% NaCl solution, only 40 mm from the bottom surface was immersed (**Fig. 3.6**). Further, exposure was continued until around 530 days.

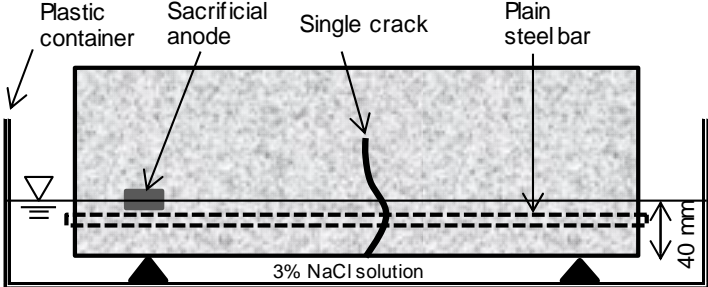


Fig. 3.6 Immersion in 3% NaCl solution

Table 3.7 List of test specimen (cracked concrete)

Specimen series	Maximum crack Width (mm)	Average crack width	Exposure condition
A1	0.15	0.06	Air curing at temperature (T): $20\pm 2^\circ\text{C}$ , relative humidity (RH): 60%
A2	0.22	0.15	
A3	0.38	0.25	
A4	0.45	0.31	
B1	0.14	0.09	Immersion in 3% NaCl solution
B2	0.17	0.17	
B3	0.30	0.20	
B4	0.45	0.32	
C1	0.18	0.09	Dry/wet cycles (2 days in 3% NaCl solution & 5 days dry)
C2	0.25	0.18	
C3	0.37	0.29	
C4	0.45	0.34	

### 3.3 Electrochemical Tests

Electrochemical tests include half-cell potential, on potential, instant-off potential, protective current, polarization behavior of sacrificial point anode, anodic-cathodic polarization curve and polarization resistance of steel bar. In addition, visual observation was also carried

out at the end of test periods. **Table 3.8** is summarized the electrochemical tests and visual observation for each specimen.

Table 3.8 Summary of electrochemical tests and visual observation each specimen

Test item	Chloride contaminated concrete	Repaired concrete	Cracked concrete
Half-cell potential	o	o	o
On potential	×	o	o
Instant-off potential	o	×	×
Protective current	o	×	×
Polarization behavior of sacrificial anode	o	o	o
Anodic-cathodic polarization curve of steel bar	×	o	o
Polarization resistance of steel bar	o	×	×
Visual observation	×	o	o

o : Tested; ×: No tested;

**(a) Half-cell potential (PS: Plain steel bar)**

Half-cell potential of PS was monitored by using a digital voltmeter (Yokogawa) and the silver/silver chloride reference electrode (Ag/AgCl). The interpretation of potential readings of PS was carried out according to ASTM C876-09<sup>(3.4)</sup> as described in **Table 3.9**.

Table 3.9 Corrosion probability<sup>(3.4)</sup>

Half-cell potential (mV;CSE)	Corrosion probability
-200 < E	90% no corrosion
-350 < E < -200	Uncertainty
E > -350	90% corrosion

**(b) On potential and instant-off potential (PSCP: Plain steel bar with sacrificial anode)**

The “On-potential” and the instant-off potential (within one second after current interruption) of PSCP were recorded periodically using similar method and equipment in half-cell potential measurement. Judgment for the PSCP is based on the protective potential of steel bar is lower than -750 mV vs. CSE<sup>(3.5)</sup>.

**(c) Protective current and depolarization tests**

The protective current of sacrificial anode was measured by using the ammeter.

Depolarization tests were regularly carried out by disconnecting the steel bar from the sacrificial point anode. The difference between instant-off potential and 24 hours off potential was assumed as a decay potential. Cathodic protection applied to steel in concrete is commonly considered as effective if the 24 hours depolarization value is more than 100 mV in accordance with Concrete Library 107, JSCE, Japan <sup>(3.6)</sup>. In this study, 300 mV depolarization value (On-potential – natural potential), was used to demonstrate the effectiveness of the sacrificial point anode in the repaired and cracked concrete. While for chloride contaminated concrete is 100 mV.

**(d) Anodic Polarization behavior of sacrificial point anode**

Anodic polarization behavior of the sacrificial point anode was measured after depolarization tests. Anodic polarization behaviors were obtained by the contact method (repaired concrete and cracked concrete) and immersion method (chloride contaminated concrete). The contact method is a measuring method using double layer counter electrode contacted on the surface of the specimen. Immersion method is a measuring method in which the measurement is carried out with the specimen be immersed in a solution. Potentiostat (HA-151A Hokuto Denko) and function generator (HB-III Hokuto Denko) were used for this anodic polarization test with scan speed of 1 mV/sec. The current at each potential sweep was recorded.

**(e) Anodic-cathodic polarization curve of steel bar**

Anodic polarization curve is related to the passivity condition of steel bars (**Table 3.10**). When the current density becomes larger, the grade of passivity film of steel bars becomes worse <sup>(3.7)</sup>. Cathodic polarization curve is related to diffusion of oxygen (O<sub>2</sub>). When the current density becomes larger, the level of O<sub>2</sub> diffusion becomes larger. For this, similar method and testing equipment in anodic polarization behavior of sacrificial point anode was used. The potential of steel bar ( $E_{corr}$ ) was shifted to +700 mV for anodic polarization curve and -700 mV for cathodic polarization curve from the natural potential with a scan speed of 1 mV/sec.

**(f) Polarization resistance of steel bar**

Contact method was conducted to measure polarization resistance of steel bar. Rebar corrosion meter (SRI-CM-III) and double counter electrode sensor with amplitude + 10 mV and frequency ranges of 10 mHz to 100 Hz were used. Set up for polarization resistance

measurement is shown in **Figure 3.7**. In addition, judgement of polarization resistance based on the value proposed by Mehta and Monteiro<sup>(3.8)</sup> as presented in **Table 3.11**.

**(g) Visual observation**

Corroded area of steel bar was measured after completely removed from the concrete specimen. Then corroded area of steel bar was calculated using software ImageJ v1.49p<sup>(3.9)</sup>. Also, corrosion of the steel bar and leaching products of sacrificial point anode in the cracked area was observed.

Table 3.10 Grade of passivated film associated with anodic polarization curve<sup>(3.7)</sup>

Grade	Polarization curve	Condition of passivity
Grade 0	Potential between 0.2 and 0.6 V (vs SCE), current density is over 100 $\mu\text{A}/\text{cm}^2$ at least one time.	No passivity exist
Grade 1	Potential between 0.2 and 0.6 V, current density between 10 to 100 $\mu\text{A}/\text{cm}^2$ .	Certain degree of passivity exist
Grade 2	Potential between 0.2 and 0.6 V, current density is over 10 $\mu\text{A}/\text{cm}^2$ at least one but not qualified to grade 1 and 3.	
Grade 3	Potential between 0.2 and 0.6 V, current density is between 1 to 10 $\mu\text{A}/\text{cm}^2$ .	
Grade 4	Potential between 0.2 and 0.6 V, current density is over 1 $\mu\text{A}/\text{cm}^2$ at least one but not qualified to grade 1, 2 and 3.	
Grade 5	Potential between 0.2 and 0.6 V, current density is less than 1 $\mu\text{A}/\text{cm}^2$ .	Excellent passivity exist

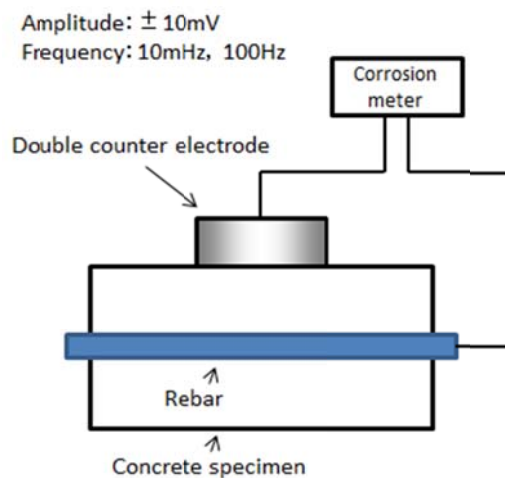


Fig 3.7 Setup for polarization resistance measurement

Table 3.11 Typical polarization resistance for steel in concrete <sup>(3.8)</sup>

Rate of corrosion	Polarization resistance $R_p$ ( $k\Omega.cm^2$ )	Corrosion penetration $p$ ( $\mu m/year$ )
Very high	$0.25 < R_p < 2.5$	$100 < p < 1000$
High	$2.5 < R_p < 25$	$10 < p < 100$
Low/moderate	$25 < R_p < 250$	$1 < p < 10$
Passive	$250 < R_p$	$P < 1$

### 3.4 Chloride Contaminated Concrete

#### 3.4.1 Half-cell potential and instant-off potential of steel bars

Half-cell potential of the steel bar without sacrificial point anode (PS) is presented in **Fig. 3.8**. During 150 days exposed in the air curing, the specimen without chloride shows that the potential of steel bar is around -120 mV. In the case of specimens with  $4 \text{ kg/m}^3$  and  $10 \text{ kg/m}^3$  of chloride, the potential of steel bars are about -250 mV. In the dry/wet cycles, it is observed that the potential of steel bar without chloride are shifted to more negative, about -300 mV. This is attributed to the effect of environmental changes, which is promote the corrosion current. In the case of  $4 \text{ kg/m}^3$  and  $10 \text{ kg/m}^3$  of chloride, the potential of steel bar closed to -450 mV and -400 mV respectively, which indicates the 90% probability of corrosion according to ASTM C 876-95 <sup>(3.4)</sup>. This is caused by the presence of water and oxygen on the steel surface during dry/wet cycles, which is accelerates the onset of corrosion.

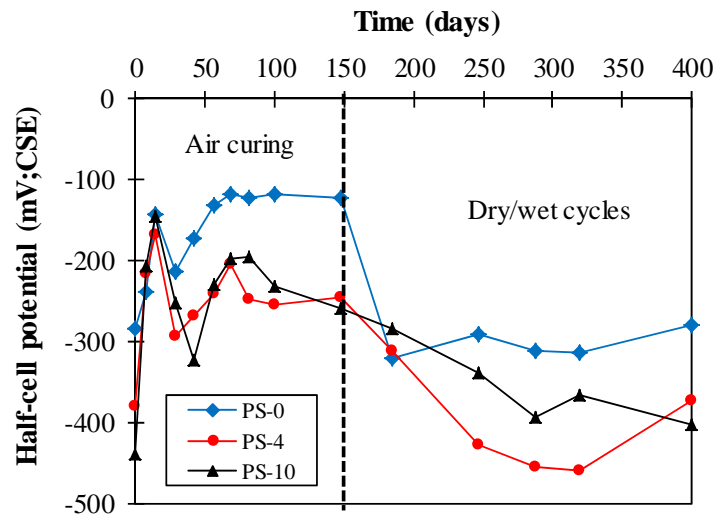


Fig. 3.8 Half-cell potential of the steel bar without sacrificial point anode (PS)

**Figure 3.9** represents the relationship between instant-off potential of steel bars with sacrificial point anode (PSCP) versus time. At the very beginning (after 24 hours connecting with the sacrificial point anode), the instant-off potential of all steel bars shift to negative values

around -950 mV. Nevertheless, after 150 days exposed in the air curing, the instant-off potential moved to noble value around -600 mV for all steel bars. As the dry/wet cycle started, it is observed that the instant-off potential value of steel bars decreased to negative values between -800 mV to -950 mV at 400 days. This implies that the sacrificial point anode reached the protective potentials less negative than -750 mV vs. CSE<sup>(3,5)</sup> in high humidity (moisture) condition. In addition, a larger protective potential was found in the specimens without chloride (0 kg/m<sup>3</sup>) even the environmental condition is changed to dry/wet cycles.

For specimen including 4 kg/m<sup>3</sup> of chloride with gap of 15 mm, no significant difference in the instant-off potential was observed than that without gap. It seems that the existence of the gap does not have any influence on the protective effectiveness.

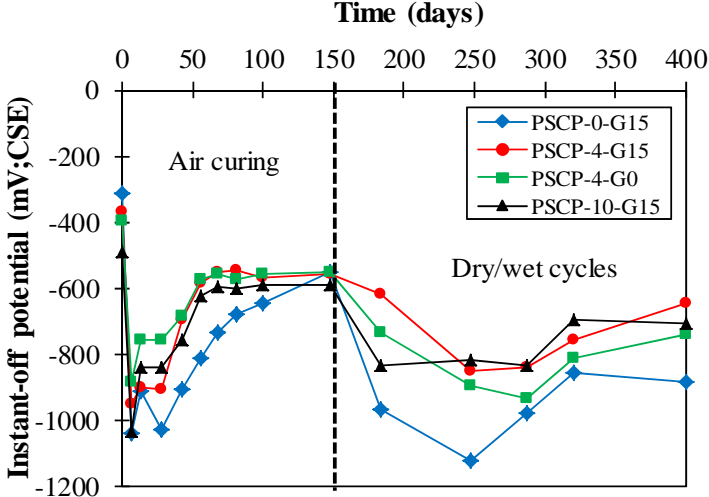


Fig. 3.9 Instant-off potential of the steel bars with sacrificial point anode (PSCP)

### 3.4.2 Instant-off potential of the sacrificial point anode

Figure 3.10 shows the instant-off potential value of the sacrificial point anode with time. At 150 days of exposure in the end of air curing, the sacrificial point anode reached potential value about -700 to -800 mV. Afterward, the specimens were exposed to dry/wet cycles. It is observed that the potential value of sacrificial point anode shifted to more negative about -1000 mV, which is similar to natural potential of Zn alloys (e.g., ~ -1000 mV). Also the specimen without chloride (0 kg/m<sup>3</sup>) achieved more negative potential value, which similar trend of the instant-off potential of steel bar.

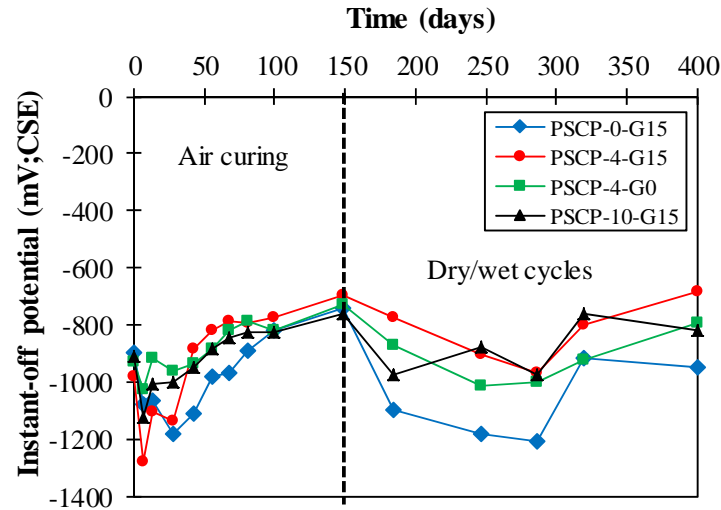


Fig. 3.10 Instant-off potential of the sacrificial point anode

### 3.4.3 Protective current of the sacrificial anode

The protective current of sacrificial point anode versus time is shown in **Fig. 3.11**. It is observed that the initial protective current is around 80 mA/m<sup>2</sup> and decreased substantially to 5 mA/m<sup>2</sup> for all specimens after 150 days exposure in the air curing. One reason may be due to the high resistivity of concrete, which decrease the current output of the sacrificial point anode to the steel bars <sup>(3.5)</sup>. On the other hand, when the specimens exposed to dry/wet cycles, it was found that the current output of sacrificial point anode shifted to higher value between 15 mA/m<sup>2</sup> to 20 mA/m<sup>2</sup>. This is caused by the high moisture condition of the concrete. Thus, the sacrificial point anode became active. These levels of protective current are within the design limits of cathodic protection between 2 - 20 mA/m<sup>2</sup> as specified in EN 12696 <sup>(3.10)</sup>.

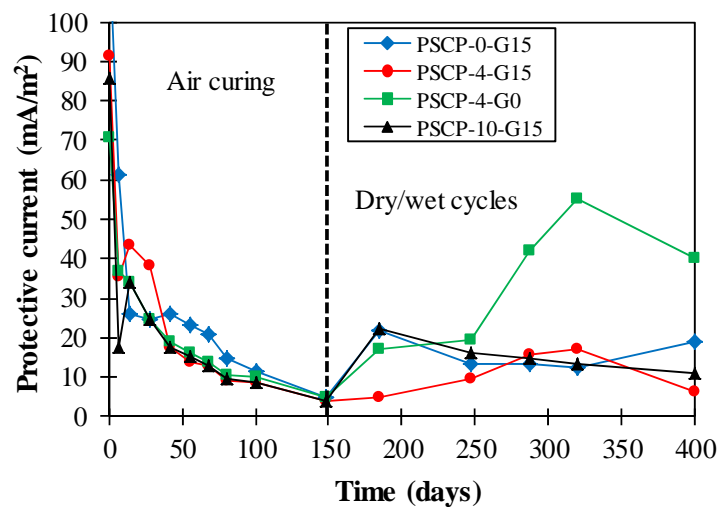


Fig. 3.11 Protective current of the sacrificial point anode

Another interesting observation is the effect of gap between steel bars and the sacrificial point anode after exposed to dry/wet cycles. It was clearly seen that the protective current of sacrificial point anode with gap shows a stable value around 10 - 20 mA/m<sup>2</sup> after 400 days exposure compare to without a gap. This indicates that the presence of the gap makes the current output of sacrificial point anode to the steel bar stable.

**3.4.4 Depolarization Tests**

Depolarization tests were regularly carried out by disconnecting the steel bars from the sacrificial point anode for 24 hours. **Figure 3.12** illustrates the depolarization value of the steel bars during exposure. Depolarization value of steel bars tends to decrease from 600 mV to 350 mV during 150 days exposed in the air curing. These behaviors were found similar to the instant-off potential of steel bars and current output of the sacrificial point anode. In the dry/wet cycles exposure, it was found that the specimen without chloride provide a larger value around 600 mV at 400 days. Meanwhile specimens 4 kg/m<sup>3</sup> and 10 kg/m<sup>3</sup> of chloride with gap of 15 mm, depolarization value was around 400 mV. For the specimen without gap in the concrete with 4 kg/m<sup>3</sup> of chloride, it was observed that the depolarization value is higher than with gap around 550 mV at 400 days. This implies that the sacrificial point anode is much effective in the high humidity condition, however, it is also effective even in the low humidity.

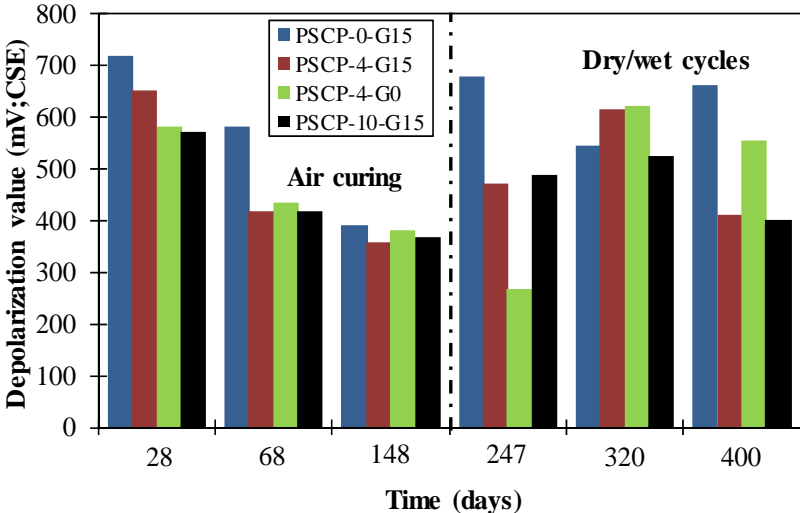


Fig. 3.12 Depolarization values of steel bars in chloride contaminated concrete

**3.4.5 Anodic Polarization behavior of the sacrificial anode**

**Figure 3.13** shows the anodic polarization behaviors of the sacrificial point anode for each exposure condition. The initial current density of the sacrificial point anode is in the range



of  $10 - 20 \mu\text{A}/\text{cm}^2$ . After 150 days in the air curing, the current densities of the sacrificial point anode significantly decreased to around  $2 \mu\text{A}/\text{cm}^2$  for all specimens.

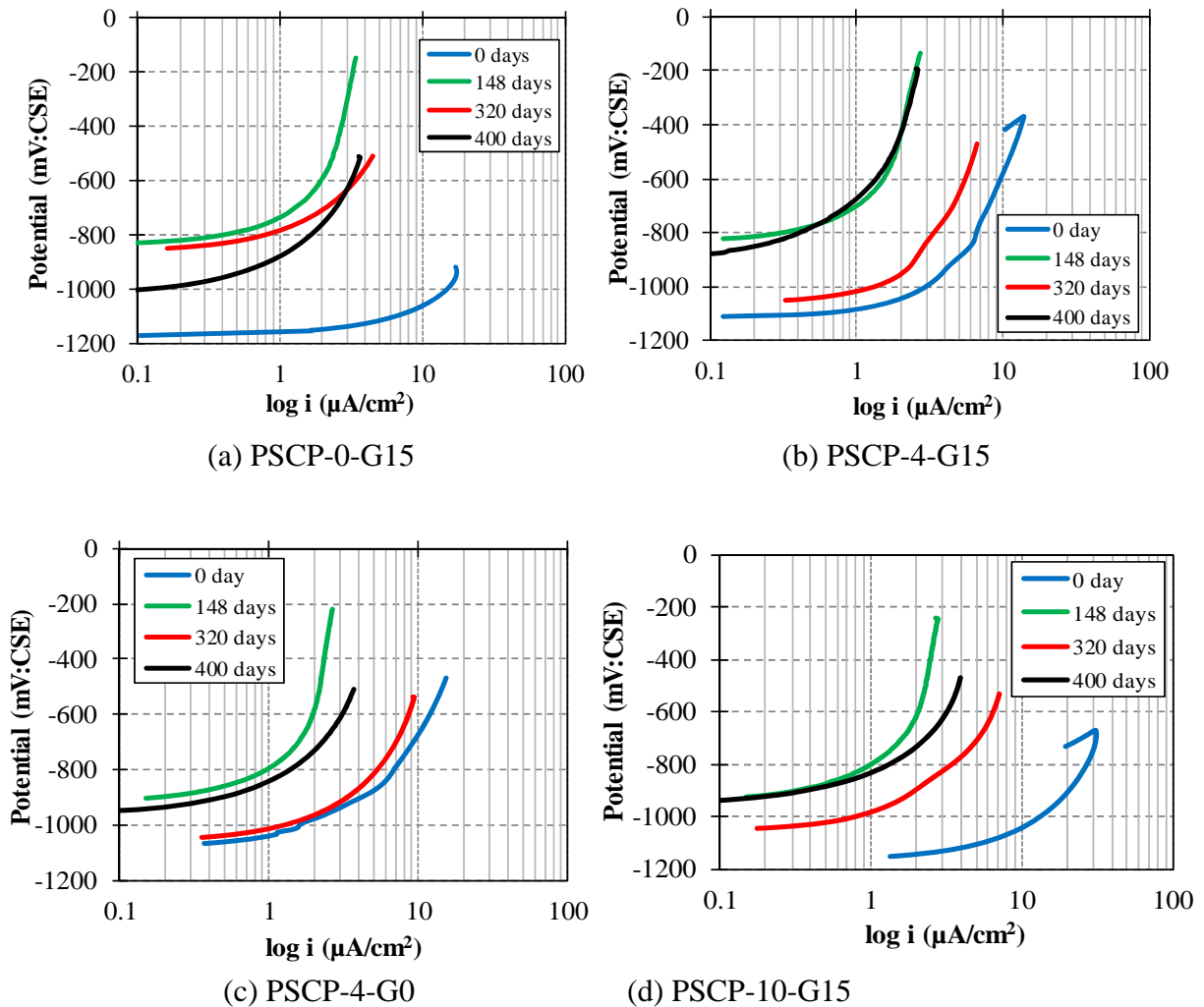


Fig. 3.13 Anodic polarization behaviors of the point anode: 0 day, 148 days (air curing); 320 days, 400 days (dry/wet cycles)

### 3.4.6 Polarization resistance and corrosion current density

Polarization resistance ( $R_p$ ) and corrosion current density ( $i_{\text{corr}}$ ) of steel bars at the end of testing are presented in **Table 3.12**. For specimens without sacrificial point anode with  $4 \text{ kg}/\text{m}^3$  and  $10 \text{ kg}/\text{m}^3$  of chloride, the  $R_p$  values is less than  $250 \text{ k}\Omega\cdot\text{cm}^2$ , which indicates the low/moderate corrosion rate <sup>(3.8)</sup>. On the other hand, specimens with sacrificial point anode show a passive corrosion rate even with chloride content of  $4 \text{ kg}/\text{m}^3$  and  $10 \text{ kg}/\text{m}^3$ . It can be said that sacrificial point anode could increase the polarization resistance of steel bars in concrete.

In the view point of the  $i_{\text{corr}}$ , it is observed that the specimens without sacrificial point anode shows values higher than  $0.1 \mu\text{A}/\text{cm}^2$ , which represent that the steel bar is active in

concrete with 4 kg/m<sup>3</sup> and 10 kg/m<sup>3</sup> of chloride. Meanwhile for specimens with sacrificial point anode shows the levels of  $i_{corr}$  below 0.1  $\mu\text{A}/\text{cm}^2$ .

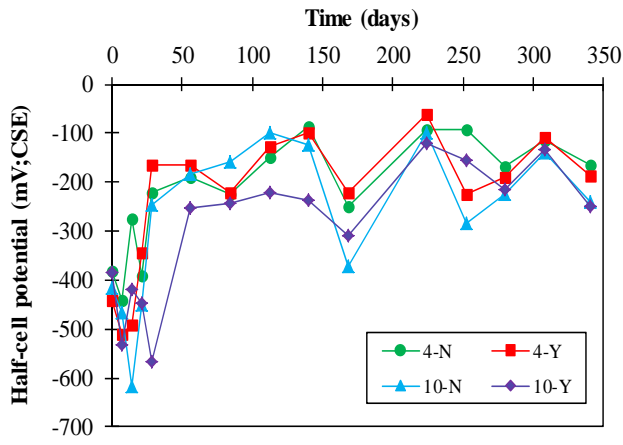
Table 3.12 Polarization resistance and corrosion rate of steel bars at 400 days

Specimen	Polarization resistance (k $\Omega$ .cm <sup>2</sup> )	Corrosion current density ( $\mu\text{A}/\text{cm}^2$ )	Corrosion penetration ( $\mu\text{m}/\text{year}$ )	Rate of corrosion
PS-0	365	0.086	0.79	Passive
PS-4	241	0.127	0.94	Low/moderate
PS-10	222	0.173	1.02	Low/moderate
PSCP-0-G15	701	0.037	0.43	Passive
PSCP-4-G15	896	0.029	0.34	Passive
PSCP-4-G0	972	0.017	0.31	Passive
PSCP-10-G15	408	0.061	0.74	Passive

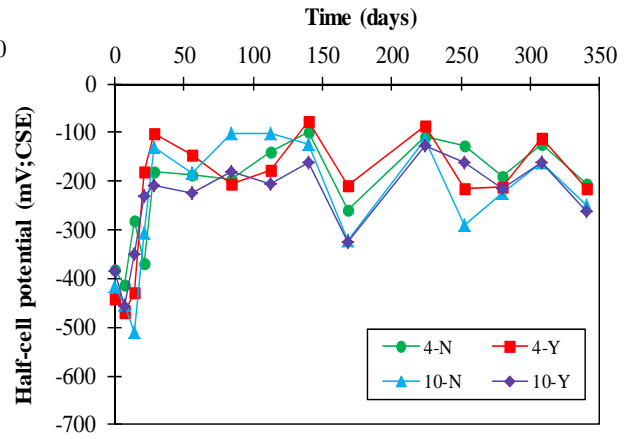
### 3.5 Repaired Concrete

#### 3.5.1 Half-cell potential and on-potential of steel bars

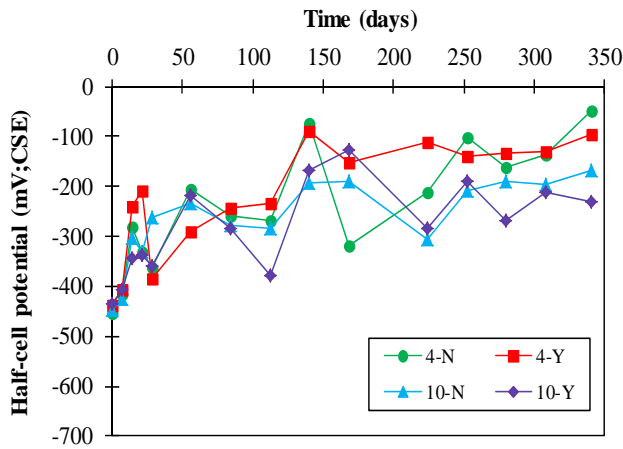
Time dependent changes in half-cell potential of plain steel bar (PS) are illustrated in **Fig. 3.14**. In N53.5, PS in RPC which contained 4 kg/m<sup>3</sup> of chloride with and without epoxy materials shows the potential value about -200 mV. By adding 10 kg/m<sup>3</sup> of chloride, PS shows the potential value around -275 mV in both specimens with and without epoxy materials. While the potential value of PS in N40 becomes more positive than N53.5, both specimens contained 4 kg/m<sup>3</sup> and 10 kg/m<sup>3</sup>. It indicates that the lower W/C ratio have a good resistance against penetration of chloride ions into repaired concrete. On the other hand, the half-cell potential value of PS in BB40 becomes more positive than N53.5 and N40. It seems that replacement of cement with 50% BFS significantly helps to prevent corrosion activity in repaired concrete. Further, specimens with epoxy materials showed no significant different in potential value than without epoxy materials. It indicates that the addition of epoxy materials does not influence to minimize the corrosion activity in RPC.



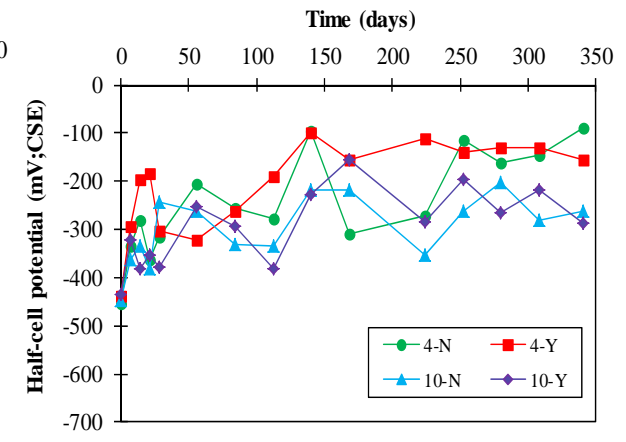
(a). Repaired concrete N53.5



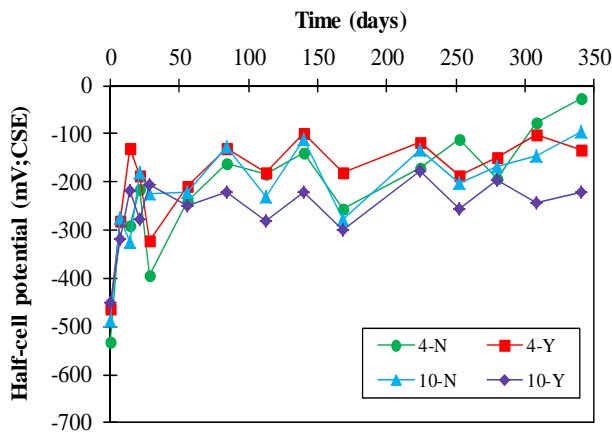
(b). Existing concrete N53.5



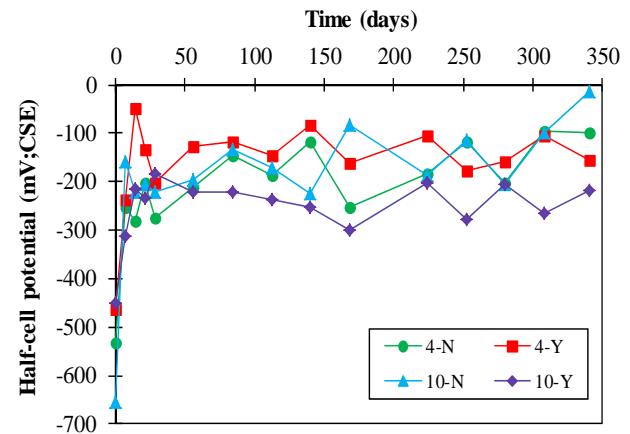
(c). Repaired concrete N40



(d). Existing concrete N40



(e). Repaired concrete BB40



(f). Existing concrete BB40

Fig. 3.14 Half-cell potential of PS with time

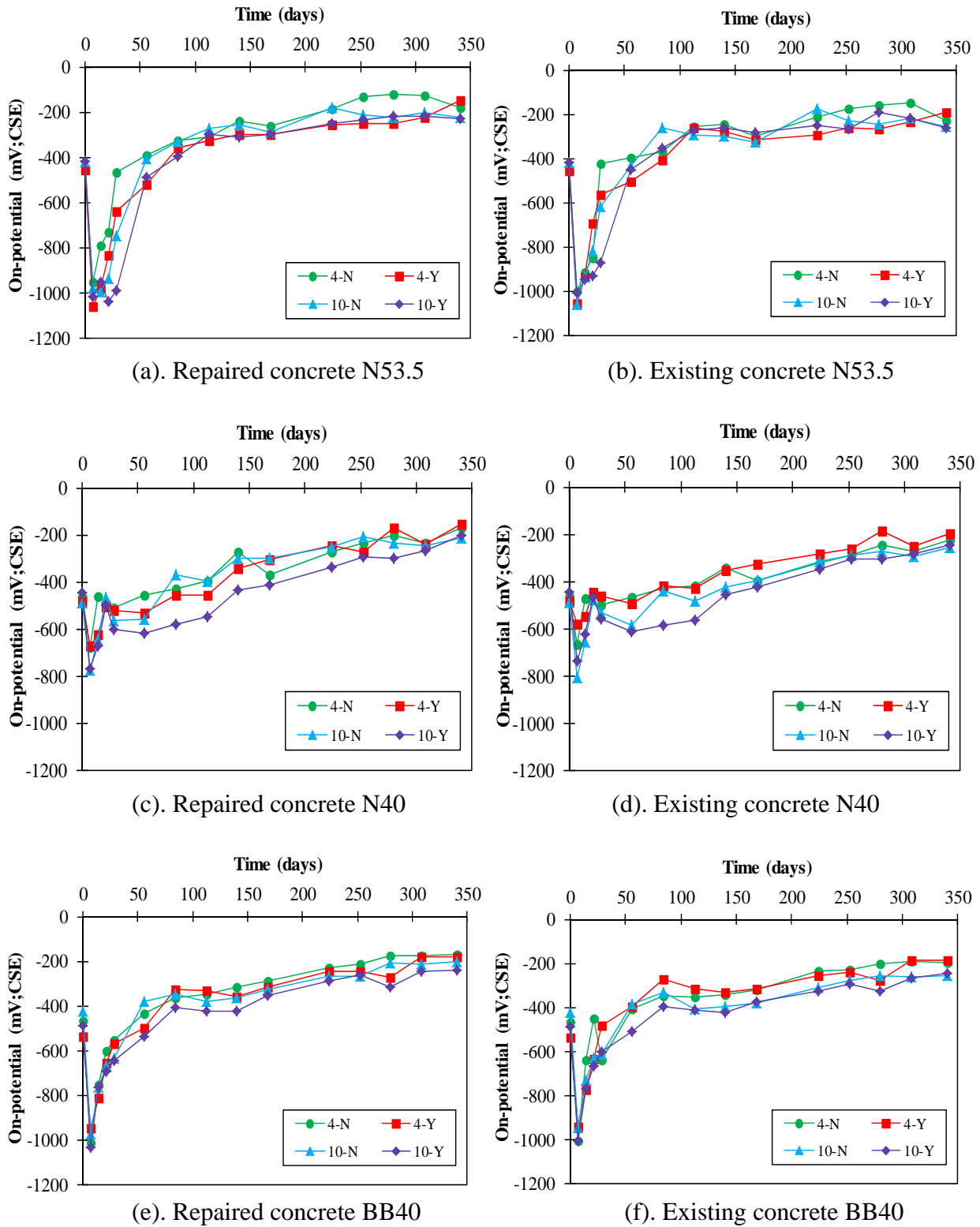


Fig. 3.15 On-potential of PSCP with time

**Figure 3.15** shows the on-potential values of plain steel bar with point anode (PSCP). It is shown that the point anode active at an early age and reached potential value around  $-1000$  mV for N53.5 and BB40. While for N40, it was found that the potential value is higher than in

N53.5 and BB40, which was around -800 mV. This potential difference at the early age may be due to high resistivity of concrete in N40. However, after 100 days the potential shifted to noble value about -250 mV both RPC and EC for all mix concrete. This behavior was also observed in concrete contained chloride exposed in the air curing. It is might be due to low humidity inside concrete, thus the point anodes hardly to active. Even though the potential value is decreased, it was observed that the potential of steel bars on the stable condition with time. It indicates that the steel bar is under protected condition. These results were confirmed by visual observation of steel bars at the end of testing that is no corrosion appearance in the repaired concrete (RPC).

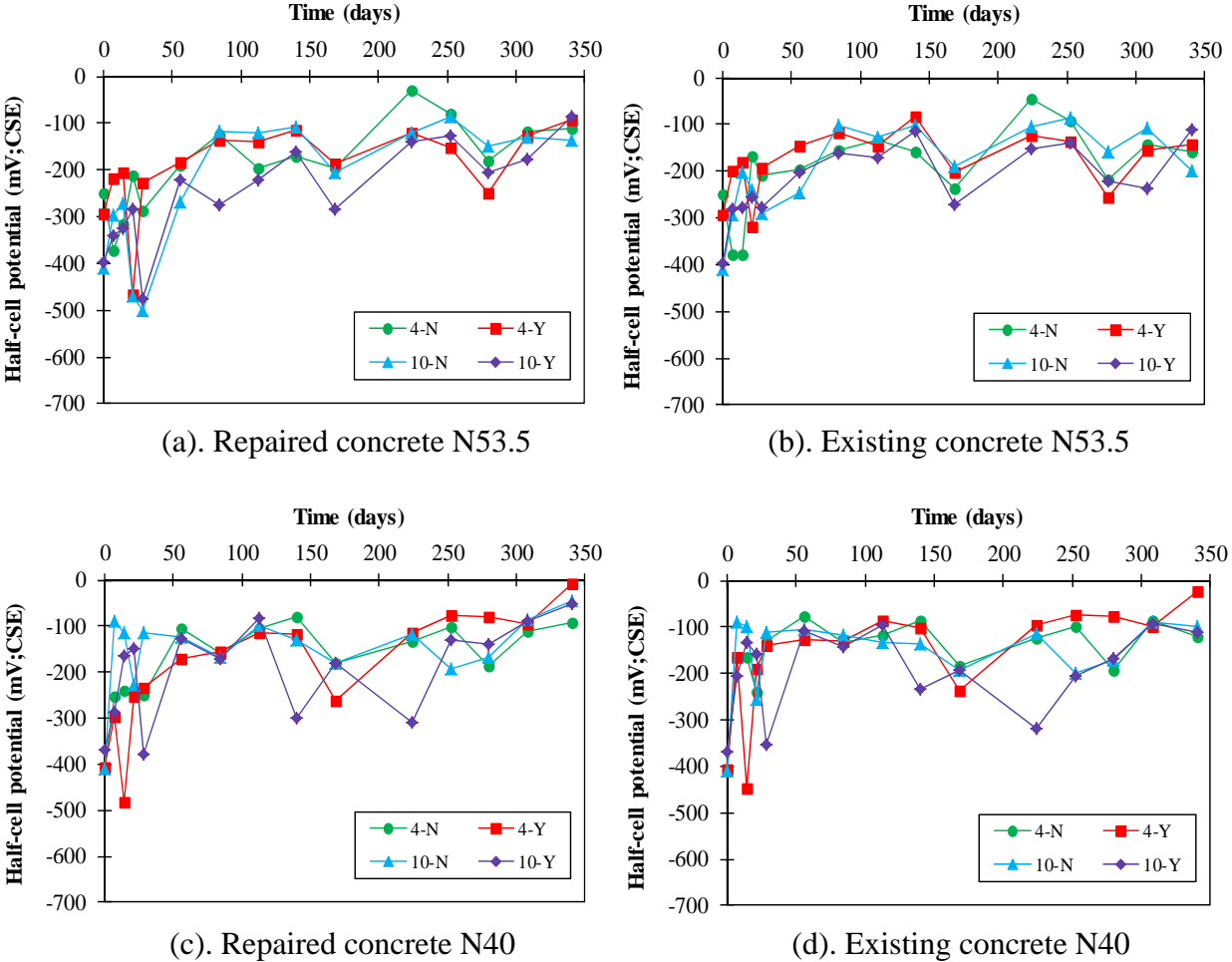


Fig. 3.16 Half-cell potential of PSE with time

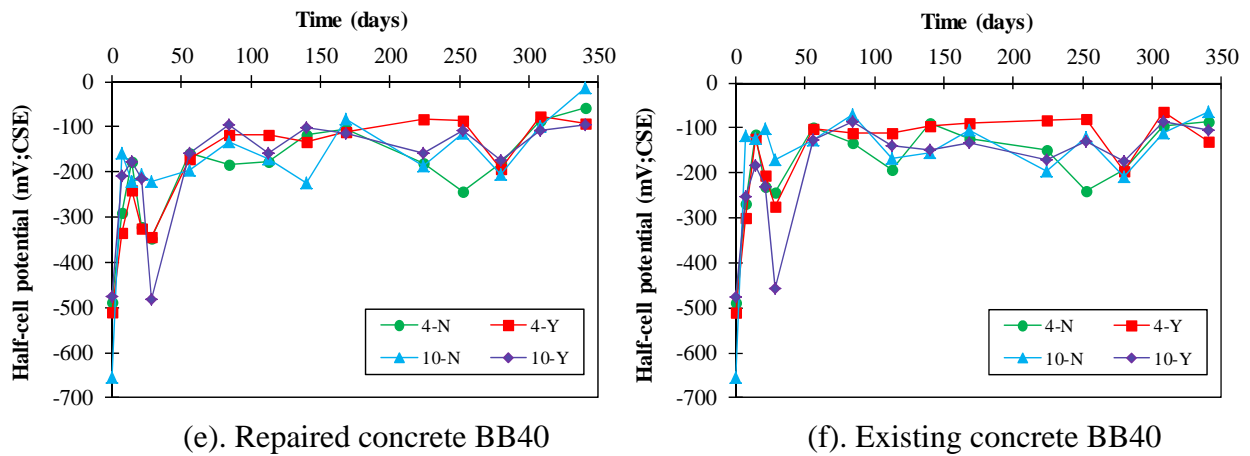


Fig. 3.16 (Continued) Half-cell potential of PSE with time

**Fig 3.16** shows the half-cell potential values of epoxy coated steel bar (PSE) versus time. PSE reached the potential value more positive than PS. The value with 4 kg/m<sup>3</sup> of chloride shows the potential around -120 mV with and without epoxy materials. While concrete with 10 kg/m<sup>3</sup> of chloride shows the potential value about -170 mV with and without epoxy materials. This implies that PSE provided excellent corrosion protection and delayed the onset of corrosion in repaired concrete than PS.

### 3.5.2 Depolarization tests

At the end of tests, three specimens with 10 kg/m<sup>3</sup> of chloride without epoxy materials (N53.5-N-10, N40-N-10 and BB40-N-10) were open, and the point anodes removed from steel bars. **Table 3.13** shows the rest potential and depolarization values after 24 hours, taken in the repaired section. It was observed that the depolarization value for all steel bars less than 300 mV. It is due to the low humidity condition, which decrease the protective potential of the point anode. Nevertheless, the rest potential values of the steel bars around -200 mV, which indicates that 90% no corrosion probability per ASTM C876-95<sup>(3,4)</sup>. In addition, the natural potential of the point anode still in the higher value about -850 mV vs. CSE as shown in **Fig. 3.17**.

Table 3.13 The rest potential and depolarization values

Specimen	On-potential (mV;CSE)	Rest potential (mV;CSE)	Depolarization (mV;CSE)
N53.5-N-10	-252	-224	28
N40-N-10	-334	-257	77
BB40-N-10	-297	-253	44

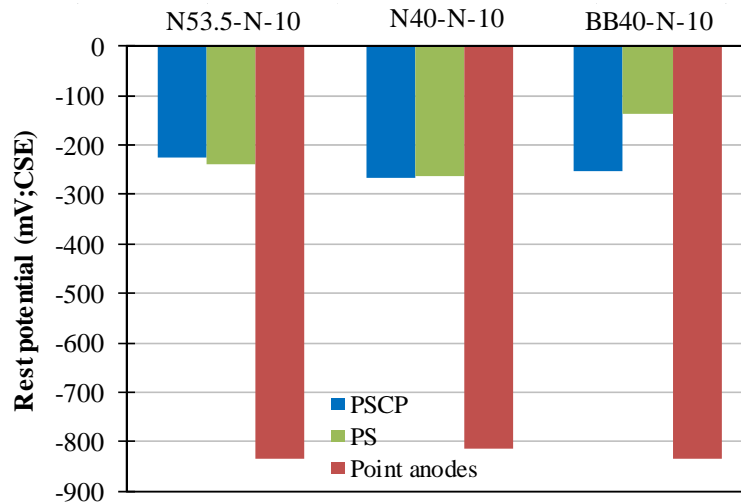


Fig. 3.17 Rest potential of the steel bars and the sacrificial point anode at the end of tests

### 3.5.3 Polarization behavior of the sacrificial point anode

Figure 3.18 shows the polarization behavior of point anode after removing from the steel bars. It was found that the current density of the point anode around  $4 \mu\text{A}/\text{cm}^2$ ,  $7 \mu\text{A}/\text{cm}^2$  and  $8 \mu\text{A}/\text{cm}^2$  for N53.5, BB40 and N40 respectively. Comparing with the initial current density obtained in concrete contained chloride (specimen with  $10 \text{ kg}/\text{m}^3$  of chloride), the protective effectiveness decreased after one year exposed in the air curing (T:  $20 \pm 2^\circ\text{C}$ , RH: 60%). It is due to the low humidity of the concrete thus the sacrificial point anode hardly to be active to protect the steel bars.

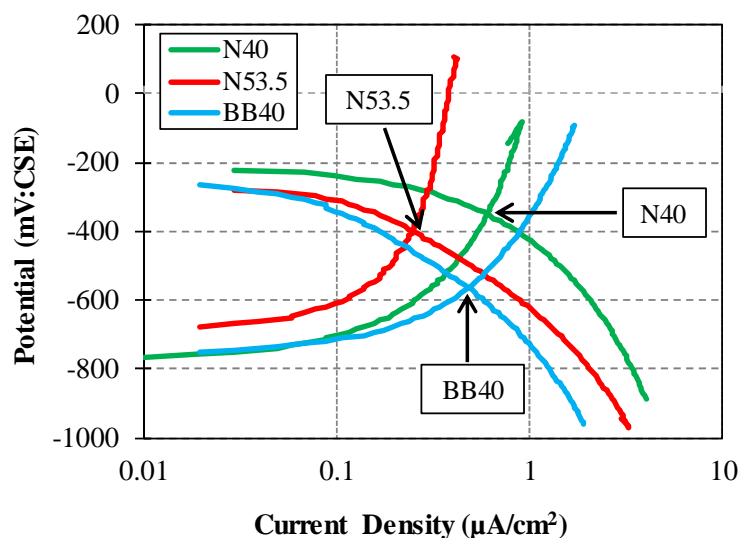


Fig. 3.18 Polarization behavior of the sacrificial point anode

### 3.5.4 Anodic-cathodic polarization curve of steel bars

Anodic-cathodic polarization curve of steel bars is presented in **Fig. 3.19**. Except N40, it is observed that no significant different in anodic-cathodic polarization curve between PSCP and PS for all mixed concrete. It means that the point anodes does not affected on the anodic-cathodic polarization curve of steel bars exposed in the air curing.

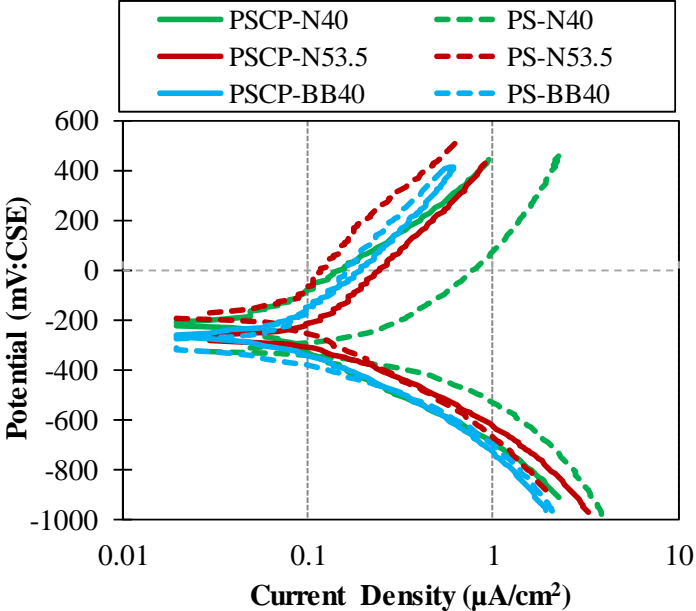


Fig. 3.19 Anodic-cathodic polarization curve of PS and PSCP

### 3.5.5 Visual observation

**Figure 3.20** shows results of visual examined of the steel bars. It was observed that PS for N53.5 exhibits larger corrosion area than N40 and BB40 in repaired concrete. It seems that the lower W/C ratio gave influence in preventing corrosion activity in RPC. Also, replacement of cement by 50% BFS showed a good condition. On the other hand, it is clearly seen that PSCP showed no corrosion appearance in RPC in all mixed concrete. The results indicate that the sacrificial point anode can delay anodic reactions in RPC even if the protective potential slightly shifted to noble potential during exposure periods. In addition, it was also observed that PSE show a good resistance against corrosion.



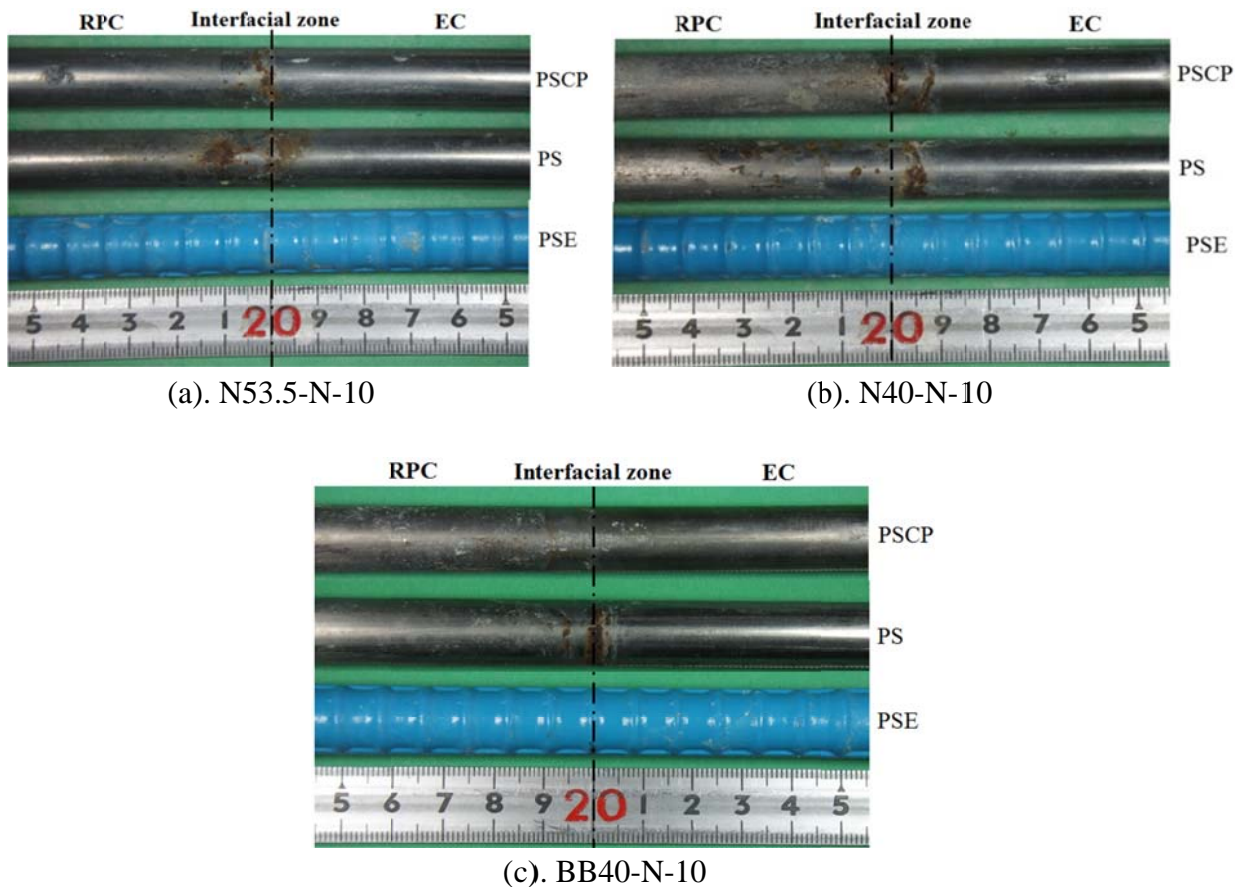


Fig. 3.20 Visual observation of the steel bars (repaired concrete)

### 3.6 Cracked Concrete

#### 3.6.1 Half-cell potential and on-potential of steel bars

The half-cell potential of PS under different exposure condition is shown in **Fig. 3.21**. It was observed that the potential value of PS in air curing was about -250 mV for all crack width until 50 days as presented in **Fig. 3.21a**. However, the half-cell potential value became more positive around -150 mV from 50 to 150 days exposure. It is found that the relationship between potential value and crack width at the early age is existed and changed by time because the steel bars remain passive condition. After 150 days exposure, it was observed that the potential of PS shifts to negative values between -200 mV to -270 mV for all crack width and categorized uncertain probability of corrosion.

**Figure 3.21b** shows the half-cell potential of PS immersed in 3% NaCl solution. It is found that the potential value becomes more positive to -100 mV for crack width 0.21 mm up to 300 days exposure. Nevertheless, it is obvious that the potential of PS falls to -350 mV after 530 days exposure for crack width of 0.21 mm. This is caused by the amount of oxygen and chloride ions are sufficient to accelerate the corrosion of steel bar. On the other hand, for

specimen whose crack width of 0.32 mm, it is evidenced that, after 50 days exposure the potential value of PS falls to -450 mV and categorized the 90% probability of corrosion. It indicates that crack width affect the corrosion rate.

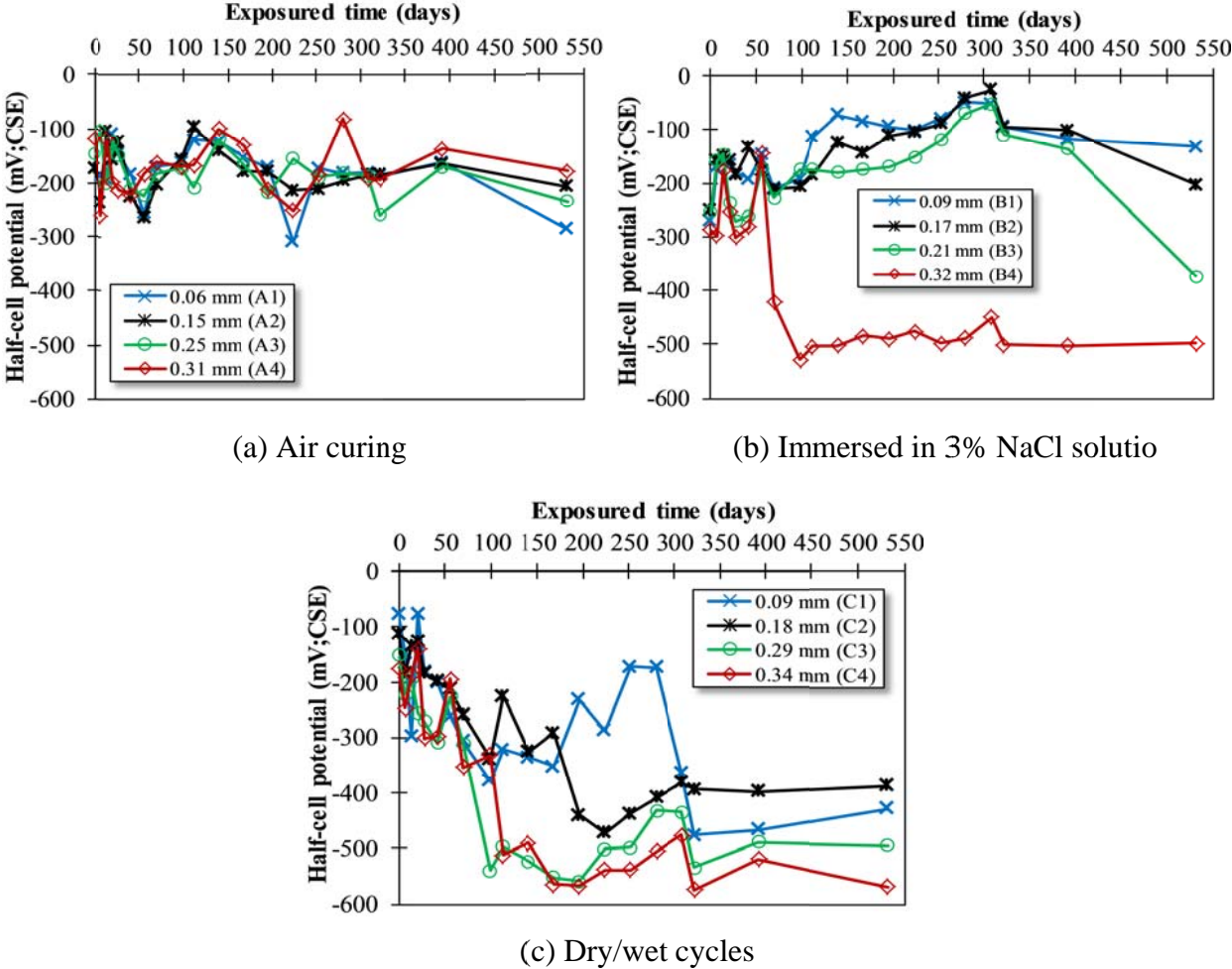


Fig. 3.21 Half-cell potential of PS at cracked area: (a) air curing; (b) immersed in 3% NaCl solution; (c) dry/wet cycles.

The half-cell potential value of PS under dry/wet cycles is shown in **Fig. 3.21c**. It shows that crack width less than 0.10 mm reached the potential value around -250 mV at early age and relationship between crack width and potential value changed to more positive value with time. However, after 350 days the potential values shifts to -450 mV and categorized of 90% of corrosion probability. It implies that the chloride ions and oxygen can reach the surface of steel bars after certain period. While for specimen whose crack width is larger than 0.10 mm, it is observed that the potential value shifts to the 90% of corrosion probability at 90, 100 and 320 days for crack width of 0.34 mm, 0.29 mm and 0.18 mm respectively. This is attributed to the effect of crack which permitted easy access of chloride ions and oxygen to the steel bars and

accelerated the onset of corrosion. The results indicate that the relationship between crack width and corrosion rate is existed due to the environmental condition.

**Figure 3.22a** shows the on-potential value of PSCP exposed in the air curing. It is observed that potential value of PSCP reached to about -550 mV at the initial stage, and moved to noble value around -300 mV after 530 days exposure. This may be due to the increasing of resistivity of concrete with time, which decreases the current flow of the sacrificial point anode to the steel bar. Although the protective potential of steel bar changes to noble value with time, however, the potential of steel bars are in a stable condition. It means that the steel bar is protected. This result is confirmed by visual observation of steel bar at the end of test periods.

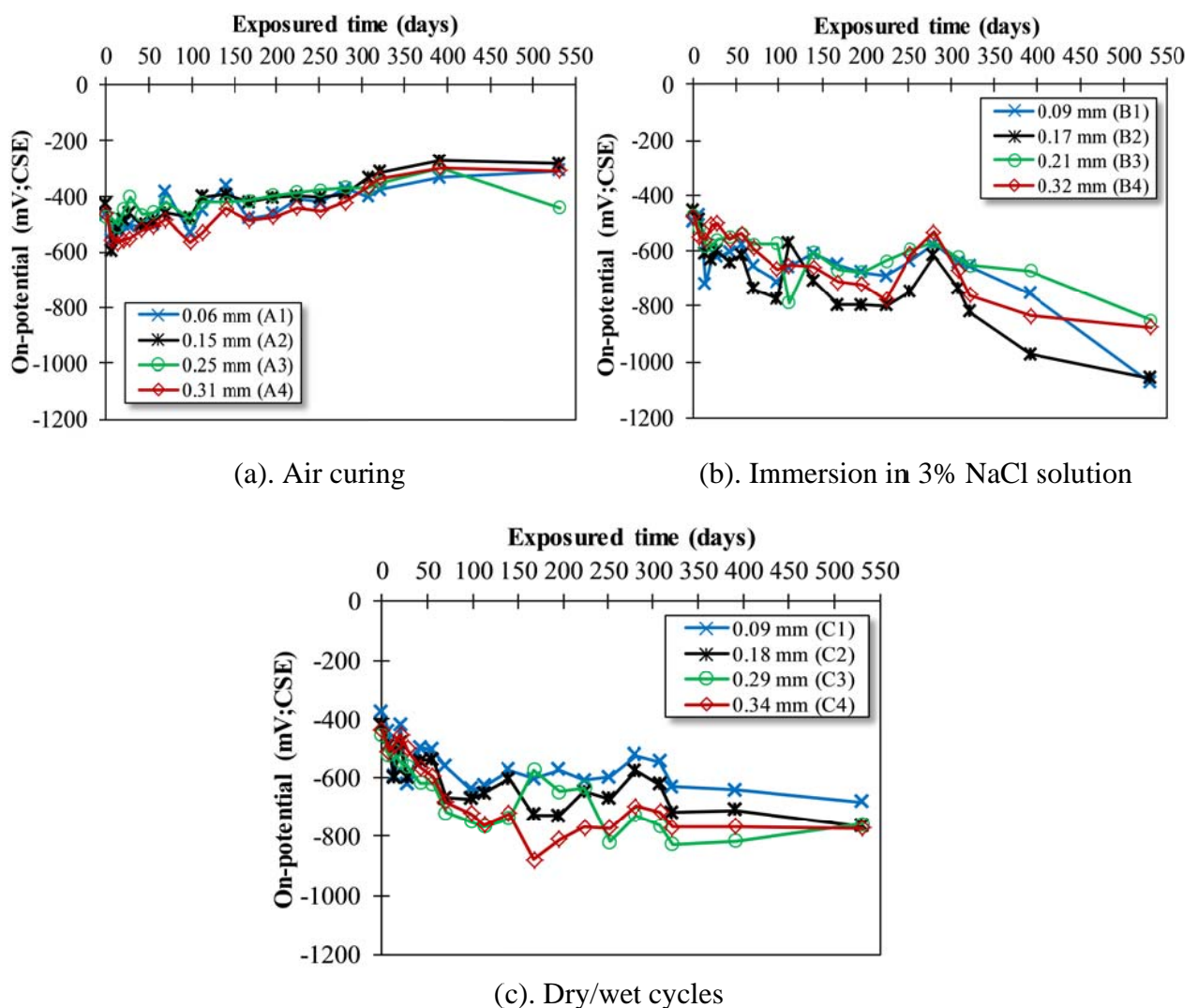


Fig. 3.22 On-potential of PSCP at cracked area: (a) air curing; (b) immersed in 3% NaCl solution; (c) dry/wet cycles

The on-potential of PSCP immersed in 3% NaCl solution is presented in **Fig. 3.22b**. It is found that the potential value of PSCP is around -800 mV to -1000 mV, which satisfies the

protective potential (lower than -750 mV vs. CSE) for all crack width at 530 days exposure. It is due to the presence of water in concrete pores, thereby reducing the resistivity of concrete. From **Fig. 3.22c**, it can be observed that for crack width of 0.09 mm, PSCP under dry/wet cycles showed the on-potential about -650 mV. Meanwhile, specimens whose crack width of 0.18 mm, 0.29 mm and 0.34 mm are presented similar protective potential of steel bar around -750 mV. From these results, it can be concluded that the sacrificial point anode is more effective in the high moisture condition even in the larger crack width of 0.30 mm.

**3.6.2 Depolarization tests**

Specimens whose crack width is larger than 0.30 mm were investigated 24 hours after removing the point anode from the steel bar. Depolarization values of PSCP are presented in **Table 3.14**. The result shows that the depolarization value of the specimen exposed in the air curing is smallest. While for specimens exposed in dry/wet cycles and immersed in 3% NaCl solution, the depolarization values were achieved 687 mV and 532 mV respectively.

Table 3.14 The rest potential and depolarization value of PSCP at the end of test

Exposure condition	On-potential (mV;CSE)	Rest potential (mV;CSE)	Depolarization value (mV)
Air curing	-347	-208	139
Immersed in 3% NaCl	-930	-243	687
Dry/wet cycles	-874	-342	532

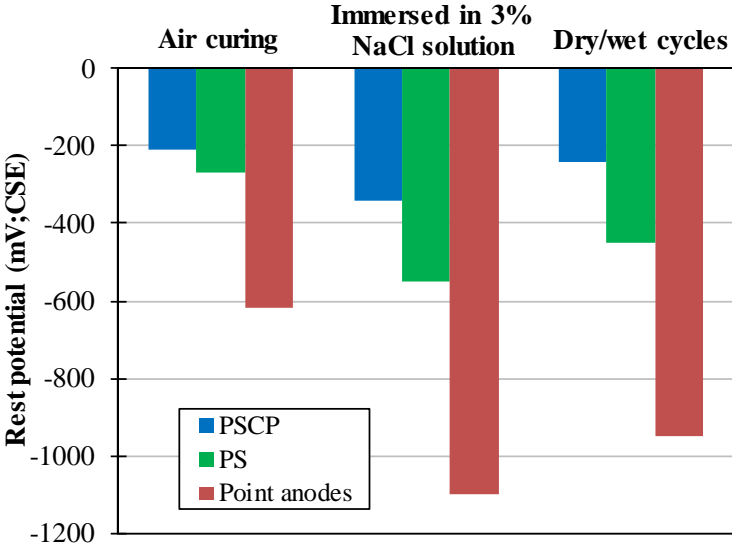


Fig. 3.23 The rest potential of steel bars and sacrificial point anodes (crack width: 0.31mm, 0.32mm, and 0.34mm)

The rest potential of steel bars and sacrificial point anode of specimen whose crack width is 0.31mm, 0.32 mm and 0.34 mm are shown in **Fig. 3.23**. It is found that PS shows the rest potential lower than -350 mV, while PSCP shows the value between -220 mV to -340 mV under dry/wet cycles and immersed in 3% NaCl solution. It indicates that sacrificial point anode could be effective to prevent steel corrosion in the presence of crack. In addition, it was also observed that the rest potential of sacrificial point anode under dry/wet cycles and immersed in 3% NaCl solution is about -1000 mV vs. CSE, which is similar to natural potential value of Zn alloys<sup>(3.11)</sup>. It means that the protective criteria is changed due to the environmental condition.

**3.6.3 Polarization behavior of the sacrificial anode**

The polarization behavior of the sacrificial point anode at the end of tests for crack width of 0.31 mm, 0.32 mm and 0.34 mm is shown in **Fig. 3.24**. It is clear that specimens exposed in dry/wet cycles and immersed in 3% NaCl solution is provided large current density about 3  $\mu\text{A}/\text{cm}^2$  and 4  $\mu\text{A}/\text{cm}^2$  respectively. On the other hand, the specimen in the air curing provided smaller current density of 0.3  $\mu\text{A}/\text{cm}^2$ . This difference may be caused by the moisture content inside concrete. High moisture content make the sacrificial point anode more active to provide larger current protect.

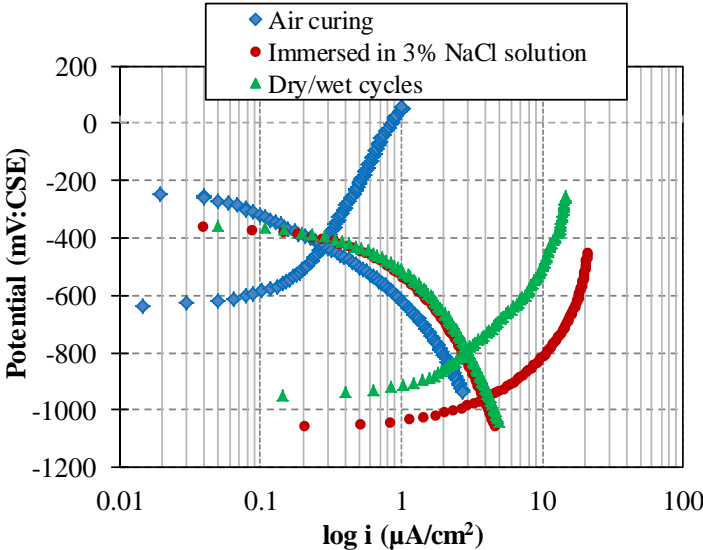


Fig. 3.24 Anodic polarization behavior of the sacrificial point anode and cathodic polarization curve of steel bar

As reported by previous studies<sup>(3.12), (3.13)</sup>, current density of 0.2  $\mu\text{A}/\text{cm}^2$  is sufficient for cathodic prevention before corrosion initiation. From the test results, the current densities of

all sacrificial point anodes are still over the range of cathodic prevention for all exposure conditions after 530 days.

### 3.6.4 Anodic-cathodic polarization curve

Figure 3.25 shows anodic-cathodic polarization curve of specimens for crack width of 0.31 mm, 0.32 mm and 0.34 mm at 530 days exposure. Based on the grade of the passivity film of steel bar proposed by Otsuki (3.7), the passivity of steel bars was Grade 4 (good condition) both PSCP and PS in air curing. For specimen immersed in 3% NaCl solution, it is observed that PS is categorized into Grade 3 (worse condition), and PSCP in Grade 4 (good condition). On the other hand, conditions of PSCP and PS under dry/wet cycles categorized into Grade 4 (good condition) and Grade 3 (worse condition) respectively. This indicates that the passivity of PS becomes worse both in dry/wet cycles and immersed in 3% NaCl solution, and it was confirmed by visual observation of steel bars after removing from concrete specimens. Compared to the anodic polarization behavior, the difference in cathodic behavior is small in all exposure conditions. It can be said that the environmental condition greatly affect the grade passivity of steel bar.

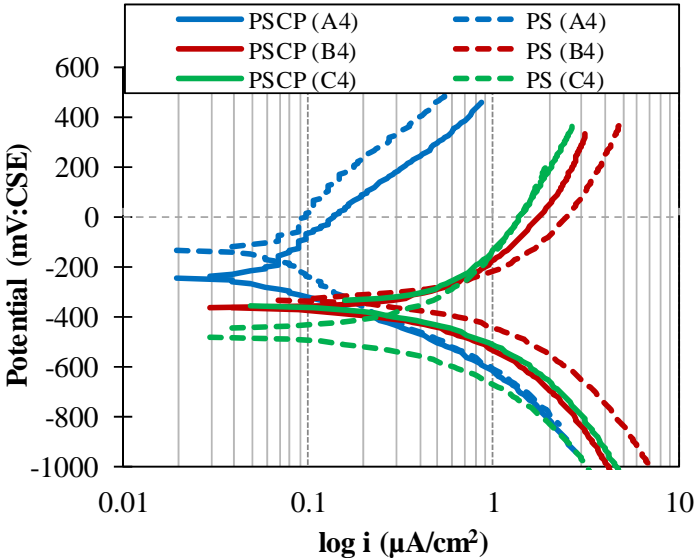


Fig. 3.25 Anodic-cathodic polarization curve (crack width: 0.31mm, 0.32mm, 0.34mm) at 530 days

### 3.6.5 Visual observation and corrosion area

For specimens exposed in dry/wet cycles and immersed in 3% NaCl solution, rust products from PS were observed along the crack (Fig. 3.26). It indicates that the passivity film of steel bar is damaged and corrosion was already initiated. While for PSCP exposed in dry/wet



cycles, the leaching product from the inside anode were found at the bottom surface of the specimen along the crack, which may decrease the performance of sacrificial point anode for long-term exposure <sup>(3.5). (3.11)</sup>. Also, it was confirmed by visual observation of PSCP in dry/wet cycles that a little pitting corrosion is existed on the steel surface.

From the visual observation of steel bars as shown in **Fig. 3.27**, it is found that corrosion occurred in the cracked area of specimens (microcell corrosion) for PS exposed in dry/wet cycles and immersed in 3% NaCl solution. Also, the passivity film of steel bars was broken due to the increasing of black colored corrosion product. Meanwhile, it was observed that PSCP shows a better condition than PS for both exposed in dry/wet cycles and immersed in 3% NaCl solution. This indicates that point anode can prevent the microcell corrosion in cracked area although the chloride ions and oxygen are available on the steel surface through the crack.

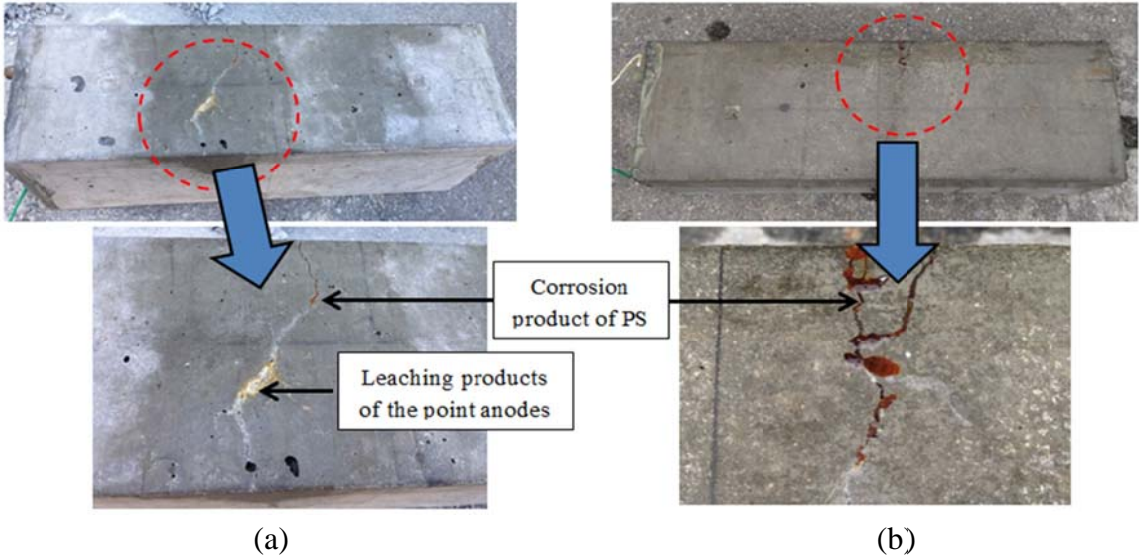


Fig. 3.26 Corrosion and leaching products at the cracked area: (a) dry/wet cycles; (b) immersed in 3% NaCl solution.

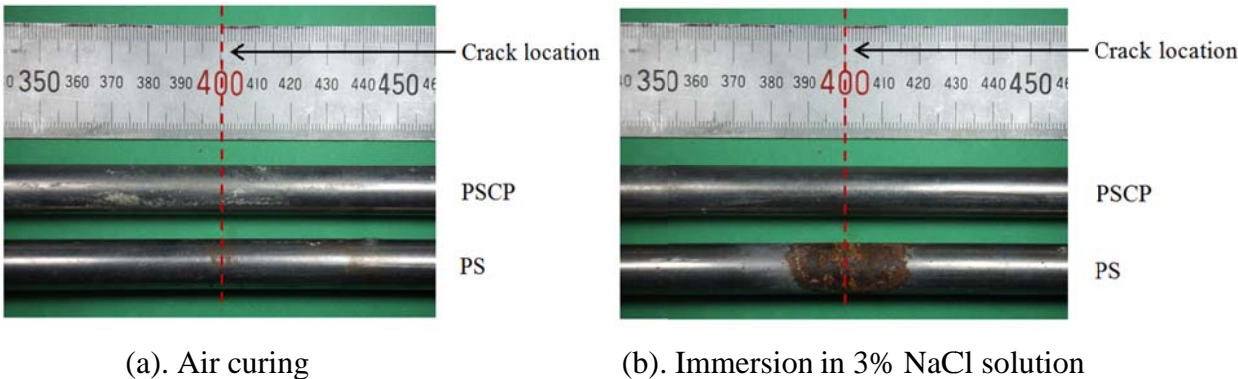


Fig. 3.27 Corrosion appearances of steel bars



(c). Dry/wet cycles

Fig. 3.27 (Continued) Corrosion appearances of steel bars

The condition of the sacrificial point anode after removing from the concrete specimen are shown in **Fig. 3.28**. A little corrosion product in PSCP under dry/wet cycles are found. This is probably derived from expansive oxide or hydroxide of zinc as a corrosion product of sacrificial point anode <sup>(3.11)</sup>.



(a). Air curing



(b). Immersed in 3% NaCl solution



(c) Dry/wet cycles

Fig. 3.28 Condition of the sacrificial point anode after removing from concrete specimen:

(a) air curing; (b) immersed in 3% NaCl solution; (c) dry/wet cycles



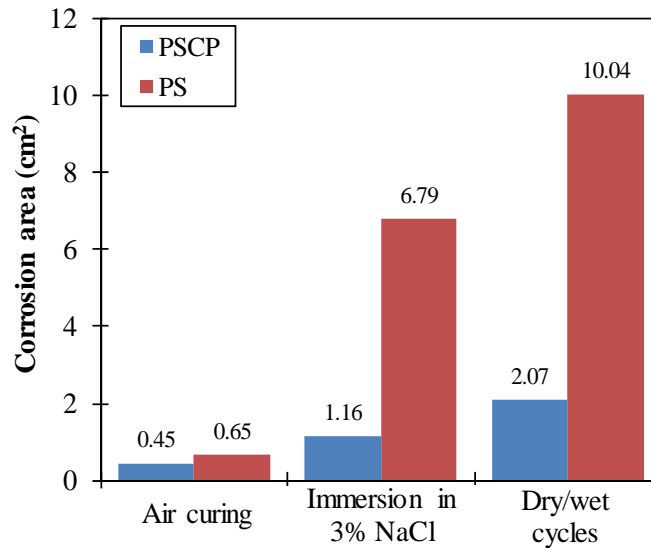


Fig. 3.29 Total corroded area of the steel bars (crack width: 0.31 mm, 0.32 mm, 0.34 mm)

The corroded area of steel bars for crack width, 0.31 mm, 0.32 mm and 0.34 mm is shown in **Fig. 3.29**. The result shows that the specimen exposed in the air curing had a corroded area of 0.45 cm<sup>2</sup> and 0.65 cm<sup>2</sup> for PSCP and PS respectively. This was significantly lower than the average corroded area for the specimens exposed in dry/wet cycles and immersed in 3% NaCl solution. The specimen immersed in 3% NaCl solution showed an average corroded area of 1.16 cm<sup>2</sup> and 6.79 cm<sup>2</sup> for PSCP and PS respectively. While specimens exposed in dry/wet cycles, PSCP had 2.07 cm<sup>2</sup> of corroded area and 10.04 cm<sup>2</sup> for PS. Compared to PSCP, it is found that PS shows 5 times larger of corroded area than PSCP for both exposed in dry/wet cycles and immersed in 3% NaCl solution.

#### 4. Conclusions

This study has presented the effectiveness of commercially available sacrificial point anode for corrosion prevention of steel bar under various application namely chloride contaminated chloride, repaired concrete and cracked concrete. The following conclusions can be drawn from this study:

1. Sacrificial point anode has presented a better protection and could achieve the protective potential less -750 mV vs. CSE under dry/wet cycles and immersed in 3% NaCl solution due to the presence of water in the concrete pores, which increases the humidity of concrete.

2. In the air curing, although the protective potential of steel bars changes to noble value during exposure, the potential of steel bars are in a stable condition, which indicates that the steel bars are under protected condition.
3. The levels of depolarization value showed more than 100 mV for both dry/wet cycles and immersed in 3% NaCl solution reveals the effectiveness of this sacrificial point anode.
4. A stable value of protective current is found in the specimen with gap of 15 mm between steel bar and sacrificial point anode.
5. The visual observation showed that the sacrificial point anode is successfully prevents microcell and macrocell corrosion of steel bar in the presence of chloride ions in concrete.
6. The leaching product from the point anode may decrease the performance of sacrificial point anode in long-term exposure.
7. The results from this study suggest that this type of sacrificial point anode is effective to increase the resistance of steel bar from corrosion initiation caused by chloride ions.

## References

- 3.1 Tabatabai, H., et al. "Laboratory Evaluation of Select Methods of Corrosion Prevention in Reinforced Concrete Bridges," *International Journal of Concrete Structures and Materials*, 8(3), 2014, pp. 201-212.
- 3.2 Qian, S., et al, "Theoretical and Experimental Study of Microcell and Macrocell corrosion in Patch Repairs of Concrete Structures." *Cement and Concrete Composites*, 28, 2006, pp. 685-695.
- 3.3 Takewaka, K., "Cathodic Protection for Reinforced Concrete and Prestressed Concrete Structures," *Corrosion Science*, Vol. 35, 1993, pp. 1617-1626.
- 3.4 ASTM C 876-95, "Standard Test Method for Half-cell Potentials of Uncoated Reinforcing Steel in Concrete," Philadelphia: American Society of Testing and Materials, 1999.
- 3.5 Rincon, O. T., et al, "Environmental Influence on Point Anode Performance in Reinforced Concrete," *Construction and Building Materials*, 22, 2008, pp. 494-503.
- 3.6 Concrete Library 107, "Recommendation for Design and Construction of Electrochemical Corrosion Control Method," Tokyo: Japan Society of Civil Engineers, 2011, pp. 67-68.
- 3.7 Otsuki, N., "A Study of Effectiveness of Chloride on Corrosion of Steel Bar in Concrete," Report of Port and Harbor Research Institute (PHRI), Japan, 1985, 127-134.
- 3.8 Mehta, P. K. and Monteiro, P. J. M., "Concrete: Microstructure, Properties and Materials," 3<sup>rd</sup> Ed. New York: Mc Graw Hill, 2006.
- 3.9 <http://imagej.nih.gov/ij/>
- 3.10 EN 12696, "Cathodic Protection of Steel in Concrete," European Standard, 2000.
- 3.11 Dugarte, M. J. and Sagues, A. A., "Sacrificial Point Anode for Cathodic Prevention of Reinforcing Steel in Concrete Repairs: Part 1 – Polarization Behavior," *Corrosion*, NACE International, Houston, 70(3), 2014, pp. 303-317.
- 3.12 Bertolini, L., et al, "Cathodic Protection of New and Old Reinforced Concrete Structures," *Corrosion Science*, 35, 1993, pp. 1633-1639.
- 3.13 Pedferri, P., "Cathodic Protection and Cathodic Prevention," *Construction and Building Materials*, 10(5), 1996, pp. 391-402.

## CHAPTER 4. DEVELOPMENT OF STEEL PASSIVITY IN CONCRETE BY CATHODIC PROTECTION WITH ENVIRONMENT IMPROVEMENT EFFECTS

### 4.1 Introduction

Deterioration mechanism due to the corrosion of steel bars becomes a primary problem in reinforced concrete (RC) structure. This is usually caused by diffusion of chloride ions ( $\text{Cl}^-$ ) and oxygen ( $\text{O}_2$ ) into the concrete, thus, destroyed the passivity film and led the corrosion initiation on the steel surface. As results, it was produced crack and spalling in concrete by expansion pressure of corrosion products. Among the various available corrosion control methods, cathodic protection (CP) is a standard technique adapted to stop the corrosion of steel embedded in concrete and re-established the passivity film of steel bar. Researchers and practitioners have regarded the 100 mV decay potential as the most rational CP criterion in reinforced concrete structure<sup>(4.1)</sup>. In some cases, the 100 mV decay potential criteria could not achieve due to the insufficient protective current. In this case, the more significant current protection is required to satisfy the 100 mV criterion<sup>(4.2)</sup>. However, it creates adverse effects such as bond loss, hydrogen embrittlement and decreasing the anodic performance due to dry up of water in anode surface<sup>(4.3), (4.4)</sup>.

For RC structure exposed in the atmospheric zone where the  $\text{O}_2$  supply is larger, CP current may increases pH and decreases the  $\text{Cl}^-$  on the steel surface by electrophoresis due to the cathodic reaction as shown in Eq (1). This phenomenon is called “environmental improvement.”



By continuing applied CP, the ratio concentration of  $\text{Cl}^-/\text{OH}^-$  will decrease due to the environmental improvement effects. As reported by previous researchers<sup>(4.5), (4.6)</sup>, for the case of

high corrosion rate in the atmosphere condition the most important protective effect is to induce passivity by improving the local environment at the steel surface. In this case, the protection of steel can be achieved after certain periods. This study aims to investigate the development of steel passivity in concrete exposed to the atmosphere by CP considering environmental improvement effects.

## 4.2 Preparation of Specimens

### 4.2.1 Mix proportion

Specimens were manufactured using Ordinary Portland Cement (OPC). Tap water at  $20\pm 2$  °C was introduced as the mixing water. Washed sea sand and crushed stone were used as aggregates. The physical properties of concrete materials are similar those in **Table 3.1, Chapter 3**. Further, a deformed steel bar of 19 mm in diameter was used for reinforcement.

Concrete mix with water to cement (W/C) ratio of 55% was used throughout all specimens. Air entraining admixture (AE) was used to obtain the slump and air content in the range of  $10\pm 2.5$  cm and  $4.5\pm 1.5\%$  respectively. Chloride ions of  $2\text{ kg/m}^3$ ,  $5\text{ kg/m}^3$  and  $10\text{ kg/m}^3$  were added as sodium chloride (NaCl) through the mix concrete. Mix design of concrete is presented in **Table 4.1**.

Table 4.1. Mix design of concrete

W/C (%)	Water ( $\text{kg/m}^3$ )	Cement ( $\text{kg/m}^3$ )	Sand ( $\text{kg/m}^3$ )	Gravel ( $\text{kg/m}^3$ )	Chloride ( $\text{kg/m}^3$ )	AEWR ( $\text{kg/m}^3$ )	AE ( $\text{mL/m}^3$ )
55	190	345	841	956	2, 5, 10	1.08	1036

AEWR: Air Entrained Agent Water Reducer; AE: Air Entrained Agent

### 4.2.2 Specimens design

Specimens were casted in the form of reinforced concrete prism with dimensions of 120 mm x 120 mm x 200 mm. Each specimen consist of deformed steel bar of 19 mm in diameter centrally located with an exposed length of 180 mm. Both end side of exposed steel bar was covered with PVC pipe ( $\text{Ø}20$  mm) contain resin to avoid penetration of chloride during accelerated corrosion test. Two ribbon mesh titanium electrode with iridium oxide as catalyst layer (width = 13 mm) were embedded 10 mm from the concrete surface as a counter electrode and anode. The embedded counter electrode was used for polarization test. The detail of the specimen is shown in **Fig. 4.1**. At 24 hours after casting, specimens were demoulded and cured

in the wet towel sealing for 28 days at  $20\pm 2^{\circ}\text{C}$  constant room temperature. In addition, specimens were sealed with epoxy resin after 28 days curing room.

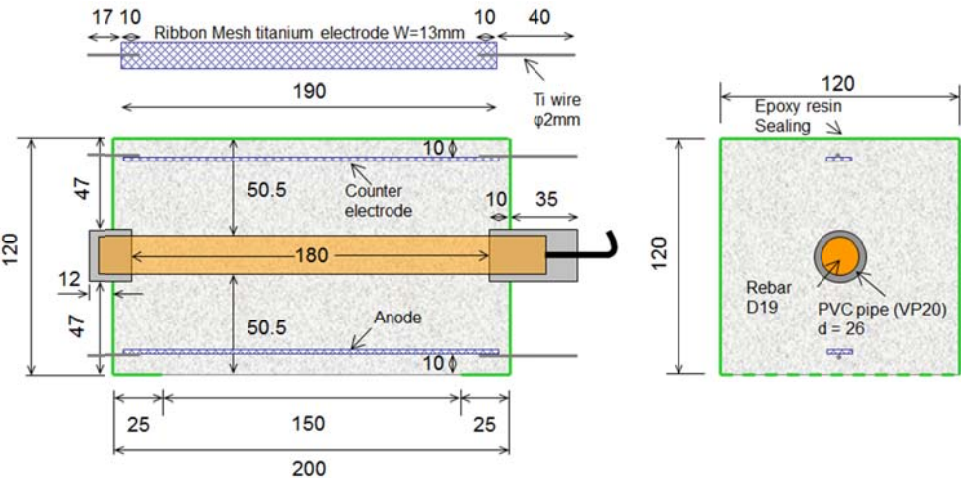


Fig. 4.1 Detail of specimen (unit: mm)

**4.2.3 Accelerated corrosion test**

Prior to CP tests, specimens were subjected to an accelerated corrosion test to generate corrosion on the steel surface. For this, specimens were immersed in 3% NaCl solution and applied constant current of 14.4 mA by using power supply (DC). The steel bar was connected to the positive terminal of DC power and negative terminal to stainless steel plate as a counter electrode (Fig. 4.2). This test was performed eight days for concrete with  $10\text{ kg/m}^3$  of chloride and 14 days for  $2\text{ kg/m}^3$  and  $5\text{ kg/m}^3$ .

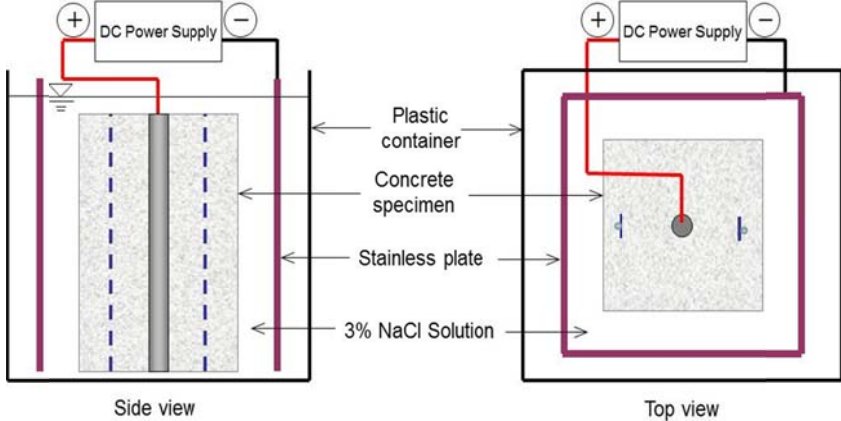


Fig. 4.2 Setup for accelerated corrosion tests

### 4.3 Method of Investigation

#### 4.3.1 Cathodic Protection (CP) instrumentation

Nine level constant current densities were applied to the steel bars embedded in concrete specimens. Each chloride content consist of three different current density. Current densities were calculated according to the initial potential shift value of 100 mV, 50 mV and 25 mV at the initial stage (0 day) for each chloride content and kept continuously during CP tests. **Table 4.2** summarized the specimens used in this investigation. A constant current power supply unit was manufactured to provide cathodic current to the specimens. The negative terminal of power supply was connected to the steel bar and a positive terminal to the anode. A constant cathodic current were maintained on each specimen by adjusting the semi-fixed resistor of power supply. The schematic of CP is illustrated in **Fig. 4.3**.

Table 4.2. Summary of specimens

Chloride content (kg/m <sup>3</sup> )	Series	Initial potential shift value (mV)	Protective current density (mA/m <sup>2</sup> )	Test duration (days)
2	A2-No CP	-	-	193
	A2-25 mV	25	2	
	A2-50 mV	50	5	
	A2-100 mV	100	10	
5	A5-No CP	-	-	193
	A5-25 mV	25	5	
	A5-50 mV	50	10	
	A5-100 mV	100	20	
10	A10-No CP	-	-	230
	A10-25 mV	25	10	
	A10-50 mV	50	20	
	A10-100 mV	100	100	

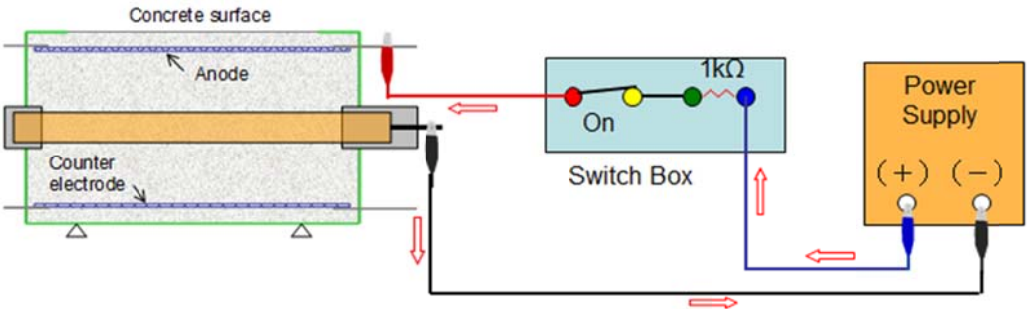


Figure 4.3 The schematic of CP tests

CP tests were performed approximately 230 days for concrete with 10 kg/m<sup>3</sup> of chloride. Meanwhile, for concrete with 2 kg/m<sup>3</sup> and 5 kg/m<sup>3</sup> of chloride was around 193 days. All specimens were kept in constant room temperature of 20±2°C and relative humidity of 60% during test periods. In addition, sat.KCl(aq)/AgCl/Ag electrode (SSE) was used as a reference electrode and converted to copper/copper sulfate electrode (CSE) standard.

**4.3.2 Measurement method**

**a. Instant-off potential (E<sub>i0</sub>)**

Instant-off potential (E<sub>i0</sub>) was monitored periodically by using Instant-off potential meter (TTR frequency 60 Hz and interruption time 0.3 ms) after CP current interruption via switch box for a few second. The schematic measurement of E<sub>i0</sub> is shown in **Fig. 4.4**.

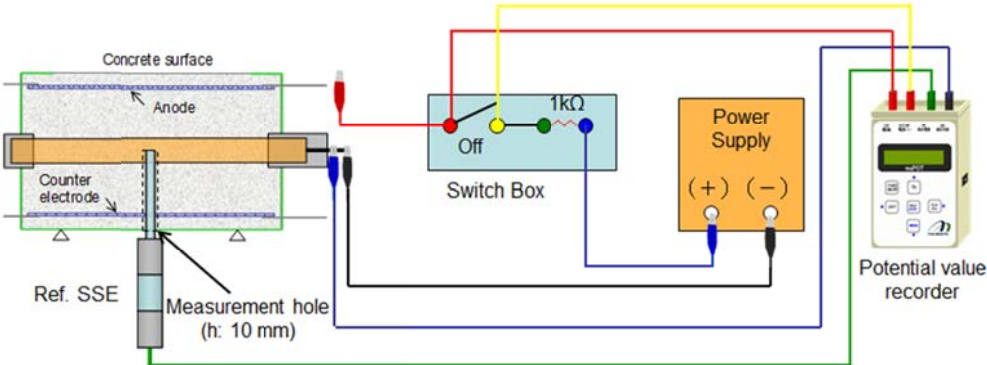


Figure 4.4 The schematic measurement of the E<sub>i0</sub>

**b. Depolarization test**

Depolarization tests were regularly carried out by disconnecting the steel bar from anode for 24 hours and monitoring the decay of the potential. The difference between 24 hours off potential (E<sub>off</sub>) and E<sub>i0</sub> can be assumed to represent the 100 mV decay potential. The 100 mV depolarization value accepted as indicative of efficient CP system <sup>(4.1), (4.7)</sup>. **Figure 4.5** illustrated depolarization test and method of measurement the E<sub>off</sub>.

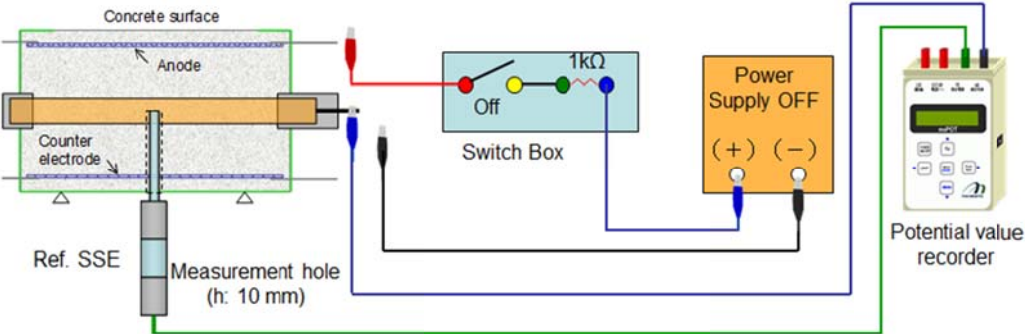


Figure 4.5 Depolarization test and measurement of the E<sub>off</sub>



### c. Anodic-cathodic polarization curve

The anodic polarization curve were obtained by shifting the  $E_{\text{off}}$  gradually every 3 minutes until reached the anodic potential difference around 250 mV. Galvanostat TTR PS14 and potential value recorder TTR were used to maintain the current density and to monitor the potential change of steel bar respectively. Similar method was used to perform the cathodic polarization curve and just different in the cathodic potential shifted about 150 mV. The schematic measurement of anodic-cathodic polarization curve is shown in **Fig. 4.6**.

In this test, the amount of the current density supplied each specimen is same during anodic-cathodic polarization test. Hence, the judgment is based on increasing the anodic-cathodic polarization curve with exposure periods.

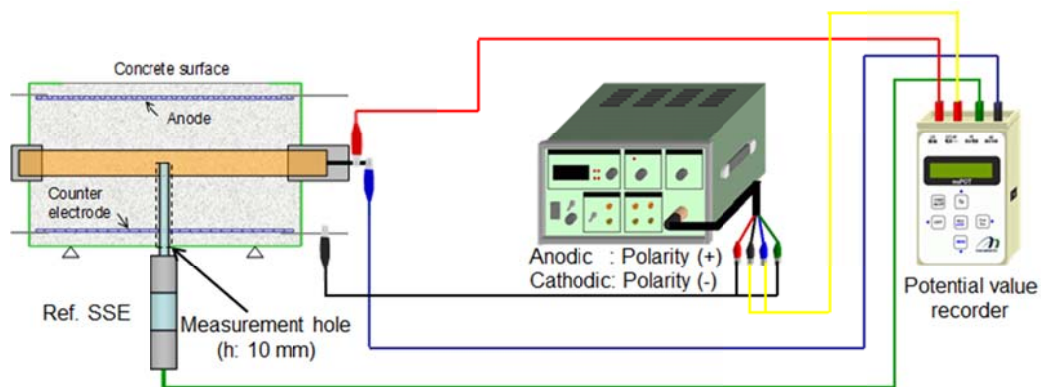


Fig. 4.6 Anodic-cathodic polarization curve test

### d. Corrosion rate

Measurements of corrosion rate were carried out in two methods namely the open-circuit corrosion rate (corrosion rate in the absence of protection) and corrosion rate under protection (CP connecting with steel bar). The open-circuit corrosion rate were estimated from the negative potential shift achieved and the applied current density <sup>(4.8)</sup>. Corrosion rate estimation based on the anodic-cathodic polarization curve and assuming anodic ( $\beta_a$ ) and cathodic ( $\beta_c$ ) Tafel slope of 60 mV and 120 mV<sup>(4.8)</sup> respectively (**Fig. 4.7a**). The balanced condition between anodic curve and cathodic curve was determined as the open-circuit corrosion rate of steel bar.

On the other hand, the corrosion rate under protection was obtained from the anodic-cathodic polarization curve under CP applied. Firstly, cathodic polarization curve were created by decreasing the protective current gradually every 3 minutes until zero value. After that, the anodic polarization curve was obtained by increasing the protective current until the  $E_{i_0}$  shifted about 120 mV. From these curve, the corrosion rate under protection was calculated. Similar

method in the open-circuit corrosion rate was used for calculation. In the case of under protection, the cathodic slope ( $\beta_c$ ) is based on the protective potential value under CP (Fig. 4.7b). In addition, the open-circuit corrosion rate for passive steel bar in concrete is less than  $1 \text{ mA/m}^2$  (4.9).

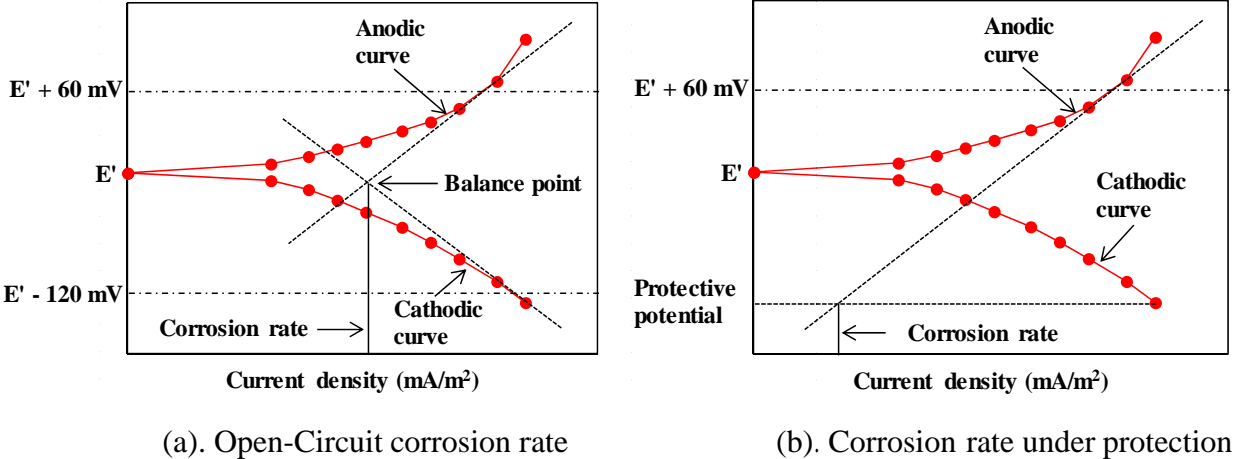


Fig. 4.7 Estimation of corrosion rate of steel bar

**e. Visual observation and corrosion weight loss**

The specimens were open after CP tests for visual examination. After completely remove the steel bars from concrete specimen, the corrosion weight loss was calculated. Due to the lack information of the initial weight of steel bars, an approach method was used to calculate the corrosion weight loss. For this, one set non-corroded steel bar of 50 mm in length with similar properties of corroded steel bar was prepared as control. Then, corroded steel bars were cut with same length and orientation (Fig. 4.8).

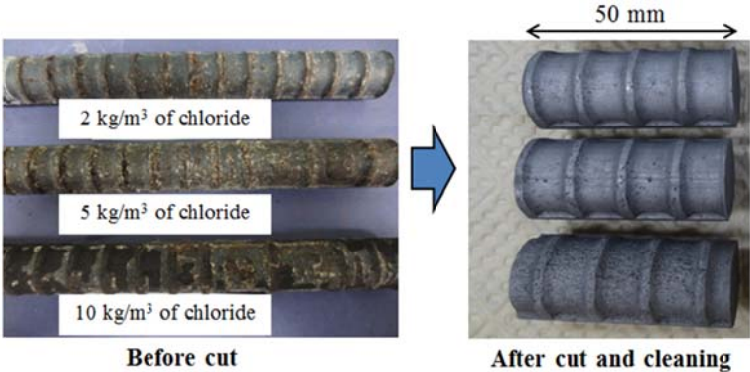


Fig. 4.8 Steel bars condition before and after cutting then cleaning

After that, weight of steel bars were measured before immersed in 10% diammonium hydrogen citrate solution for one week and then the rust was cleaning by a steel wire brush. The

difference in weight between control and corroded steel bars after cleaning was defined as the corrosion weight loss (weight per running length).

## 4.4 Results and Discussion

### 4.4.1 Initial potential shift versus current density

The difference between natural potential ( $E_{corr}$ ) and  $E_{i0}$  at the initial stage (0 days) was determined as initial potential shift. From there, current density of each specimen was calculated. The relationship between initial potential shift and current density for each chloride content is presented in **Fig. 4.9**. For concrete contained  $2 \text{ kg/m}^3$  of chloride, the initial potential shift of 25 mV, 50 mV and 100 mV required current densities of  $2 \text{ mA/m}^2$ ,  $5 \text{ mA/m}^2$  and  $10 \text{ mA/m}^2$  respectively. While for  $5 \text{ kg/m}^3$  and  $10 \text{ kg/m}^3$  of chloride initial shift potential of 25 mV, 50 mV and 100 mV provided  $5 \text{ mA/m}^2$ ,  $10 \text{ mA/m}^2$ ,  $20 \text{ mA/m}^2$  and  $10 \text{ mA/m}^2$ ,  $20 \text{ mA/m}^2$ ,  $100 \text{ mA/m}^2$  respectively. This implies that the higher chloride content require a greater protective current density.

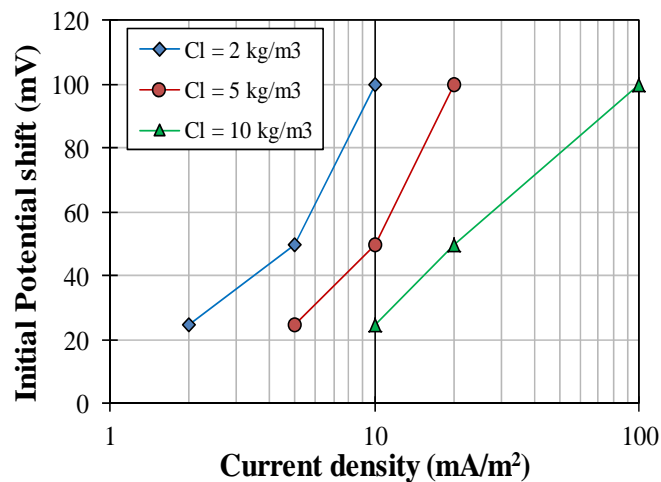


Fig. 4.9 The relationship between initial potential shift and current density

### 4.4.2 Instant-off potential ( $E_{i0}$ )

**Figure 4.10** shows the relationship between the  $E_{i0}$  with time. It is shown that the higher initial shift potential provided the most negative potential and reached stable condition after 40 days in all chloride content. In the concrete contained  $2 \text{ kg/m}^3$  of chloride, it is found that no significant change in  $E_{i0}$  occurred during test periods. By adding  $5 \text{ kg/m}^3$  of chloride, it is clear from **Fig. 4.10** that the  $E_{i0}$  tends to decrease at the end of test periods. Similar trend was also found in concrete with  $10 \text{ kg/m}^3$  of chloride for protective current densities of 20 and  $100 \text{ mA/m}^2$ . One reason might be due to the decreasing of oxygen from the steel bar or continuing

the breakdown of the passivity film (4.2), (4.4), (4.10). Furthermore, for concrete with 10 kg/m<sup>3</sup> of chloride, the lower protective current density of 10 mA/m<sup>2</sup> shows that E<sub>io</sub> did not change significantly during test periods.

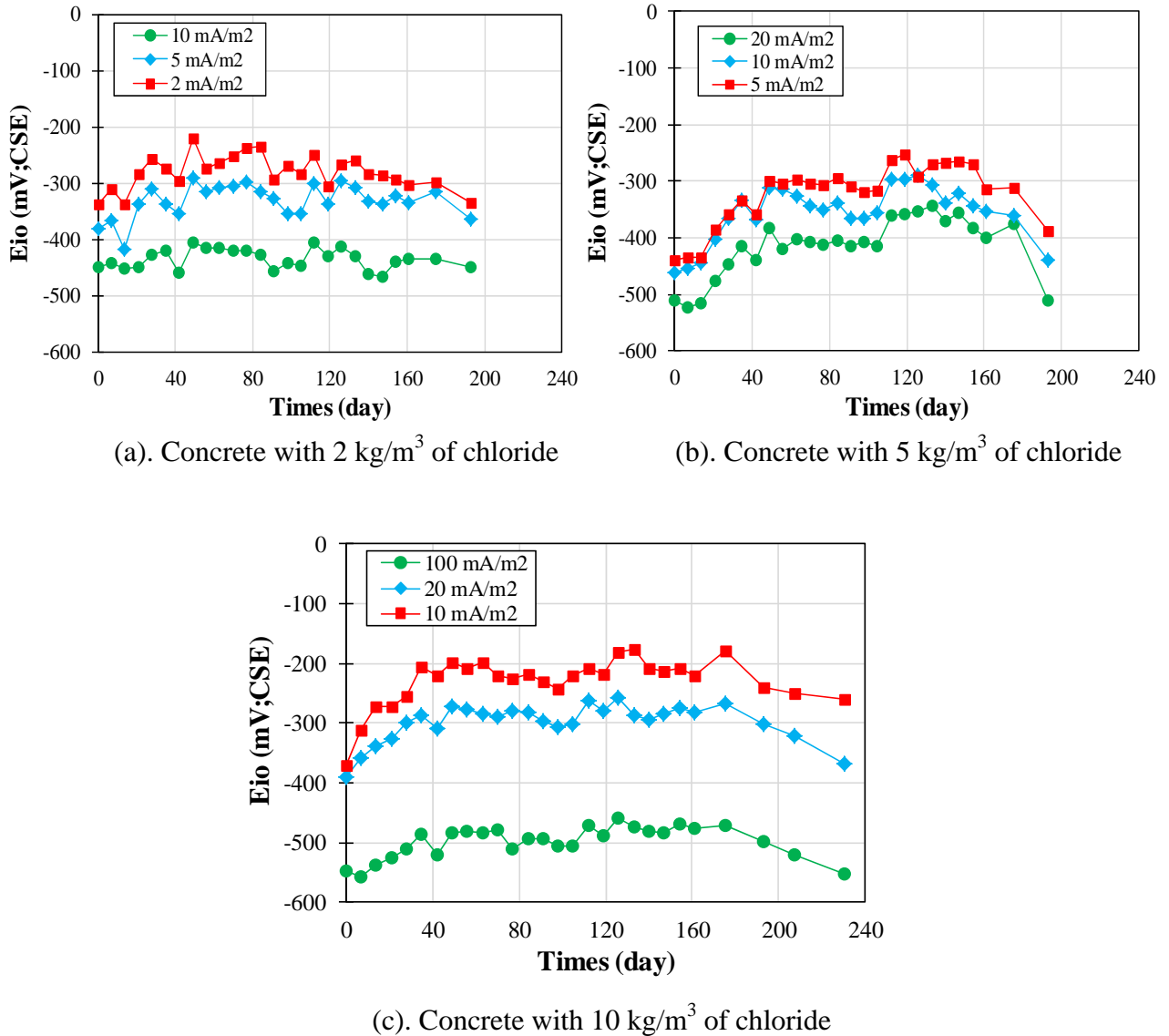
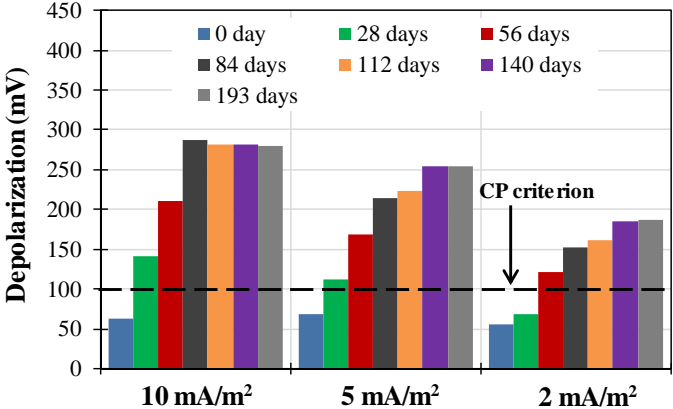


Fig. 4.10 The instant-off potential (E<sub>io</sub>) of steel bars

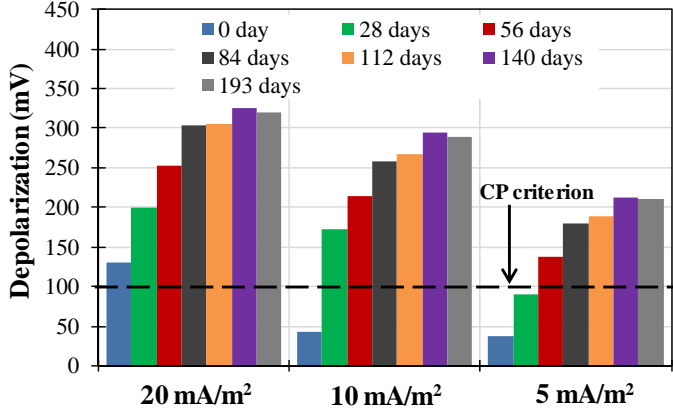
#### 4.4.3 Depolarization tests

From Fig. 4.11 it is observed that the depolarization value increased with increasing in polarization time. The 100 mV decay potential was achieved at 28 days with higher initial potential shift for all chloride content. Meanwhile, the lower protective current densities of 2, 5 and 10 mA/m<sup>2</sup> satisfies the 100 mV after 56 days polarized for all chloride content. It means that to satisfy the 100 mV decay criterion, it is not required a greater CP current at the initial stage, and can be achieved by applying small CP current with considering the environment improvement effects on the steel surface. At the end of test periods, it was observed that the

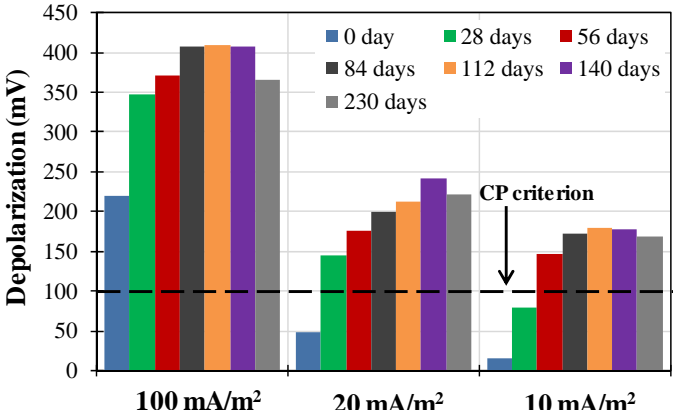
depolarization values of steel bars tend to decrease for concrete contained 5 kg/m<sup>3</sup> and 10 kg/m<sup>3</sup> of chloride. It is possible due to the largest concentration slope of DO, which delay the depolarization of steel bars.



(a). Concrete with 2 kg/m<sup>3</sup> of chloride



(b). Concrete with 5 kg/m<sup>3</sup> of chloride

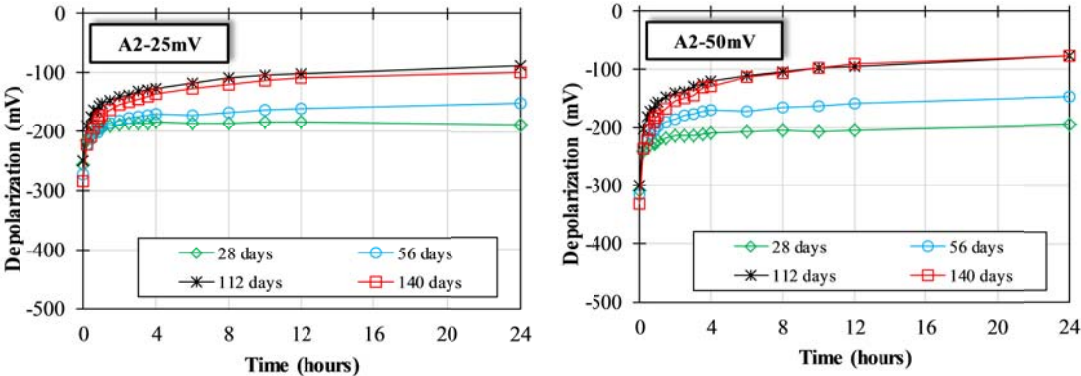


(c). Concrete with 10 kg/m<sup>3</sup> of chloride

Fig. 4.11 Depolarization values of steel bars after 24 hours disconnecting

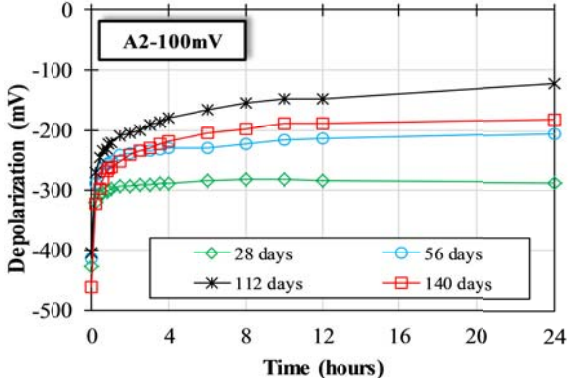
Figure 4.12 shows the time dependence of depolarized steel potential during 24 hours disconnecting from anode in all chloride contents. The depolarization value of steel was

increased with increasing polarization time. Complete depolarization of steel potential occurs at 4, 8 and 10 hours for initial potential shift of 25 mV, 50 mV and 100 mV respectively. In addition, it is also observed that the delay of depolarization behavior at 140 days and 230 days for concrete with 2 kg/m<sup>3</sup>, 5 kg/m<sup>3</sup> and 10 kg/m<sup>3</sup> of chloride respectively, due to the increasing of the dissolved oxygen <sup>(4.4)</sup>.



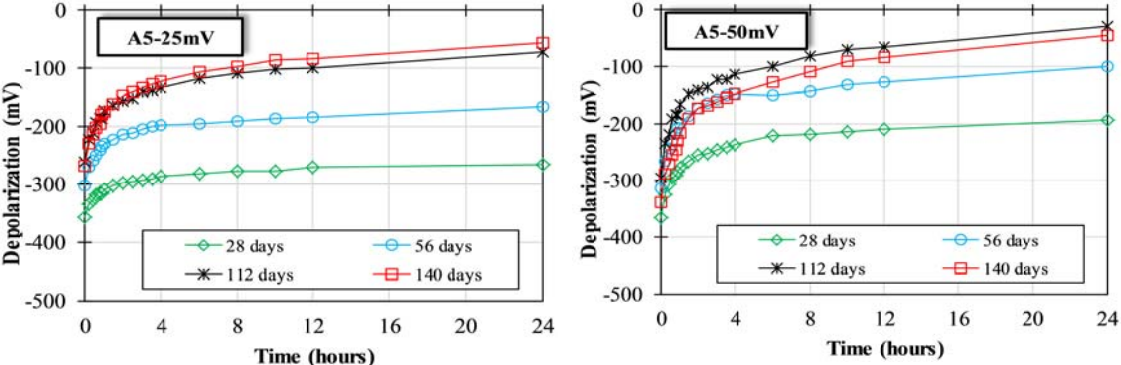
(a). Current density of 2 mA/m<sup>2</sup>

(b). Current density of 5 mA/m<sup>2</sup>



(c). Current density of 10 mA/m<sup>2</sup>

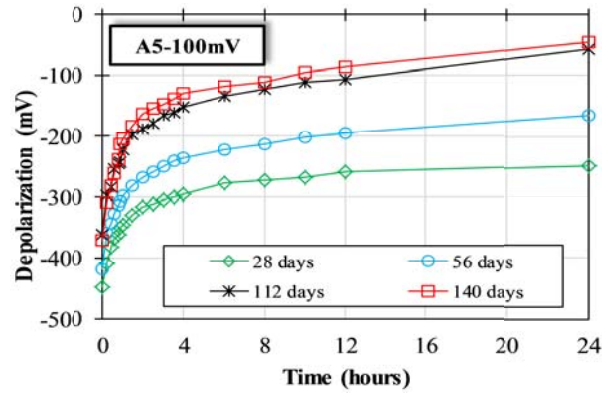
Fig. 4.12a Time dependence of depolarized steel potential with 2 kg/m<sup>3</sup> of chloride



(a). Current density of 5 mA/m<sup>2</sup>

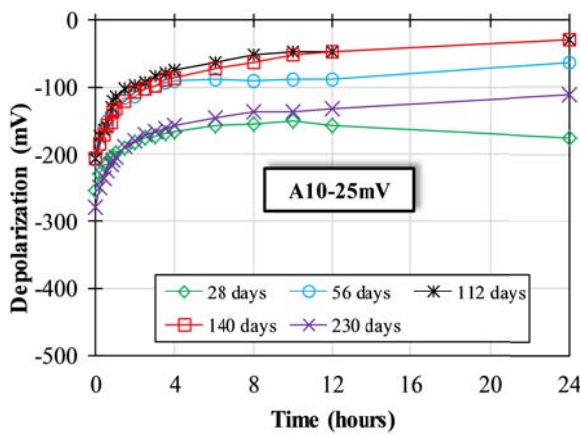
(b). Current density of 10 mA/m<sup>2</sup>

Fig. 4.12b Time dependence of depolarized steel potential with 5 kg/m<sup>3</sup> of chloride

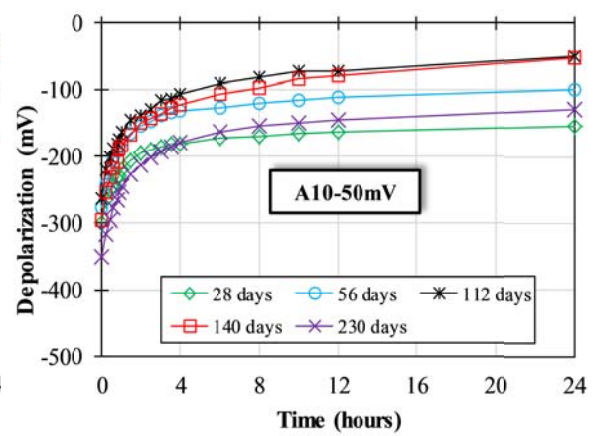


(c). Current density of 20 mA/m<sup>2</sup>

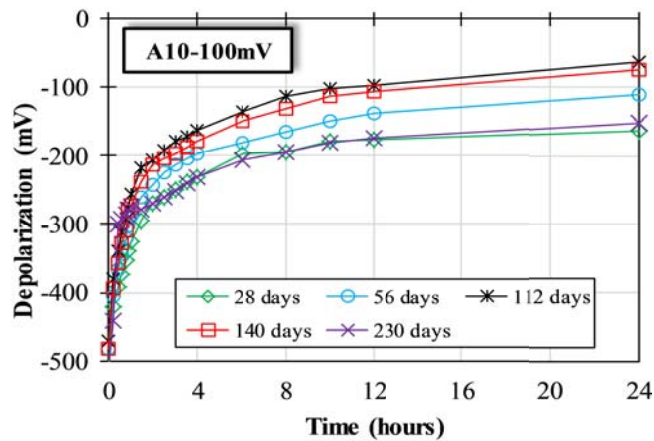
Fig. 4.12b (Continued) Time dependence of depolarized steel potential with 5 kg/m<sup>3</sup> of chloride



(a). Current density of 10 mA/m<sup>2</sup>



(b). Current density of 20 mA/m<sup>2</sup>



(c). Current density of 100 mA/m<sup>2</sup>

Fig. 4.12c Time dependence of depolarized steel potential with 10 kg/m<sup>3</sup> of chloride

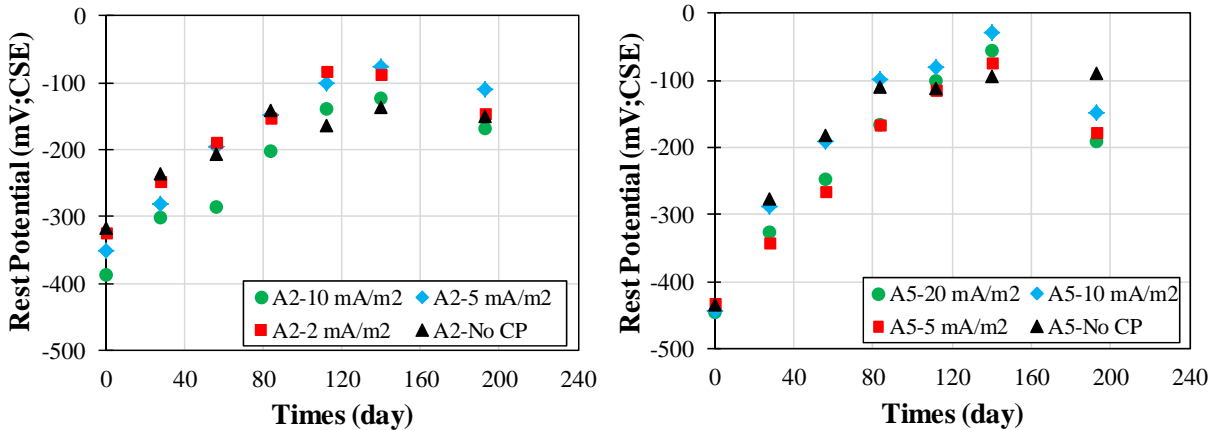
#### 4.4.4 Rest potential of steel bar ( $E_{off}$ )

The time-dependent change in the rest potential ( $E_{off}$ ) of steel bars after 24 hours disconnecting from anode are presented in **Fig. 4.13**. It is observed that the rest potential of steel bars gradually move to the positive value during 140 days polarization time even a small

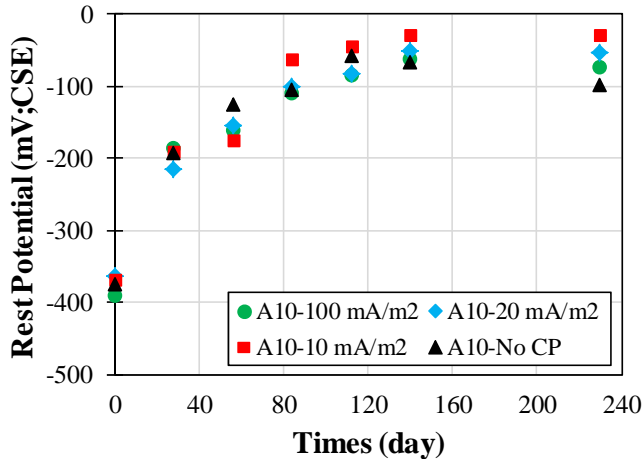


protective current density. It indicates that the improvement of passivity of the steel bars due to CP current. However, the  $E_{off}$  of steel bars tends to decrease at 193 days and 230 days for chloride content of  $2 \text{ kg/m}^3$ ,  $5 \text{ kg/m}^3$  and  $10 \text{ kg/m}^3$  respectively, as results of the diffusion of dissolved oxygen (DO).

Furthermore, it is also observed that the  $E_{off}$  of specimen without cathodic protection shifts to the positive value with time. Possible for this due to the effect of exposure condition (e.g. exposure to the atmosphere) during the hydration process, which strongly influences the hydroxide ion concentration in the pore solution <sup>(4.11)</sup>.



(a). Concrete with  $2 \text{ kg/m}^3$  of chloride      (b). Concrete with  $5 \text{ kg/m}^3$  of chloride



(c). Concrete with  $10 \text{ kg/m}^3$  of chloride

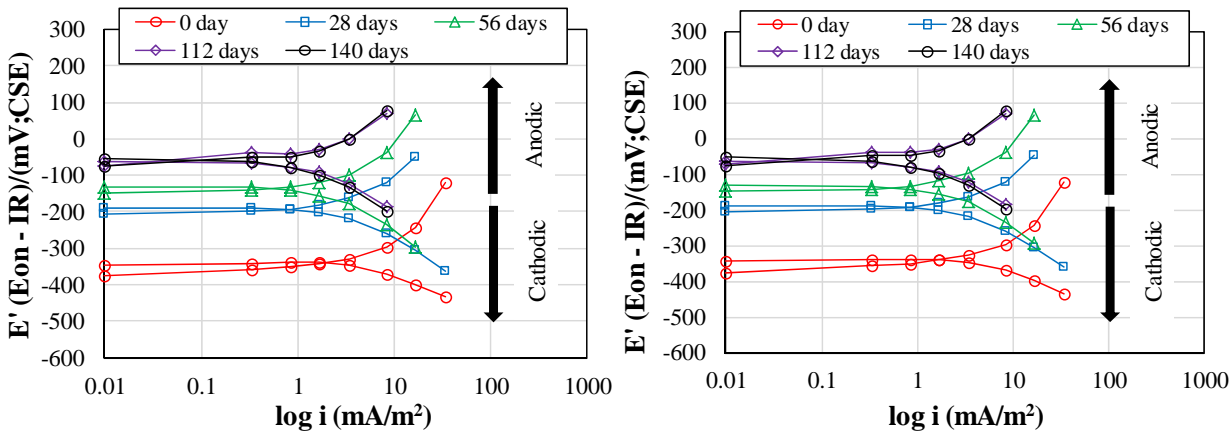
Fig. 4.13 Rest potential ( $E_{off}$ ) of steel bars

**4.4.5 Anodic-cathodic polarization curve**

Anodic polarization curve is related to passivity condition of steel bar <sup>(4.12)</sup>. While for cathodic polarization curve is related to diffusion of oxygen. As noted, the measurement periods in concrete with  $2 \text{ kg/m}^3$  and  $5 \text{ kg/m}^3$  of chloride were around 140 days and 230 days

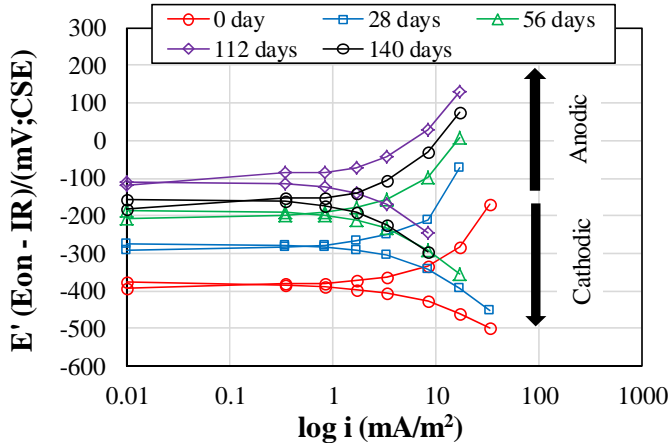


for 10 kg/m<sup>3</sup> of chloride. From **Fig. 4.14a-c**, it is clearly seen that the passivity of steel bars increased with increasing polarization time even a small current density up to 112 days in all chloride contents. It caused the environment improvement effect on the steel surface by CP current that increase pH and decreases the Cl<sup>-</sup> at the surface of steel bar. On the contrary, the anodic polarization curve of steel bars decreased in 2 kg/m<sup>3</sup> and 5 kg/m<sup>3</sup> of chloride at 140 days, and 230 days for 10 kg/m<sup>3</sup> of chloride. This is caused by depletion of oxygen, followed by the breakdown of the passivity film of steel bar. Therefore, the cathodic polarization curve increased at the same time.



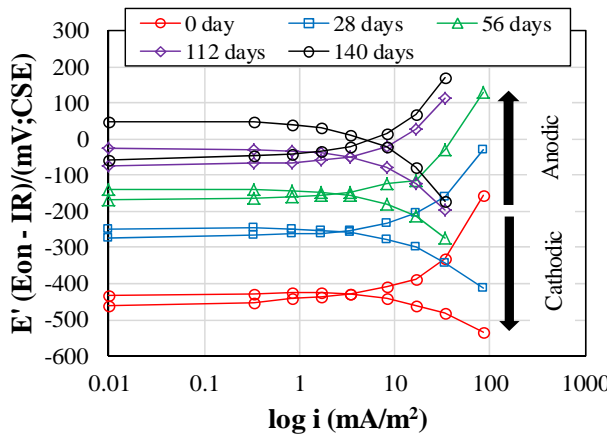
(a). Current density of 2 mA/m<sup>2</sup>

(b). Current density of 5 mA/m<sup>2</sup>

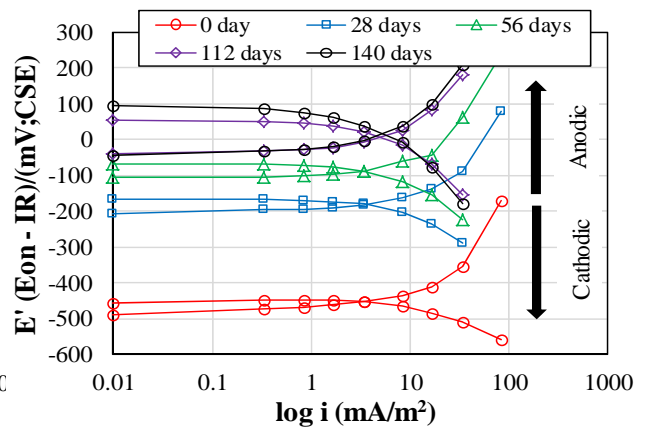


(c). Current density of 10 mA/m<sup>2</sup>

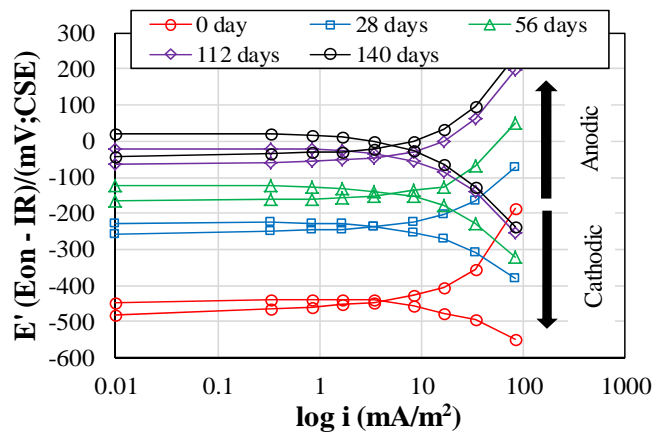
Fig. 4.14a Anodic-cathodic polarization curve with 2 kg/m<sup>3</sup> of chloride



(a). Current density of 5 mA/m<sup>2</sup>

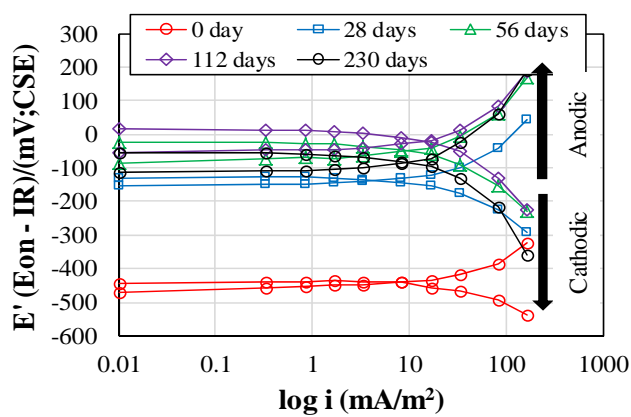


(b). Current density of 10 mA/m<sup>2</sup>

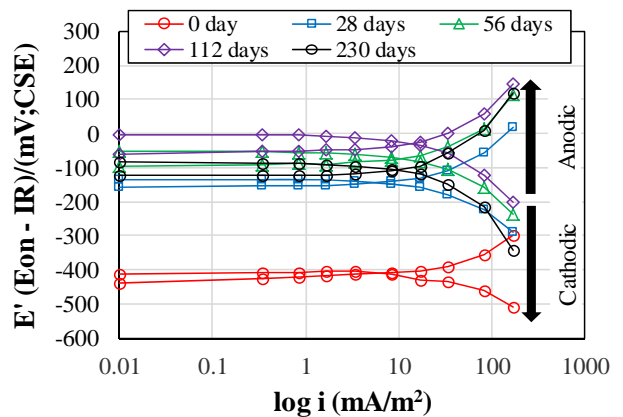


(c). Current density of 20 mA/m<sup>2</sup>

Fig. 4.14b Anodic-cathodic polarization curve with 5 kg/m<sup>3</sup> of chloride

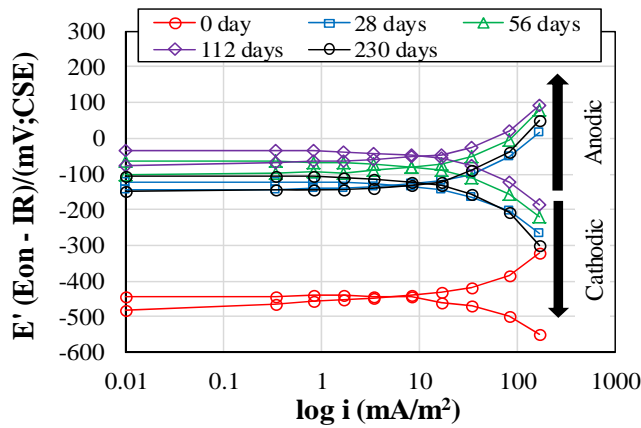


(a). Current density of 10 mA/m<sup>2</sup>



(b). Current density of 20 mA/m<sup>2</sup>

Fig. 4.14c Anodic-cathodic polarization curve with 10 kg/m<sup>3</sup> of chloride



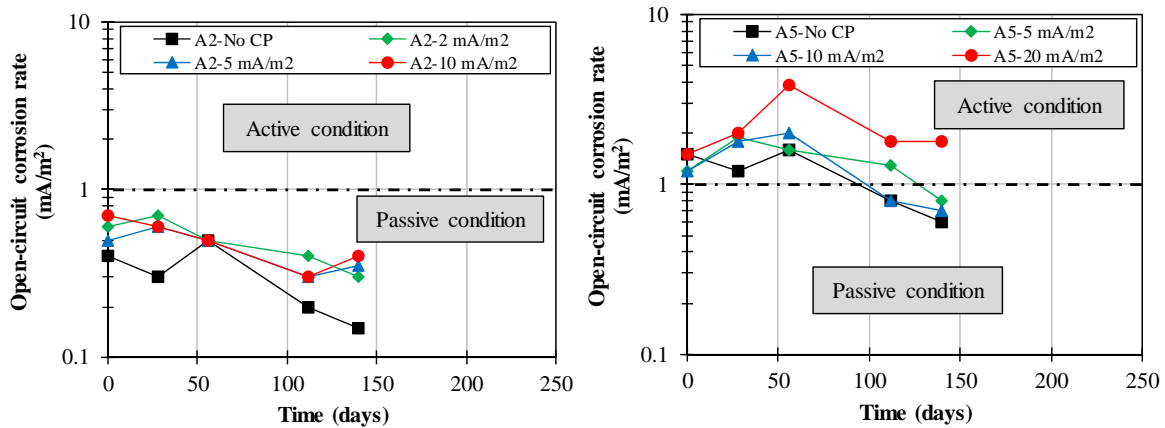
(c). Current density of 100 mA/m<sup>2</sup>

Fig. 4.14c (Continued) Anodic-cathodic polarization curve with 10 kg/m<sup>3</sup> of chloride

#### 4.4.6 Corrosion rate of steel bars

Open-circuit corrosion rate was measured at 0, 28, 56, 112 and 140 days for concrete with 2 kg/m<sup>3</sup> and 5 kg/m<sup>3</sup> of chloride. While, by adding 10 kg/m<sup>3</sup> of chloride was up to 230 days. In the case of corrosion rate under protection, measurement was conducted only in concrete with 10 kg/m<sup>3</sup> of chloride at 230 days.

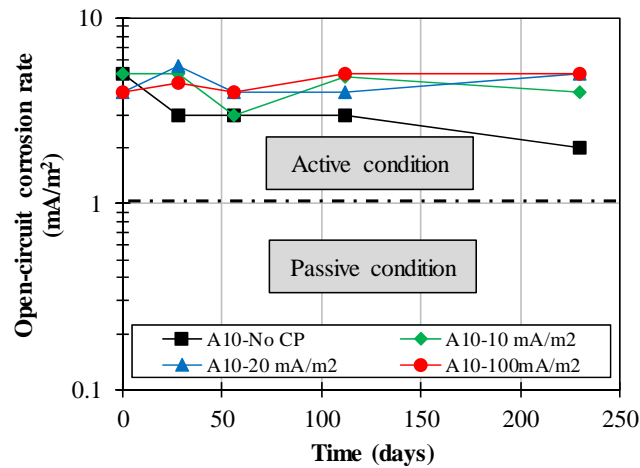
**Figure 4.15a-c** shows the reduction of the open-circuit corrosion rate versus time. The initial corrosion rate of steel bars (0 days) were 0.5 mA/m<sup>2</sup>, 1 mA/m<sup>2</sup> and 4 mA/m<sup>2</sup> for chloride 2 kg/m<sup>3</sup>, 5 kg/m<sup>3</sup> and 10 kg/m<sup>3</sup> respectively. This implies that the higher chloride content provide a largest corrosion rate. From **Fig. 4.15a-c**, it can be observed that for 2 kg/m<sup>3</sup> of chloride, open-corrosion rate of steel bars decreased with increasing polarization time. By adding 5 kg/m<sup>3</sup> of chloride, decreasing of corrosion rate was occurred after 56 days. It is due to the environment improvement effects, which reduce the ratio concentration of Cl<sup>-</sup>/OH<sup>-</sup> on the steel-concrete interface. On the contrary, no significant changes in corrosion rate was found in concrete contained 10 kg/m<sup>3</sup> of chloride even with 100 mV potential shift.



(a). Concrete with 2 kg/m<sup>3</sup> of chloride

(b). Concrete with 5 kg/m<sup>3</sup> of chloride

Fig. 4.15 Reduction of the open-circuit corrosion rate of steel bars



(c). Concrete with 10 kg/m<sup>3</sup> of chloride

Fig. 4.15 (Continued) Reduction of the open-circuit corrosion rate of steel bars

The comparison of corrosion rate of steel bars under protection and the open-circuit condition with 10 kg/m<sup>3</sup> of chloride at 230 days is presented in **Fig. 4.16**. The corrosion rate of steel bars under protection condition is below 1 mA/m<sup>2</sup> for all potential shifts. It was approximately 20, 16, and 100 times smaller than that open-circuit corrosion rate for the current densities of 10, 20 and 100 mA/m<sup>2</sup> respectively.

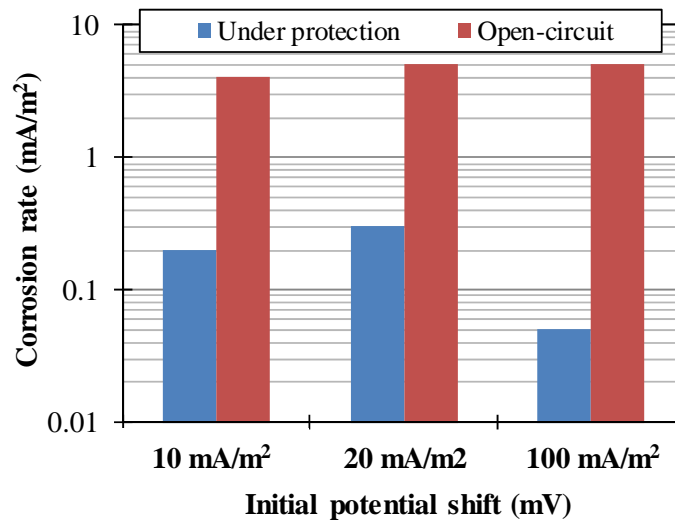


Fig. 4.16 Corrosion rate of steel bars under protection and the open-circuit condition in 10 kg/m<sup>3</sup> of chloride at 230 days

#### 4.4.7 Visual observation

Visual observations and weight loss of steel bars at the end of CP tests are shown in **Table 4.3**. It is observed that the higher chloride content shows a larger corrosion area. It can be said that corrosion area of steel bar depends on the chloride content in concrete. Also, it is observed that no significant difference in corrosion appearances for specimens with 25 mV, 50

mV and 100 mV were found for all chloride contents. The results indicate that a small current density can enhance the passivity of steel by environmental improvement effects after certain periods. In addition, specimens with CP showed a good passivity than specimen without CP.

Specimens with CP showed averages of 1.256 g, 1.830 g, and 2.032 g corrosion weight loss for 2 kg/m<sup>3</sup>, 5 kg/m<sup>3</sup> and 10 kg/m<sup>3</sup> of chloride respectively. While specimens without CP had 1.700 g, 1.820 g and 2.860 g of corrosion weight loss in the same chloride content. It is due to the CP current reduced the corrosion rate of steel bars.

Table 4.3a Corrosion appearance and weight loss of steel bars with 2 kg/m<sup>3</sup> of chloride





Chloride content (kg/m <sup>3</sup> )	Series (mV)	Corrosion appearances	weight loss (g)
2	A2 – No CP		1.700
	A2 – 25 mV		1.130
	A2 – 50 mV		1.600
	A2 – 100 mV		1.040

Table 4.3b Corrosion appearance and weight loss of steel bars with 5 kg/m<sup>3</sup> of chloride









Chloride content (kg/m <sup>3</sup> )	Series (mV)	Corrosion appearances	weight loss (g)
5	A5 – No CP		1.820
	A5 – 25 mV		1.850
	A5 – 50 mV		1.800
	A5 – 100 mV		1.870



Table 4.3c Corrosion appearance and weight loss of steel bars with 10 kg/m<sup>3</sup> of chloride

Chloride content (kg/m <sup>3</sup> )	Series (mV)	Corrosion appearances	weight loss (g)
10	A10 – No CP		2.860
	A10 – 25 mV		2.020
	A10 – 50 mV		2.000
	A10 – 100 mV		1.980

#### 4.5 Conclusions

In this study, CP by considering “Environment Improvement” effects was carried out under various chloride content. Different current density levels were applied and kept continuously on the steel surface ranging from 2 mA/m<sup>2</sup> to 100 mA/m<sup>2</sup>. From the test results, following conclusions are drawn:

1. When chloride content in concrete is higher, a greater protective current density is required to protect the steel bar.
2. The 100 mV decay potential is achieved even with current densities of 2, 5 and 10 mA/m<sup>2</sup> after certain periods for chloride content of 2 kg/m<sup>3</sup>, 5 kg/m<sup>3</sup> and 10 kg/m<sup>3</sup> respectively.

3. A small protective current density has enhanced the passivity of steel bars under CP current. It is due to the “Environment Improvement” effects that decrease the chloride ions on the steel surface.
4. The corrosion rate of steel under protection is approximately 20, 16 and 100 times lower than the open-circuit corrosion rate for current densities of 10, 20 and 100 mA/m<sup>2</sup> respectively.
5. CP current showed no significant effect on corrosion weight loss of steel bar but reduced the corrosion rate of steel bar.
6. Appropriate CP design should be based on the “Environment Improvement” effects to avoid the over protection in which causes bond degradation steel-concrete and hydrogen embrittlement.



## References

- 4.1 Concrete Library 107, "Recommendation for Design and Construction of Electrochemical Corrosion Control Method," Tokyo: Japan Society of Civil Engineers, 2011, pp. 67-68.
- 4.2 Shinoda, Y., et al, "Discussion on Cathodic Protection Effect for Steel in Salt Damaged Concrete," Proceedings of the Third International Conference on Sustainable Construction Materials and Technologies (SCMT3), Kyoto, Japan, 2013.
- 4.3 Ali, M. G., et al, "Polarization Period, Current Density, and the Cathodic Protection Criteria," ACI Materials Journal, 89 (3), 1992, pp. 247-251.
- 4.4 Otani, S., et al, "Cathodic protection method for steel in concrete with environmental improvement effects," Proceedings of East Asia & Pacific Rim Area Conference., NACE, Kyoto, Japan, 2013.
- 4.5 Stratfull, R. F., "Criteria for the Cathodic Protection of Bridge Decks," Proceedings 1<sup>st</sup> International Symposium on Corrosion of Reinforcement in Concrete Structure, Chichester, U.K, 1983, 287-331.
- 4.6 Bromfield, J. P., "Field Survey of Cathodic Protection on North American Bridges," Mat. Perf, 31(9), 1992, 28-33.
- 4.7 EN 12696, "Cathodic Protection of Steel in Concrete," European Standard, 2000.
- 4.8 Glass, G. K., "The 100-mV Potential Decay Cathodic Protection Criterion," Corrosion, NACE, 3, 1999, pp. 286-290.
- 4.9 Rincon, O. T., et al, "Environmental Influence on Point Anode Performance in Reinforced Concrete," Construction and Building Materials, 22, 2008, pp. 494-503.
- 4.10 Glass, G. K., "CP Criteria for Reinforced Concrete in Marine Exposure Zones," Journal of Materials in Civil Engineering, Vol. 12 (2), 2000, pp. 164-171.
- 4.11 Suryavanshi, A. K., et al, "Corrosion of Reinforcement Steel Embedded in High Water-cement Ratio Concrete Contaminated with Chloride," Cement and Concrete Composites, 20, 1998, pp. 263-381.
- 4.12 Otsuki, N., "A Study of Effectiveness of Chloride on Corrosion of Steel Bar in Concrete," Report of Port and Harbor Research Institute (PHRI), Japan, 1985, 127-134.

## **CHAPTER 5. EVALUATION OF THE CATHODIC PROTECTION CRITERION LESS THAN 100 mV FOR STEEL IN CHLORIDE CONTAMINATED CONCRETE**

### **5.1 Introduction**

Corrosion of steel bar is recognized as the major cause of the deterioration of reinforced concrete structures. The presences of chloride ion in concrete play a significant role in the corrosion process. Thus, lead to structural deterioration and failure of reinforced concrete structures due to the expansive of corrosion products.

Cathodic Protection (CP) system has been well known as the most reliable technique to control corrosion of steel in concrete. The criterion in most common use today is 100 mV depolarization value. A field survey in North America (1989)<sup>(5.1)</sup> reported that the most number of reinforced concrete structures were being controlled using 100 mV depolarization criterion. However, some authors<sup>(5.2), (5.3)</sup> have suggested that the depolarization value should be raised to 150 or 200 mV to ensure the cathodic protection of steel in concrete, while others have recently suggested that it should be reduced. In summary, the 100 mV depolarization value is a reasonably accurate criterion of CP system in concrete, although it may be excessive when very little chloride concentration is presented.

This study attempts to evaluate the protection level require for steel bar in chloride contaminated concrete in the atmospherically exposed zone. Three levels of depolarization value of 25 mV, 50 mV and 100 mV were examined in concrete specimen with different chloride content.

### **5.2 Preparation of Specimens**

The materials, concrete composition and dimension of specimens are identical in **Chapter 4**. The variations were steel bars preparation, duration of accelerated corrosion and exposure area of the specimen. Before embedded in concrete, the protective films of all steel

bars were removed. For this, steel bars were immersed in 10% diammonium hydrogen citrate solution for one week and then the protective film was cleaned with using a steel wire brush. After that, steel bar was measured for initial weight. **Figure 5.1** shows the steel bar condition used in this experiment.

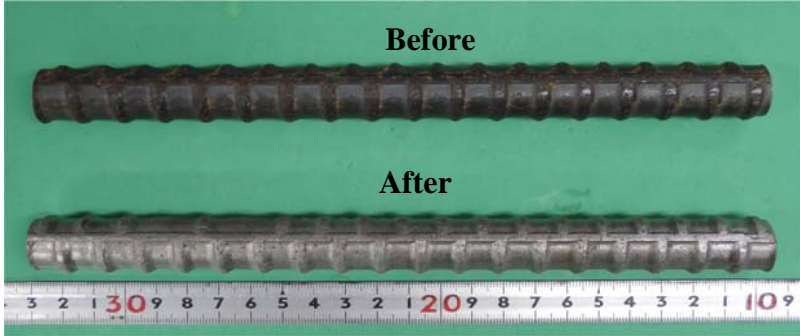


Fig. 5.1 Steel bar before and after removing the protective film

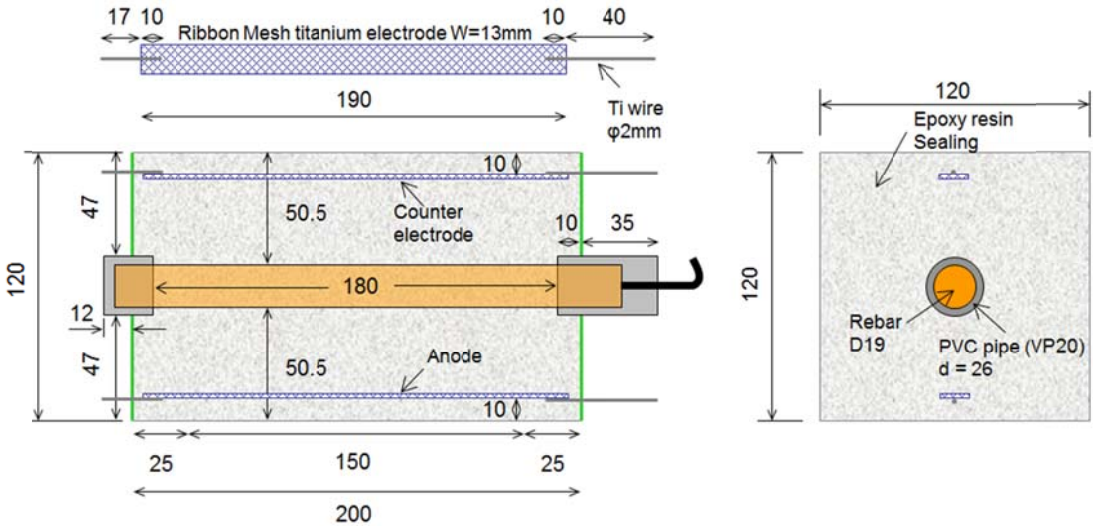


Fig. 5.2 Detail of specimen design (unit: mm)

Specimens were demoulded after 24 hours and cured under sealed condition in a wet towel for 28 days in constant room temperature at  $20\pm 2^\circ\text{C}$ . Then, accelerated corrosion test were carried out after 28 days curing. Similar method and testing equipment in **Fig. 4.2** was used. Durations of the test were 14 days for  $2\text{ kg/m}^3$  and  $5\text{ kg/m}^3$  of chloride, while six days for  $10\text{ kg/m}^3$  of chloride. After accelerated corrosion test, both end parts of the specimen were sealed with epoxy resin. The detail of specimen is shown in **Fig. 5.2**.

### 5.3 Method of Investigation

The schematic of CP is similar to **Fig. 4.3**. Three levels of depolarization value of 25 mV, 50 mV and 100 mV were applied to the concrete specimens. Current density was adjusted after switch off the steel bar from anode for 24 hours to achieve the target of protection level. The exposure period was around 250 days. In total, fifteen concrete specimens were prepared as listed in **Table 5.1**.

Table 5.1 List of specimens in testing

Chloride ion (kg/m <sup>3</sup> )	Series	Remark
2	B2	Accelerated corrosion test investigation
	B2 – No CP	Non-protection
	B2 – 25 mV	Depolarization value of 25 mV
	B2 – 50 mV	Depolarization value of 50 mV
	B2 – 100 mV	Depolarization value of 100 mV
5	B5	Accelerated corrosion test investigation
	B5 – No CP	Non-protection
	B5 – 25 mV	Depolarization value of 25 mV
	B5 – 50 mV	Depolarization value of 50 mV
	B5 – 100 mV	Depolarization value of 100 mV
10	B10	Accelerated corrosion test investigation
	B10 – No CP	Non-protection
	B10 – 25 mV	Depolarization value of 25 mV
	B10 – 50 mV	Depolarization value of 50 mV
	B10 – 100 mV	Depolarization value of 100 mV

All electrochemical measurements were performed using similar testing equipment and procedures as explained previously in **Chapter 4**. Additional measurements were just protective current and polarization resistance of steel bar. An ammeter AM-03 was used to measure the protective current of steel bar.

Polarization resistance ( $R_p$ ) was measured after depolarization test by contact method. Contact method is a measuring method using double layer counter electrode contacted on the specimen surface. The measuring system used in this study was a handy type polarization resistance system which commercially available from Shikoku Soken Co. Ltd. **Figure 5.3** shows detail measurement of  $R_p$  using contact method.

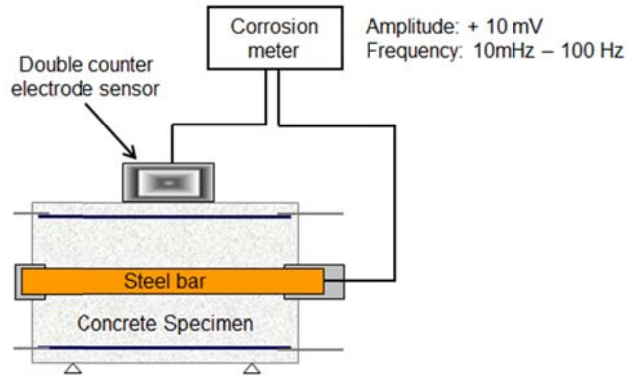


Fig. 5.3 Polarization resistance ( $R_p$ ) measurement by using contact method

After all electrochemical testing, the specimens were split open and all steel bars were observed visually for corrosion appearance. The corrosion weight losses of steel bar were measured after removing from concrete specimens. The steel bars were immersed in 10% diammonium hydrogen citrate solution for one week and then the rust was removed. The difference of initial weight and the weight after removal corrosion products was defined as the corrosion weight loss of steel bar.

## 5.4 Results and Discussion

### 5.4.1 Accelerated corrosion test

Corrosion appearances of steel bars after accelerated corrosion test are shown in **Fig. 5.4**. It was observed that the higher chloride content provide a larger corrosion area. Even though similar duration in accelerated corrosion, the more severe corrosion was found in concrete with  $5 \text{ kg/m}^3$  than in  $2 \text{ kg/m}^3$  of chloride. It can be concluded that the amount of chloride ions in concrete is significantly affected the corrosion of steel bar.

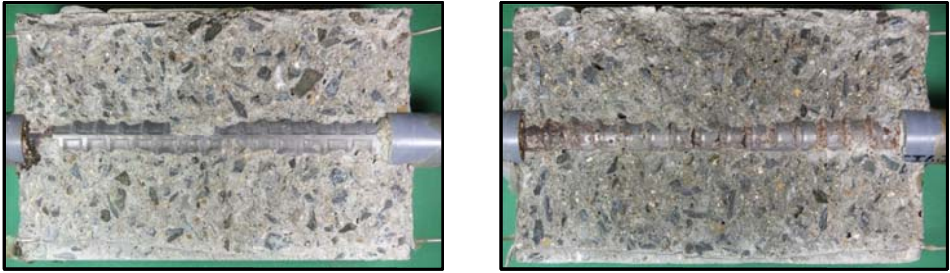
As comparison, theoretical calculation of corrosion weight loss of steel bar was carried out by using Faraday's law<sup>(5.4)</sup> as follows (**Eq. 1**):

$$W = (A \times I_{app} \times t) / (Z \times F) \quad (1)$$

where  $W$  = theoretical metal weight loss due to corrosion (g);  $A$  = atomic weight of iron (56 g);  $I_{app}$  = applied current (amp);  $t$  = time elapsed (sec);  $Z$  = valency of reacting electrode (iron) which is 2;  $F$  = Faraday's constant (96,500 amp sec).

**Table 5.2** shows the corrosion weight loss of steel bars after accelerated corrosion test both experimental and theoretical calculation. Average of corrosion weight loss is sequenced as

B10>B5>B2 with values 5.02 g, 6.48 g and 7.49 g respectively, based on the experimental results. By theoretical calculation, it is found that the corrosion weight loss of steel bar depends on the duration of applied current. From this test results, it can be said that the theoretical corrosion weight loss of steel bar using Faraday’s law does not suitable in the presence of initial chloride ions in concrete. The theoretical weight loss corrosion was used only to estimate the test duration required for the expected corrosion weight loss of steel bar.



(a). Concrete with 2 kg/m<sup>3</sup> of chloride (b). Concrete with 5 kg/m<sup>3</sup> of chloride



(c). Concrete with 10 kg/m<sup>3</sup> of chloride

Fig. 5.4 Severity corrosion of steel bars in each chloride contents

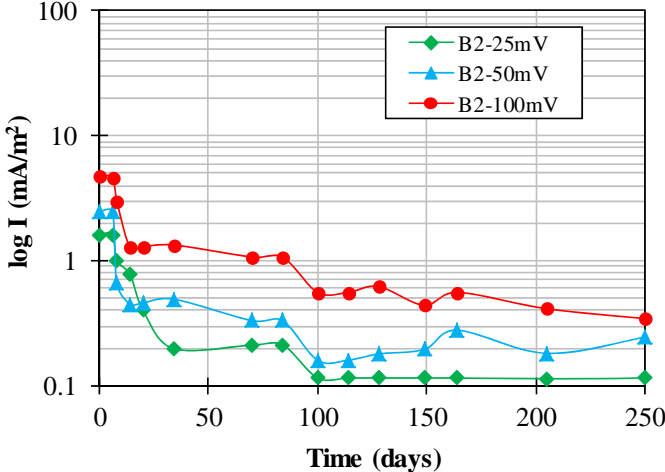
Table 5.2 Corrosion weight loss of steel bars after accelerated corrosion test

Series	Chloride (kg/m <sup>3</sup> )	Test duration (days)	Initial weight (g)	Weight after test (g)	Average weight loss (g)	
					Experiment	Theoretical
B2	2	14	479.87	474.85	5.02	5.05
B5	5	14	481.91	475.43	6.48	5.05
B10	10	6	494.88	487.34	7.49	2.17

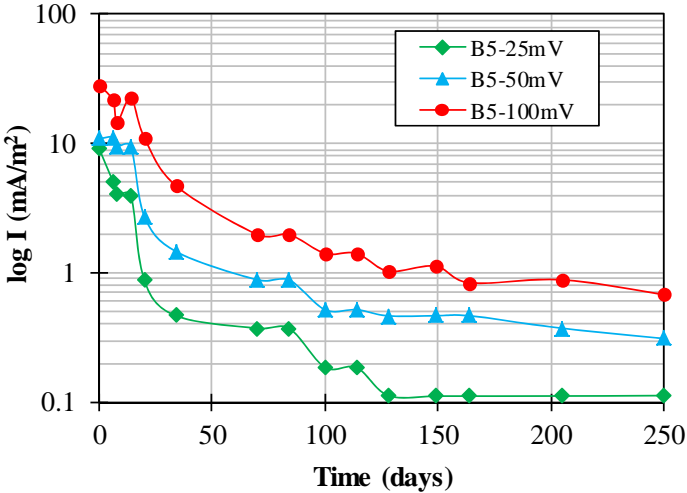
**5.4.2 Protective current**

Figure 5.5 represents the protective current of steel bars versus time. In general, the protective current tends to decrease and stable with time, which indicates the steel bars is protected. From Fig. 5.5, the similar protective current was observed for 25 mV depolarization value in all chloride contents. While 0.18 mA/m<sup>2</sup>, 0.50 mA/m<sup>2</sup> and 0.75 mA/m<sup>2</sup> are required to

achieve the 50 mV depolarization value in concrete with 2 kg/m<sup>3</sup>, 5 kg/m<sup>3</sup> and 10 kg/m<sup>3</sup> of chloride respectively. In the case of 100 mV depolarization value, it was found that protective current of 0.52 mA/m<sup>2</sup>, 1.50 mA/m<sup>2</sup> and 2.25 mA/m<sup>2</sup> were needed in concrete contained 2 kg/m<sup>3</sup>, 5 kg/m<sup>3</sup> and 10 kg/m<sup>3</sup> of chloride respectively. The result indicates that the protective current required depends on the depolarization level of steel bar and chloride content in concrete. In addition, the steady state of the protective current was achieved after 100 days for all chloride contents.

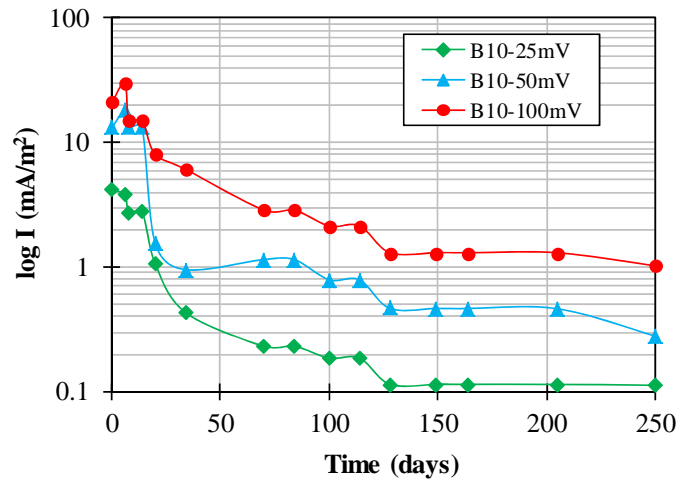


(a). Concrete with 2 kg/m<sup>3</sup> of chloride



(b). Concrete with 5 kg/m<sup>3</sup> of chloride

Fig. 5.5 Protective current of steel bars versus time

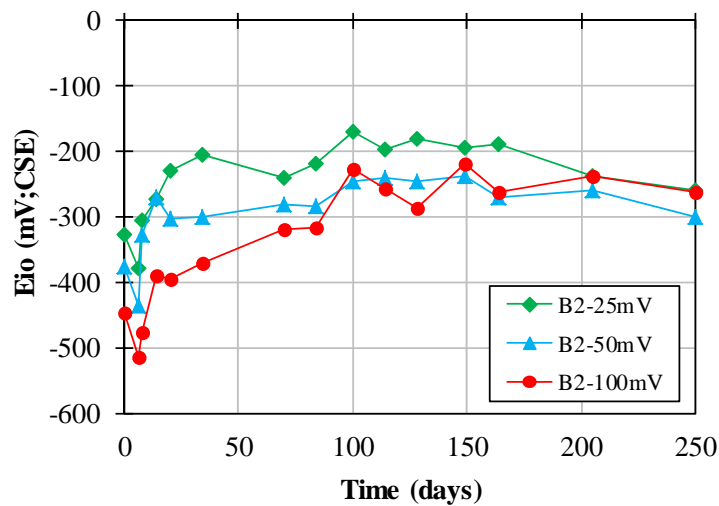


(c). Concrete with 10 kg/m<sup>3</sup> of chloride

Fig. 5.5 (Continued) Protective current of steel bars versus time

### 5.4.3 Instant-off potential ( $E_{i0}$ )

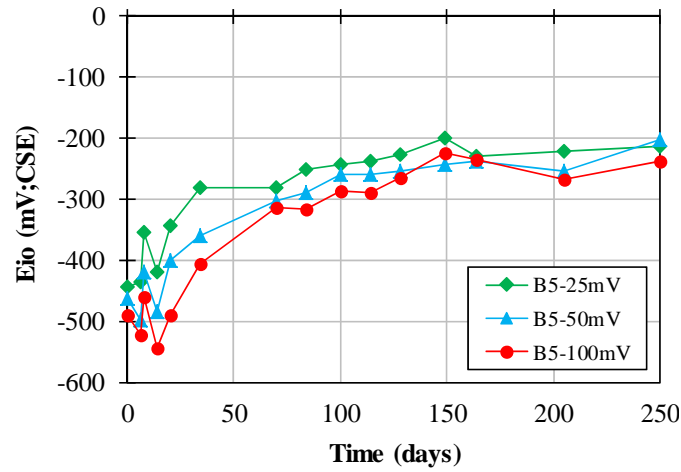
The relationship between the  $E_{i0}$ , potential shift and test periods are shown in Fig. 5.6. The data show that no significant different in  $E_{i0}$  was found with respect to the depolarization values of 25 mV, 50 mV and 100 mV in chloride content of 2 kg/m<sup>3</sup> and 5 kg/m<sup>3</sup>. By adding 10 kg/m<sup>3</sup> of chloride, it is observed that the depolarization value of 100 mV showed the  $E_{i0}$  around -200 mV that lower compare to the 25 mV and 50 mV, was around -150 mV. It means that the depolarization level affected the  $E_{i0}$  in higher chloride content in concrete. Furthermore, the stable condition of the  $E_{i0}$  was reached after 100 days for all chloride contents.



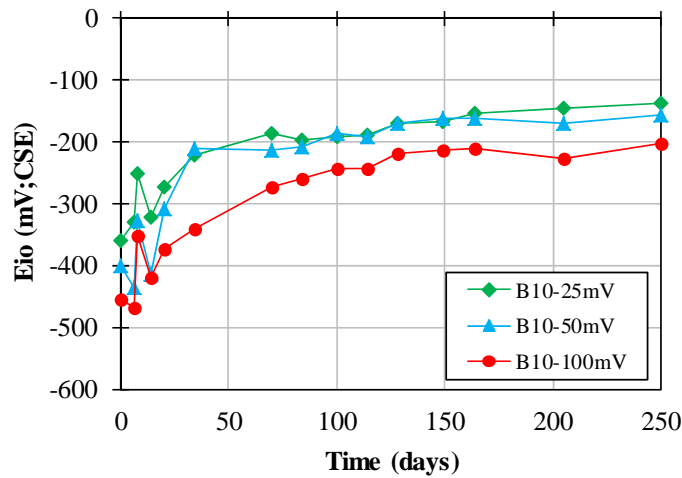
(a). Concrete with 2 kg/m<sup>3</sup> of chloride

Fig. 5.6 The instant-off potential ( $E_{i0}$ ) of steel bars





(b). Concrete with 5 kg/m<sup>3</sup> of chloride

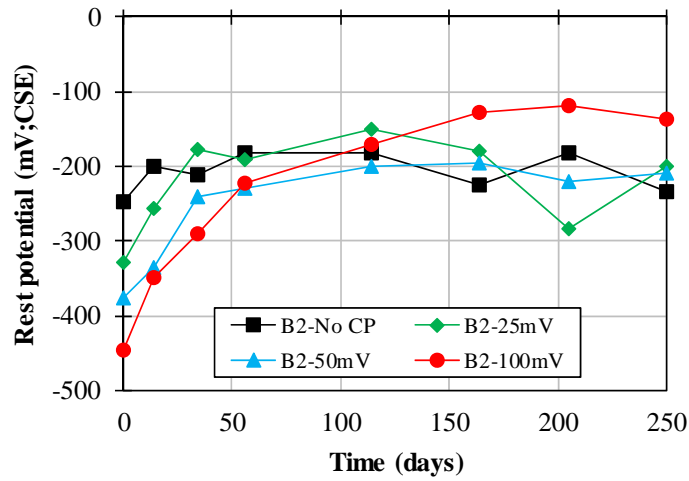


(c). Concrete with 10 kg/m<sup>3</sup> of chloride

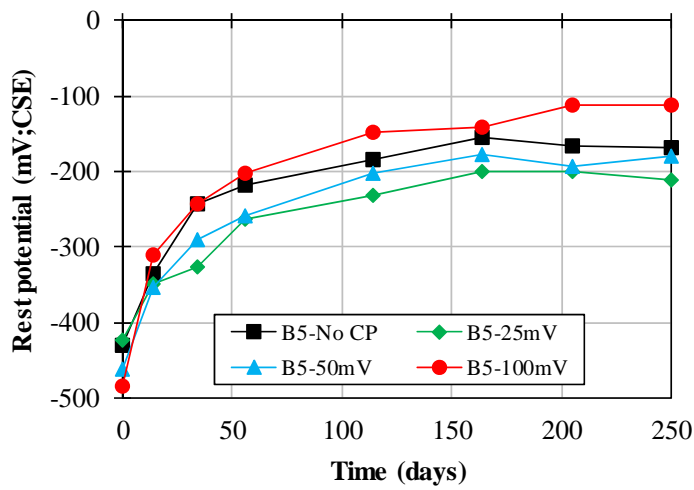
Fig. 5.6 (Continued) The instant-off potential ( $E_{io}$ ) of steel bars

#### 5.4.4 Rest potential of steel bars ( $E_{off}$ )

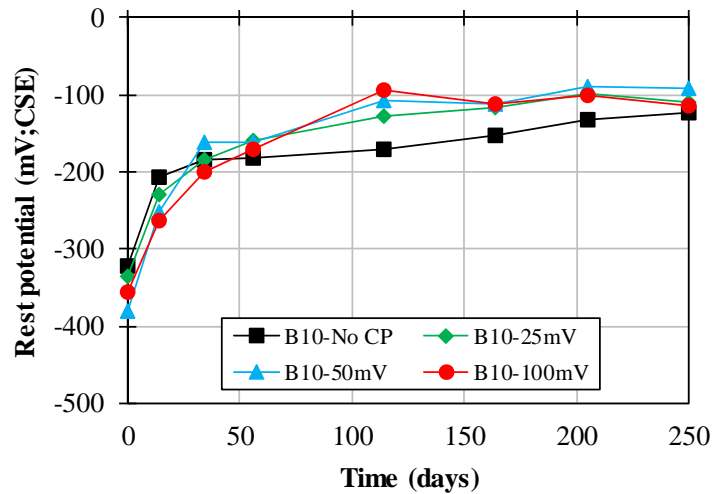
The rest potential of steel bar after switch of from anode for 24 hours is shown in **Fig. 5.7**. It is observed that 100 mV depolarization value showed the higher  $E_{off}$  in concrete with 2 kg/m<sup>3</sup> and 5 kg/m<sup>3</sup> of chloride compare to 25 mV and 50 mV depolarization value. While in concrete with 10 kg/m<sup>3</sup> of chloride, the  $E_{off}$  was similar for 25 mV, 50 mV and 100 mV depolarization. It is may be the effect of chloride content in concrete, which delay the improvement of passivity of steel bar. Overall, the CP current raised the  $E_{off}$  steel to noble value about -200 mV, -150 mV and -100 mV for 2 kg/m<sup>3</sup>, 5 kg/m<sup>3</sup> and 10 kg/m<sup>3</sup> of chloride respectively. These value are categorized 90% no corrosion probability per ASTM C876-09 <sup>(5.5)</sup>. In addition, similar behavior was found in **Chapter 4** relates to the specimens without CP.



(a). Concrete with 2 kg/m<sup>3</sup> of chloride



(b). Concrete with 5 kg/m<sup>3</sup> of chloride



(c). Concrete with 10 kg/m<sup>3</sup> of chloride

Fig. 5.7 Rest potential ( $E_{off}$ ) of steel bars

#### 5.4.5 Polarization resistance ( $R_p$ )

Polarization resistance ( $R_p$ ) of steel bar at the end of testing (250 days) is shown in **Fig. 5.8**. It was observed that the higher chloride content in concrete provided a lower  $R_p$  value. In concrete  $10 \text{ kg/m}^3$  of chloride, the  $R_p$  value of steel bars was lower than  $150 \text{ k}\Omega\cdot\text{cm}^2$  and categorized as low/moderate corrosion rate according to the **Table 3.11** <sup>(5.6)</sup>.

On the other hand, by adding  $2 \text{ kg/m}^3$  and  $5 \text{ kg/m}^3$  of chloride, the  $R_p$  show a passive condition even in the 25 mV depolarization value. In addition, the specimens without CP showed  $R_p$  value around  $100 \text{ k}\Omega\cdot\text{cm}^2$  in all chloride contents. The test results conclude that 25 mV and 50 mV depolarization value is adequate to protect the steel bar against corrosion in concrete with chloride lower than  $5 \text{ kg/m}^3$ .

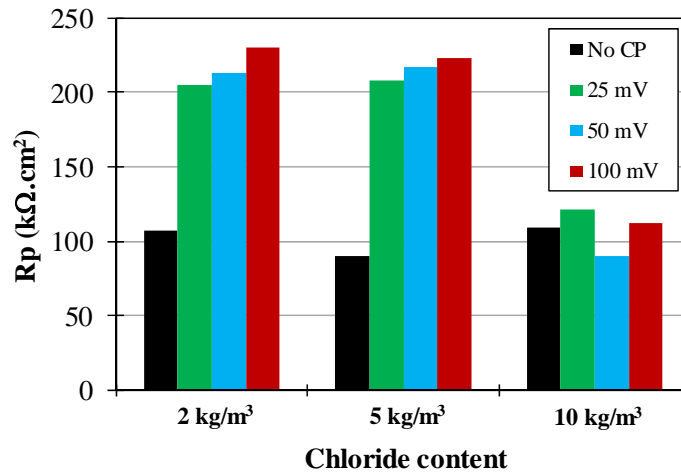


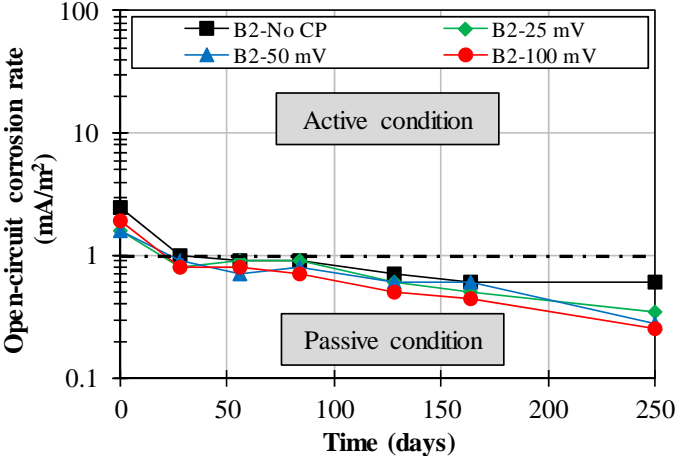
Fig. 5.8 Polarization resistance ( $R_p$ ) of steel bar at the end of testing (250 days)

#### 5.4.6 Corrosion rate of steel bars

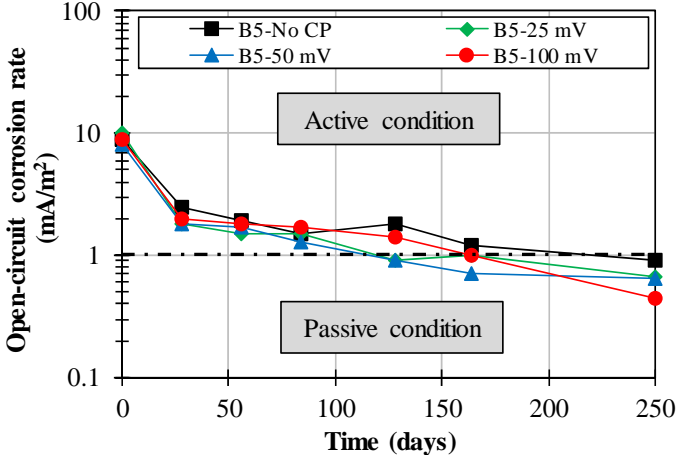
The open-circuit corrosion rate of steel bar versus time is presented in **Fig. 5.9**. The initial corrosion rate were  $3 \text{ mA/m}^2$ ,  $9 \text{ mA/m}^2$  and  $12 \text{ mA/m}^2$  in concrete with  $2 \text{ kg/m}^3$ ,  $5 \text{ kg/m}^3$  and  $10 \text{ kg/m}^3$  of chloride respectively. These values are greater than the limit of the passive state of steel bar of  $1 \text{ mA/m}^2$  <sup>(5.7)</sup>. From that figures, it is found that the open-circuit corrosion rate of steel bar gradually decreased with time due to the CP current. In the case of specimens with  $2 \text{ kg/m}^3$  and  $5 \text{ kg/m}^3$  of chloride, the open-circuit corrosion rate was below  $1 \text{ mA/m}^2$  for all depolarization levels after 250 days.

However, the open-circuit corrosion rate in concrete  $10 \text{ kg/m}^3$  of chloride showed around  $1.5 \text{ mA/m}^2$ , which was higher than the limit passive state of steel bar. It seems that the 100 mV depolarization value does not enough to apply in concrete contained  $10 \text{ kg/m}^3$  of

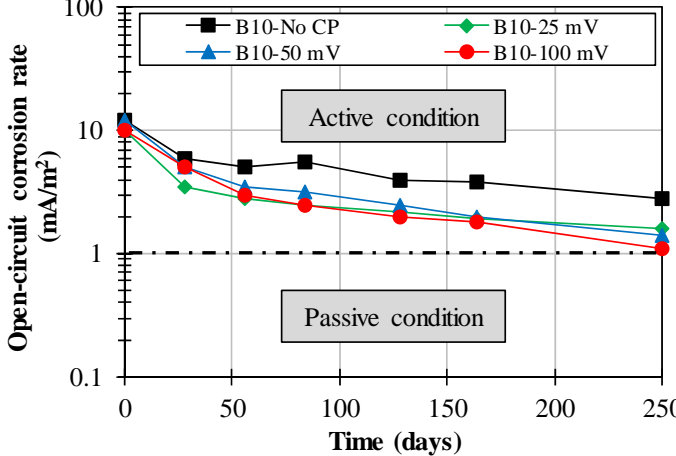
chloride. Further, specimens without CP current showed a higher open-circuit corrosion rate compare to the specimens with CP current.



(a). Concrete with 2 kg/m<sup>3</sup> of chloride



(b). Concrete with 5 kg/m<sup>3</sup> of chloride



(c). Concrete with 10 kg/m<sup>3</sup> of chloride

Fig. 5.9 Reduction in the open-circuit corrosion rate of steel bars with time

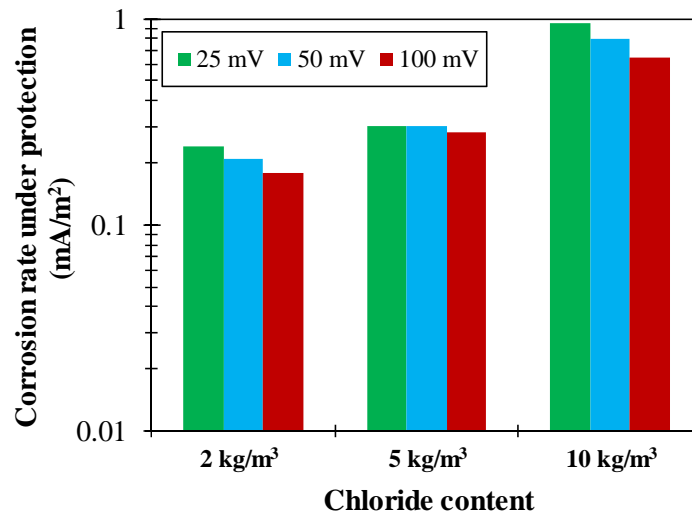


Fig. 5.10 Corrosion rate of steel bars under protection at 250 days

**Figure 5.10** shows the corrosion rate of steel bar under protection at 250 days. It can be seen that the corrosion rate of steel bar was less than  $1 \text{ mA/m}^2$  even in the concrete with  $10 \text{ kg/m}^3$  of chloride. Also, it was observed that the higher depolarization value provided a small corrosion rate. It is concluded that corrosion rate under protection is small than the open-circuit condition due to the presence of protective current at the steel surface.

#### 5.4.7 Corrosion appearances and weight loss corrosion

**Figure 5.11** shows the condition of the steel bars after spilt open for each chloride contents. It was observed that the higher chloride content exhibited larger corrosion area. No significant different corrosion area was found for specimens contained  $10 \text{ kg/m}^3$  of chloride both with and without CP. On the other hand, the specimens with CP showed a better condition than without CP in concrete  $2 \text{ kg/m}^3$  and  $5 \text{ kg/m}^3$ .

The corrosion weight loss of steel bars after CP test is presented in **Fig. 5.12**. It is observed that the effectiveness of the depolarization value of 100 mV, 50 mV and 25 mV can not be judged from the corrosion weight loss of steel bars. However, compare to the weight loss after accelerated corrosion test, it is clearly seen that weight loss slightly decreased after CP test in concrete  $5 \text{ kg/m}^3$  and  $10 \text{ kg/m}^3$  of chloride.



(a). B2 – No CP



(b). B2 – 25 mV



(c). B2 – 50 mV



(d). B2 – 100 mV

Fig. 5.11a Corrosion appearance of steel in concrete with 2 kg/m<sup>3</sup> of chloride



(a). B5 – No CP



(b). B5 – 25 mV



(c). B5 – 50 mV



(d). B5 – 100 mV

Fig. 5.11b Corrosion appearance of steel in concrete with 5 kg/m<sup>3</sup> of chloride



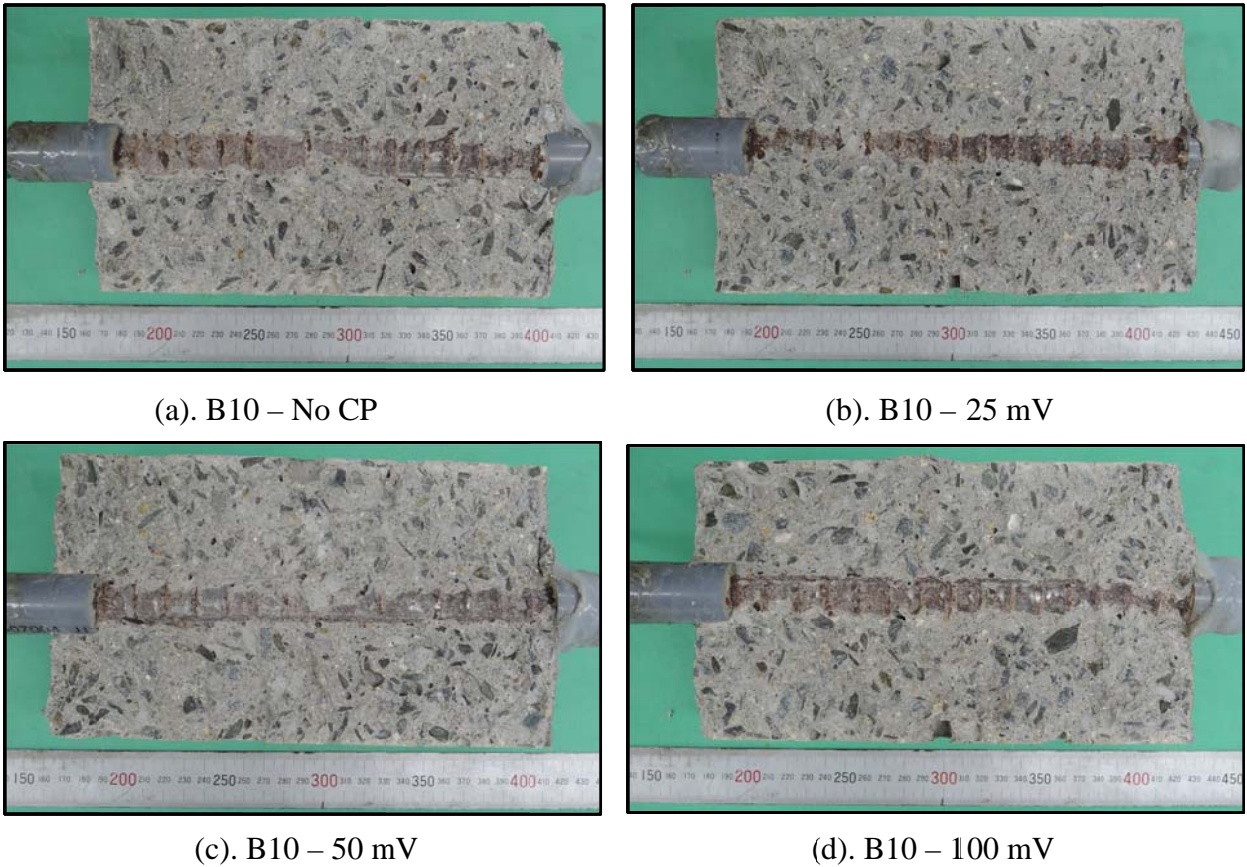


Fig. 5.11c Corrosion appearance of steel in concrete with 10 kg/m<sup>3</sup> of chloride

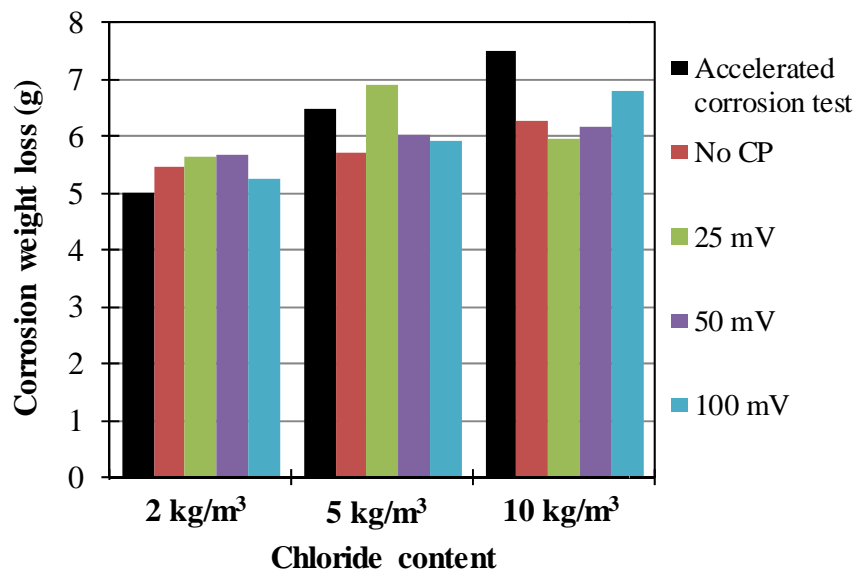


Fig. 5.12 Corrosion weight loss of steel bars after CP test

## 5.5 Conclusions

The purpose of this study is to evaluate the effectiveness of depolarization level less than 100 mV for steel bar in chloride contaminated chloride in the atmospheric exposure zone. The following conclusions can be derived from this study:

1. The amount of depolarization level required to be a function of chloride content in concrete. For instance, when the chloride content is higher, a higher depolarization level is required.
2. Protective current decreased with time and become stable after 100 days. This is stated that the protective current can be reduced during the use of CP.
3. Depolarization levels of 25 mV, 50 mV and 100 mV has raised the polarization resistance of steel bars to passive state in concrete with 2 kg/m<sup>3</sup> and 5 kg/m<sup>3</sup> of chloride. However, the depolarization level should be higher than 100 mV with respect to the polarization resistance in concrete 10 kg/m<sup>3</sup> of chloride.
4. Concerning the open-circuit corrosion rate, the depolarization level less than 100 mV is satisfy in concrete with 2 kg/m<sup>3</sup> and 5 kg/m<sup>3</sup> of chloride.

The results found in the present study suggest that the depolarization level of 25 mV and 50 mV is enough to polarize the steel bar in concrete, with chloride lower than 5 kg/m<sup>3</sup>. Therefore, if the chloride content higher than 5 kg/m<sup>3</sup> of chloride, depolarization level greater than 100 mV is necessary to polarize the steel bar.

## References



- 5.1 Han, M. K., et al, "Cathodic Protection of Concrete Bridge Components," Strategic Highway Research Program (SHRP), Progress Report for Contract SHRP-87-C-102B, April, 1989.
- 5.2 Takewaka, K., "Cathodic Protection for Reinforced Concrete and Prestressed Concrete Structures," Corrosion Science, Vol. 35, 1993, pp. 1617-1626.
- 5.3 Funahashi, M. and Young, W. T., "Investigation of 100 mV Shift Criterion for Reinforcing Steel in Concrete", NACE CORROSION/92, Paper No. 193, 1992.
- 5.4 Fontana, M. B. and Green, N. D., "Corrosion Engineering," McGraw Hill, New York, 1967.
- 5.5 ASTM C 876-95, "Standard Test Method for Half-cell Potentials of Uncoated Reinforcing Steel in Concrete," Philadelphia: American Society of Testing and Materials, 1999.
- 5.6 Mehta, P. K. and Monteiro, P. J. M., "Concrete: Microstructure, Properties and Materials," 3<sup>rd</sup> Ed. New York: Mc Graw Hill, 2006.
- 5.7 Rincon, O. T., et al, "Environmental Influence on Point Anode Performance in Reinforced Concrete," Construction and Building Materials, 22, 2008, pp. 494-503.

## CHAPTER 6. EVALUATING THE EFFECTIVENESS OF CATHODIC PROTECTION METHOD FOR STEEL IN CONCRETE

### 6.1 Introduction

Basically, Cathodic Protection (CP) aims to reduce the corrosion rate and increase resistance of steel bar against aggressive ions by a negative shift in the potential of steel bar. In the atmospherically exposed zone, CP generally operates by the current-induced improvement in the local environment at the steel bar <sup>(6.1)</sup>. The 100 mV of decay potential (depolarization value) is the commonly adopted protection criterion for atmospherically exposure zone. This decay should exclude the effects of IR drop in the concrete <sup>(6.2), (6.3)</sup>. In addition, reduction in the current density after certain periods is very important to prevent the negative effects of CP (i.e. bond loss steel-concrete, hydrogen evolution and anode deterioration).

This study has main aim to evaluate the effectiveness of CP with improvement in the local environment at the steel bars interface. Two CP methods were used: (1) constant current density and (2) constant potential shift from its natural potential of steel bar 24 hours after switch off. Both CP methods were examined in the concrete specimens with corrosive steel bar and high chloride concentration.

### 6.2 Constant CP Current

#### 6.2.1 Preparation of specimens

Concrete specimens with water to cement ratio (W/C) of 60% and contained chloride (sodium chloride) of 10 kg/m<sup>3</sup> were manufactured. Materials and dimensions of specimen are similar those in **Chapter 4** and **5**. Mix proportion of concrete is presented in **Table 6.1**.

Table 6.1 Mix proportion of concrete

W/C (%)	Water (kg/m <sup>3</sup> )	Cement (kg/m <sup>3</sup> )	Sand (kg/m <sup>3</sup> )	Gravel (kg/m <sup>3</sup> )	NaCl (kg/m <sup>3</sup> )	AEWR (kg/m <sup>3</sup> )	AE (mL/m <sup>3</sup> )
60	190	317	853	969	16.48	0.99	792

AEWR: Air Entrained Agent Water Reducer; AE: Air Entrained Agent

In order to generate corrosive condition on the surface of steel bar, the protective film of steel bars were cleaned, then dry/wet cycle's sprayed by 3% NaCl solution (one day wet : one day dry) were carried out for two weeks (**Fig. 6.1**). Both end of steel bar were covered with plastic tape to keep the exposed length of 180 mm before embedded in concrete. After 24 hours casting, all specimens were demoulded and cured under sealed conditions in a wet towel for 28 days. **Figure 6.2** shows detail of concrete specimen.



Fig. 6.1 Steel bars preparation: (a). before; (b). after dry/wet cycles sprayed

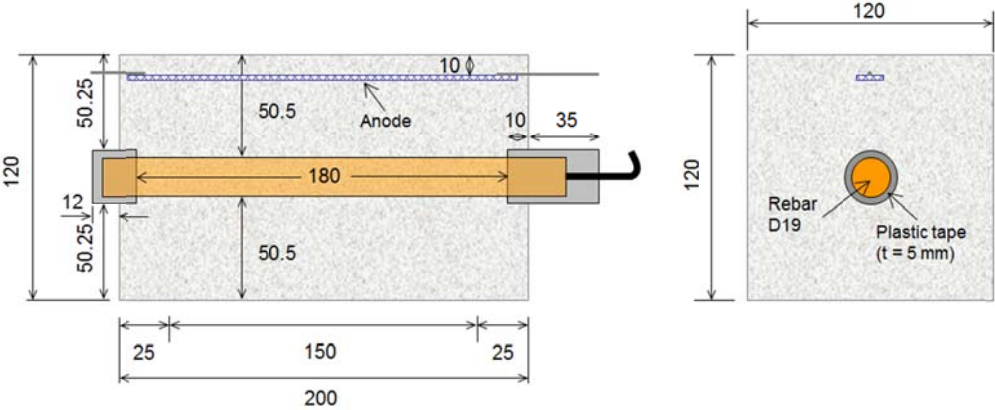


Fig. 6.2 Detail of specimen design (unit: millimeter)

Prior to the CP tests, additional accelerated corrosion tests were performed due to the corrosion rate of steel bar is smallest. In this case, the current supply was reduced gradually for cancel of potential slope. **Figure 6.3** shows reduction of current supply during accelerated corrosion test. In addition, duration of the accelerated corrosion test was around 15 days. The schematic of accelerated corrosion test is shown in **Fig. 6.4**.

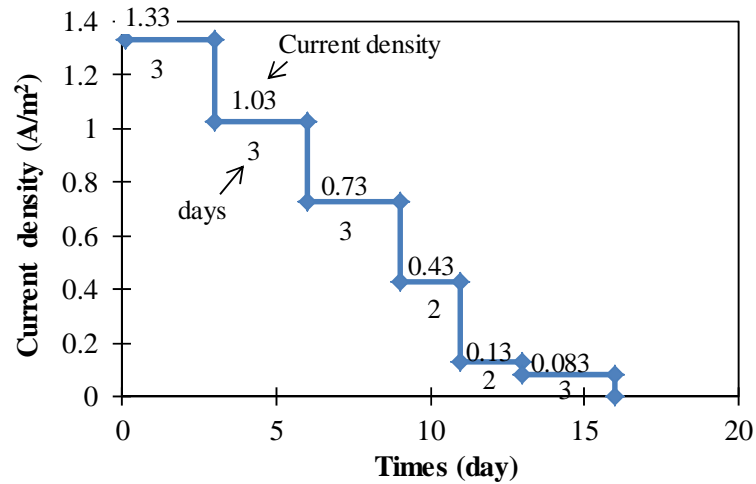


Fig. 6.3 Reduction of current supply during accelerated corrosion test

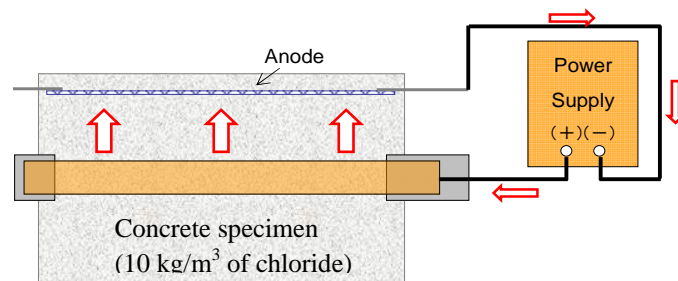


Fig 6.4 Setup of accelerated corrosion test (anode was used as counter electrode)

### 6.2.2 Cathodic protection (CP) instrumentation

The amount of current density was calculated by shifting the natural potential of steel bar ( $E_{\text{off}}$ ) to negative direction at the initial stage (0 day) for 24 hours. The  $E_{\text{off}}$  of steel bar was shifted 25 mV, 50 mV and 100 mV and represent as instant-off potential ( $E_{\text{io}}$ ). The difference between  $E_{\text{off}}$  and  $E_{\text{io}}$  after 24 hours is defined as  $\Delta E$ . Simple interpolation method was used if the  $\Delta E$  is higher or less than 25 mV, 50 mV and 100 mV. The example below shows how to calculate the current density at the initial stage.

Target of  $\Delta E = 25$  mV;  $E_{\text{off}} = -392$  mV;  $E_{\text{io}} = -448$  mV; protective current ( $I$ ) = 0.50 mA; surface area of steel bar =  $107.4 \text{ cm}^2$ .

$\Delta E = E_{\text{off}} - E_{\text{io}} = -392 \text{ mV} - (-448 \text{ mV}) = 56 \text{ mV} > 25 \text{ mV}$ . Interpolation method was used to calculate the protective current required for 25 mV potential shift as follows:

$0.50 \text{ mA} : 56 \text{ mV} = x \text{ mA} : 25 \text{ mV} \rightarrow x = 0.22 \text{ mA}$  or  $21 \text{ mA/m}^2$  to steel bar surface. This value was kept continuously during CP tests.

The schematic of CP is shown in **Fig. 6.5**. The negative terminal of power supply connected to the steel bar and positive terminal to the anode. The amount of current density was

adjusted via power supply. Six levels constant of current density were maintained to the concrete specimens and kept continuously during CP test. In addition, two specimens without CP were prepared as control. Summary of specimen tests are presented in **Table 6.2**.

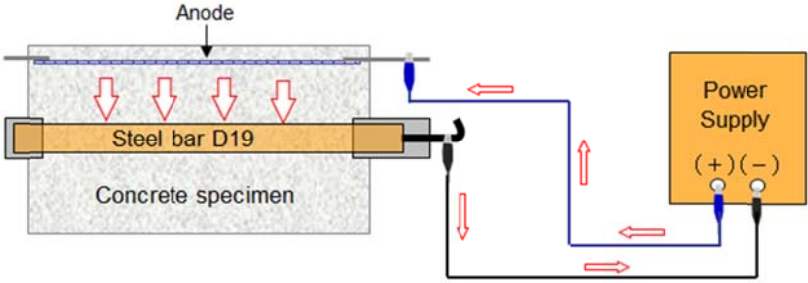


Fig. 6.5 Schematic of CP test

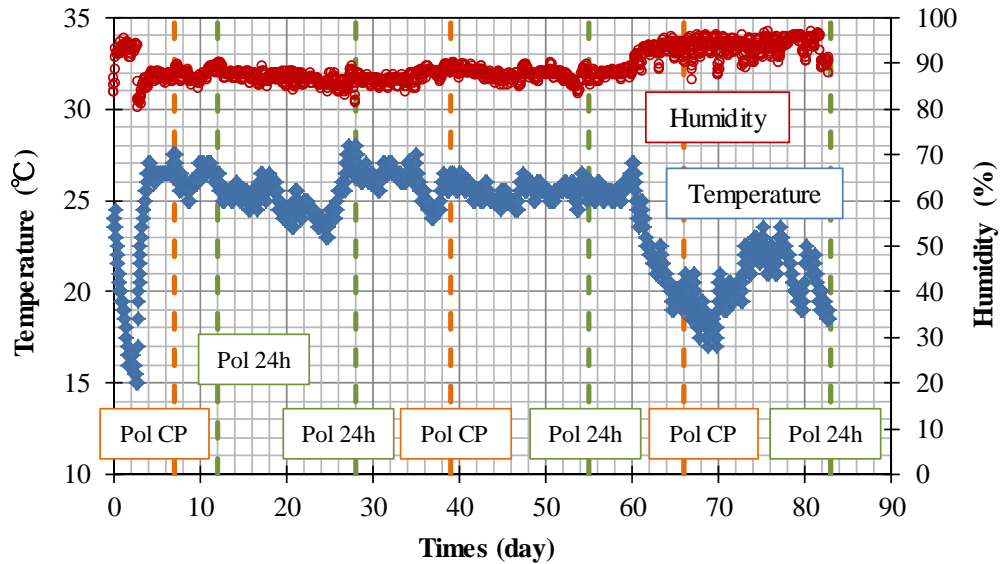
Table 6.2 Summary of the specimen tests (constant CP current)

No	$\Delta E$ target (mV)	Current density (mA/m <sup>2</sup> )	Current to electrode length (mA/m)
1	25	21	1.2 (< 3.5*)
2	25	21	1.2 (< 3.5)
3	50	43	2.4 (< 3.5)
4	50	35	1.9 (< 3.5)
5	100	112	6.3 (> 3.5)
6	100	156	8.8 (> 3.5)
7 (No CP1)	-	-	-
8 (No CP2)	-	-	-

\*Anode performance: 3.5mA/m is maximum value for design CP <sup>(6.4)</sup>.

### 6.2.3 Electrochemical tests

Instant-off potential of steel bar and anode ( $E_{i0}$ ), rest potential of steel bar and anode after 24 switch off ( $E_{off}$ ), depolarization tests, polarization resistance of steel bar ( $R_p$ ), polarization curve and corrosion rate of steel bars were carried out with similar methods and testing equipment in **Chapter 4**. Corrosion rate under CP was measured at 7, 39 and 66 days and for the open-circuit corrosion rate at 12, 55, and 83 days. The borderline corrosion rate for passive steel bar in concrete is considered to be 1 mA/m<sup>2</sup> <sup>(6.5)</sup>. In addition, all specimens were exposed in air curing at temperature (T) of 20±5°C and relative humidity (RH) of 90% for 83 days as shown in **Fig. 6.6**.



- Pol CP: polarization test under CP (7, 39, 66 days).
- Pol 24h: polarization test after 24 hours CP off (12, 55, 83 days).

Fig. 6.6 Temperature and humidity conditions during CP tests

## 6.2.4 Results and Discussion

### a. Instant-off potential ( $E_{i0}$ ) of steel bar and anode

The relationship between the  $E_{i0}$  and exposure time is presented in **Fig. 6.7**. Except specimen No.5\_112mA/m<sup>2</sup>, it was observed that the  $E_{i0}$  of steel bar increased up to 50 days exposure for all specimens even with small current density of 20 mA/m<sup>2</sup>. After 50 days, specimen No. 1, 2, 3 and 4 was reached a stable condition. While specimen No.6\_156mA/m<sup>2</sup> showed decreasing trend at the end of exposure periods. This is due to the increasing of dissolved oxygen (DO).

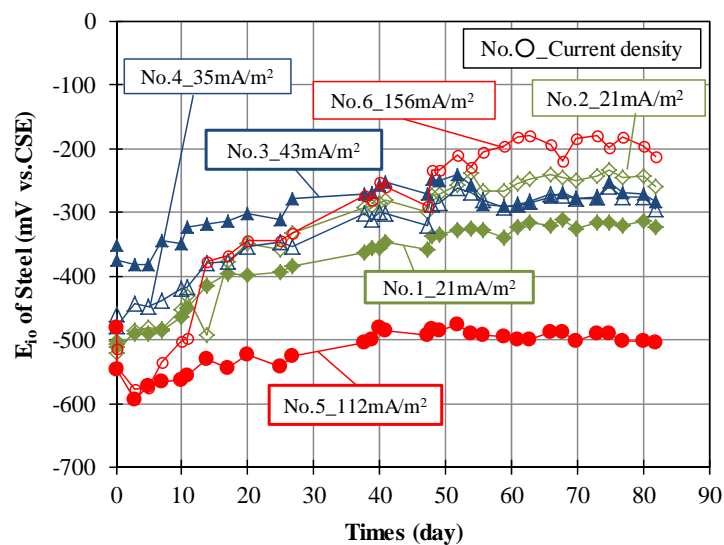


Fig. 6.7 Instant-off potential ( $E_{i0}$ ) of steel bars versus exposure time

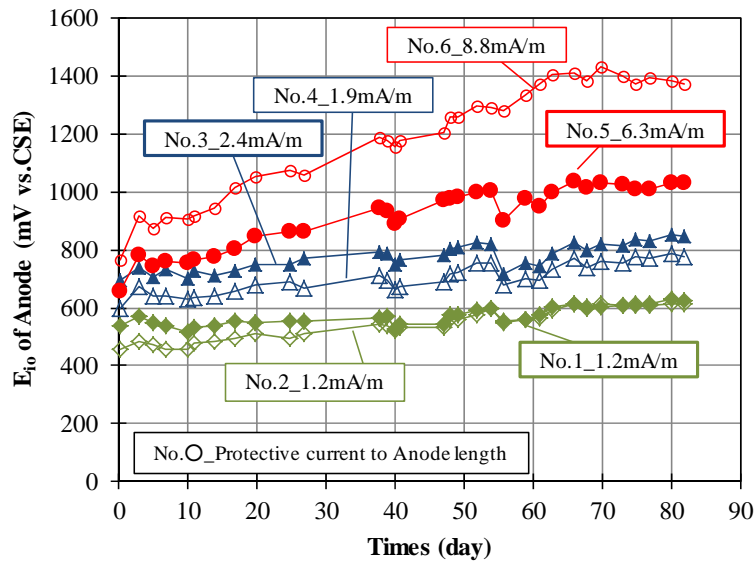


Fig. 6.8 Instant-off potential ( $E_{i0}$ ) of anode

**Figure 6.8** shows the  $E_{i0}$  of anode versus time. Variation of the  $E_{i0}$  of anode with protective current is clearly seen in view of the fact that a larger protective current, a higher  $E_{i0}$  of anode value would result. It was also observed that the protective current larger than 3.5 mA/m of length anode showed an increasing  $E_{i0}$  value with time. On the contrary, no significant change in  $E_{i0}$  value was observed for protective current less than 3.5 mA/m of length anode. Test results conclude that the larger current density could reduce the performance of anode and possible creates deleterious effects such as bond degradation between steel-concrete and hydrogen embrittlement.

### b. Depolarization tests

**Figure 6.9** shows the depolarization value of steel bars with time. It is found that the depolarization value of steel bars tends to increase with time. After 11 days of polarization, specimen No.1\_21mA/m<sup>2</sup> and No.2\_21mA/m<sup>2</sup> provides depolarization value of 40 mV and 46 mV respectively. However, these specimens satisfy the 100 mV depolarization value after 83 days exposure. For specimen No.3\_43mA/m<sup>2</sup> and No.4\_35mA/m<sup>2</sup> satisfies the 100 mV depolarization value after 28 days. On the other hand, No.5\_112mA/m<sup>2</sup> and No.6\_156mA/m<sup>2</sup> achieved 100 mV depolarization value after 11 days. At the end of tests, the specimen with larger current density (No.6\_156mA/m<sup>2</sup>) showed decreasing of depolarization value. It is conclude that to obtain 100 mV depolarization value, a larger current density does not require at the beginning of polarization. But, it will be achieved after several time by apply a small current density.

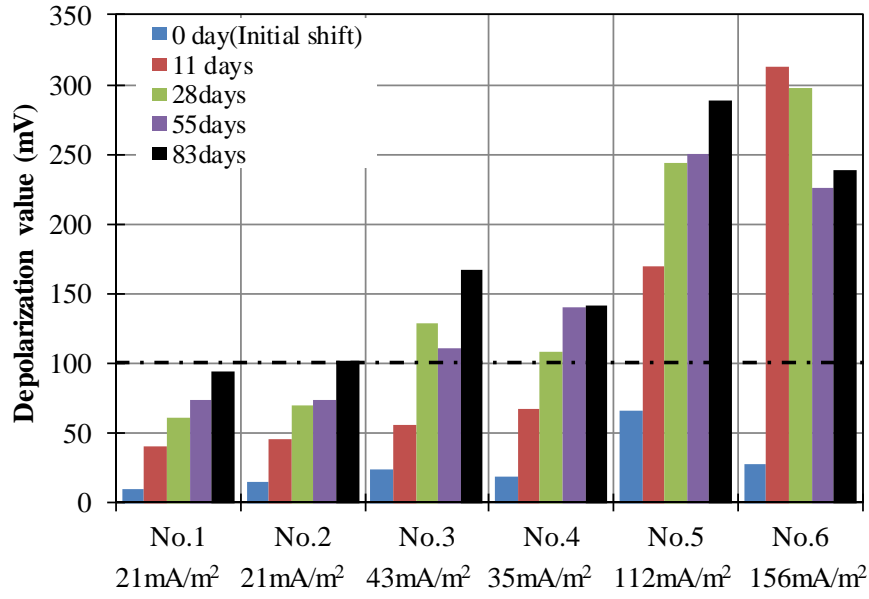


Fig. 6.9 Depolarization value of steel bars ( $E_{off} - E_{io}$ )

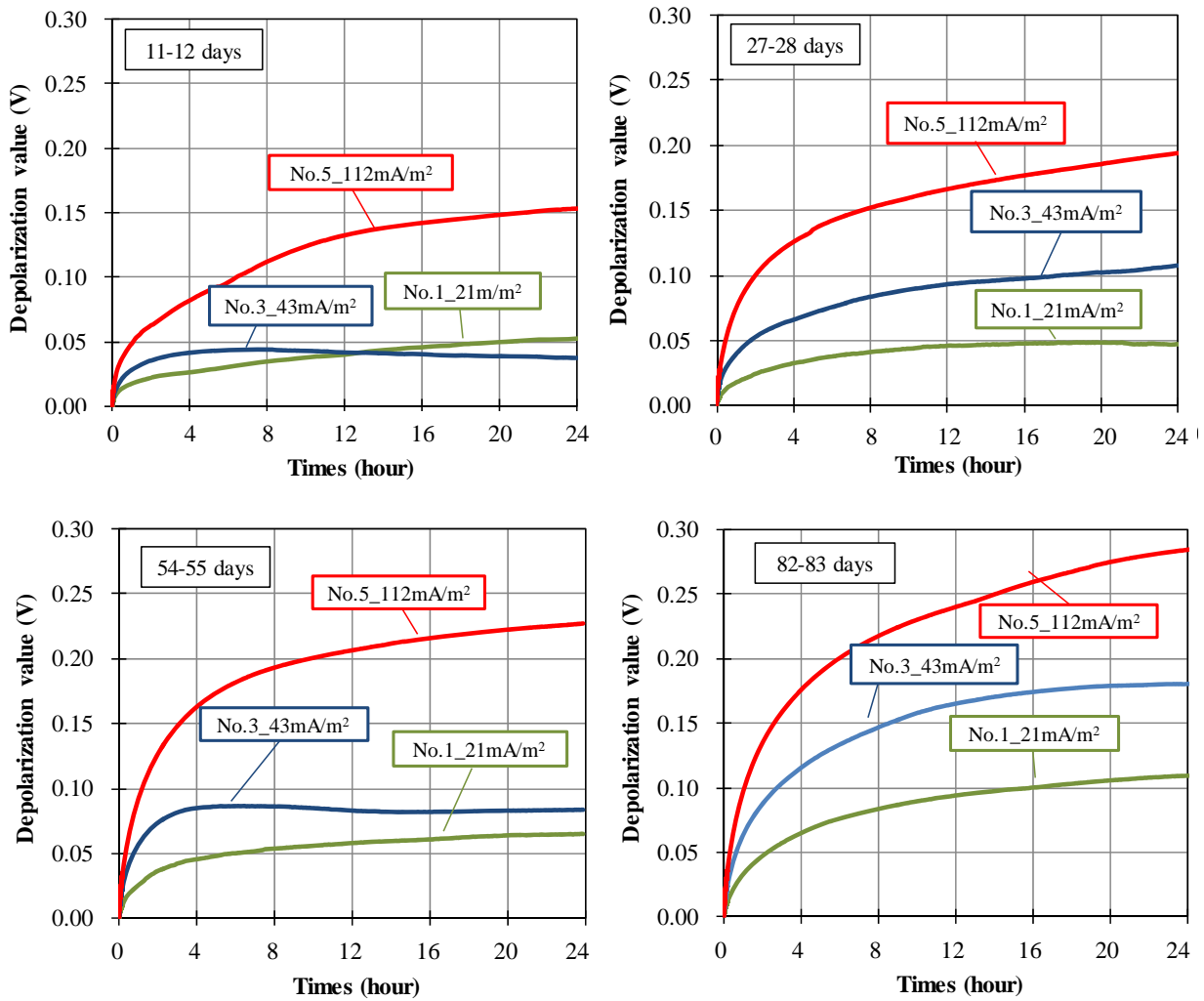


Fig. 6.10 Time dependence of depolarized of steel bars



Time dependence of depolarized steel bar during 24 hours disconnecting from anode are shown in **Fig. 6.10**. It is observed that the depolarization curve increased with exposure time which indicates that improvement of steel condition due to CP current. Also, the decay curve does not decrease at the final time of depolarization test.

**c. Rest potential ( $E_{off}$ ) of steel bars and anode**

The rest potential ( $E_{off}$ ) of steel bars versus time is presented in **Fig. 6.11**. It is found that the rest potential of all steel bars increased with time and classified as 90% no corrosion <sup>(6.6)</sup>. It indicates that the passivity of steel bar is improved. For specimens without CP, it is observed that the natural potential ( $E_{corr}$ ) of steel bars also increased with time (**Fig. 6.12**). This phenomenon also found in **Chapter 4** and **Chapter 5** in the case of specimens without CP. In this study, the specimen without CP could not judge based on the potential value only.

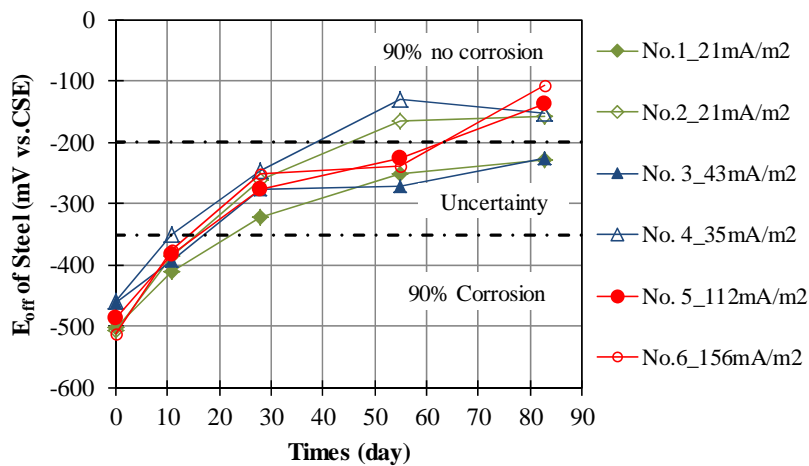


Fig. 6.11 Rest potential ( $E_{off}$ ) of steel bars

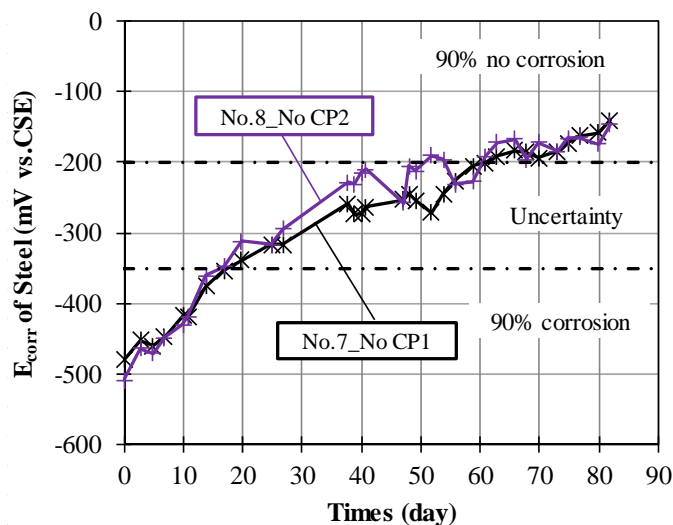


Fig. 6.12 Natural potential ( $E_{corr}$ ) of steel bar without CP

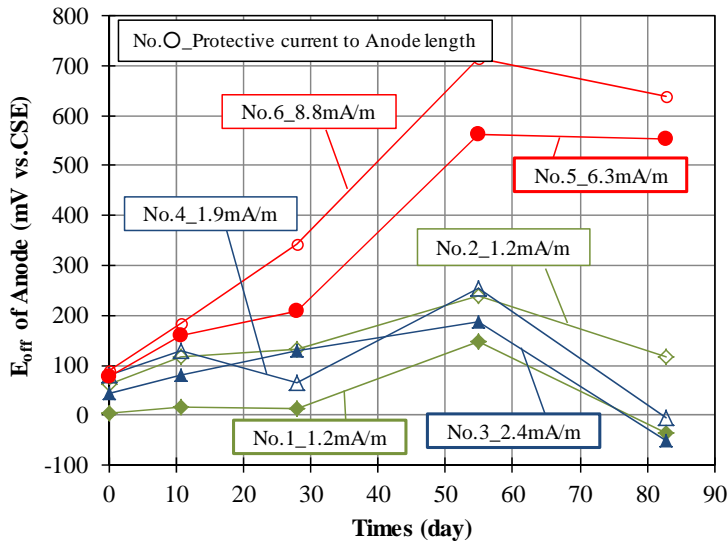


Fig. 6.13 Rest potential of anode with time

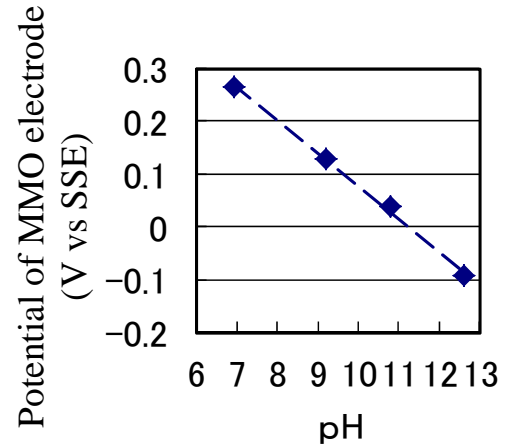


Fig. 6.14 Relationship between potential of MMO anode and pH

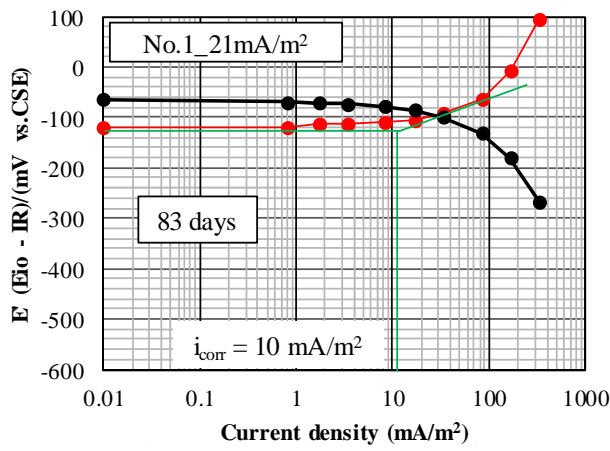
From the **Fig. 6.13**, it is observed that specimens with larger current density tend to increase in anode potential versus time. This is caused by decreasing of pH by the anodic reaction (**Fig. 6.14**). It can be said that the current density value higher than 3.5 mA/m of length anode may deteriorate early.

#### d. Corrosion rate

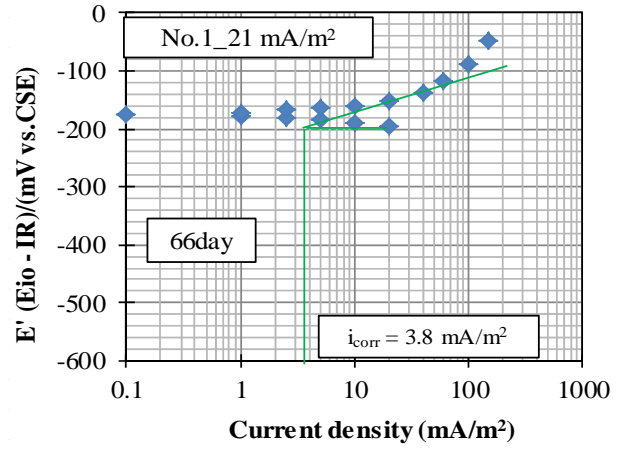
The corrosion rate of steel bar was calculated by polarization curve. **Figure 6.15** shows the polarization curve specimen No.1\_21mA/m<sup>2</sup> for both the open-circuit and under protection condition. In addition, summary of corrosion rate for open-circuit and under protection are presented in **Fig. 6.16**. From that figures, it is found that the corrosion rate under CP is small compare to the open-circuit condition. In the case of open-circuit condition, corrosion rate of steel bars was located within active condition for all specimens. On the other hand, corrosion rate of steel bar under CP current decreased with time and that classified as passive condition for the specimens with current density larger than 21mA/m<sup>2</sup> (No.3 to No.6) at the end of test periods. Meanwhile, current density of 21mA/m<sup>2</sup> (No.1 and No.2) showed in active condition, however, the corrosion rate tends to decreased with exposure time. Results of test reveal that the CP for steel in concrete should be design with small current density by considering environment improvement effects.

**Figure 6.17** shows the corrosion rate of steel bar without CP current. It is observed that the corrosion rate of steel bar in the range of passive condition around 10 mA/m<sup>2</sup>. Although the specimens without CP current showed an increase in the  $E_{corr}$ , the corrosion rate of steel bar

is higher. This indicates that the judgement of steel bar corrosion is more realistic based on the corrosion rate value than potential value in the present condition.



(a). Open-circuit condition



(b). Under CP current

Figure 6.15 Polarization curve and estimation of corrosion rate (No.1\_21mA/m<sup>2</sup>)

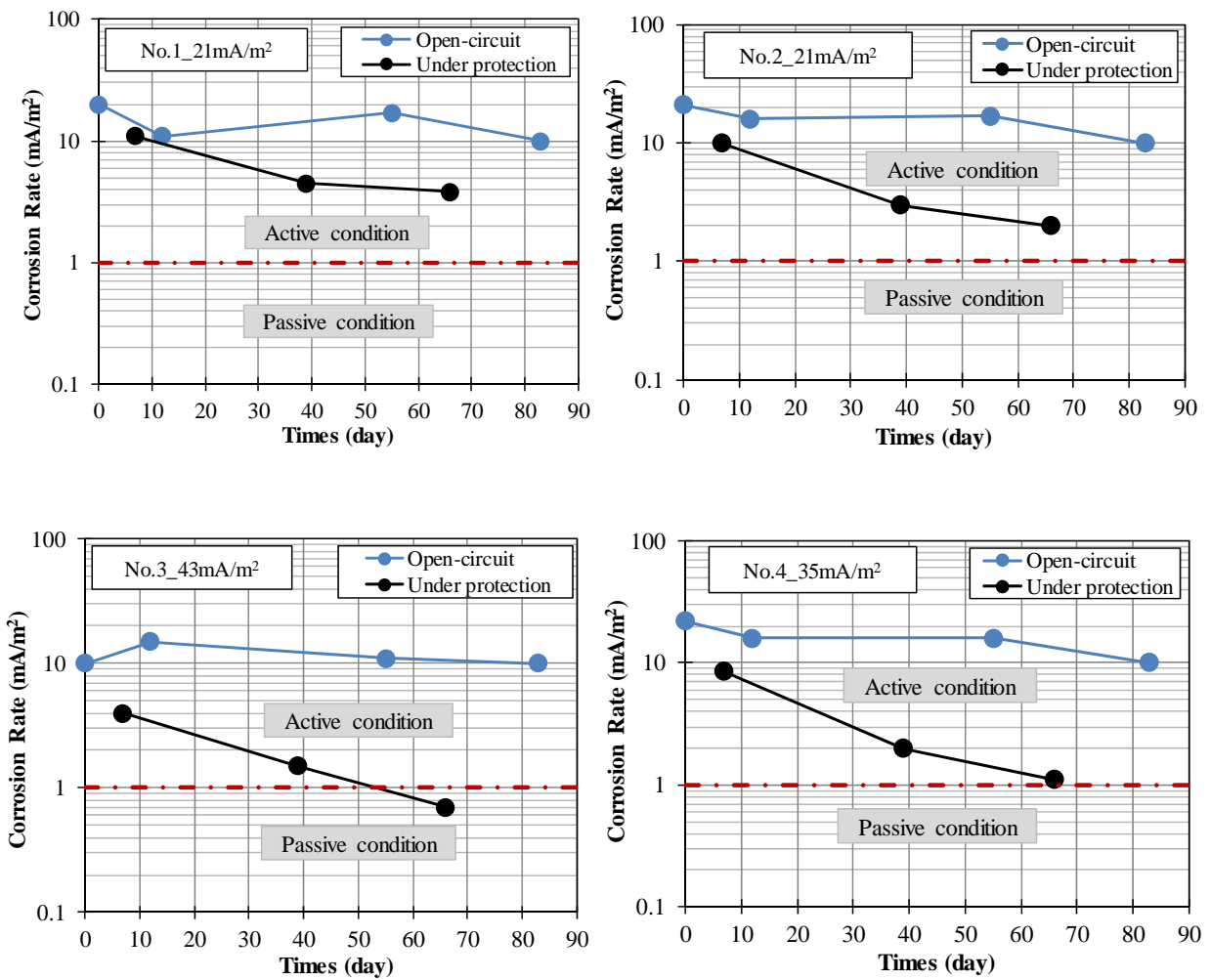


Fig. 6.16 Corrosion rate of steel bar with time

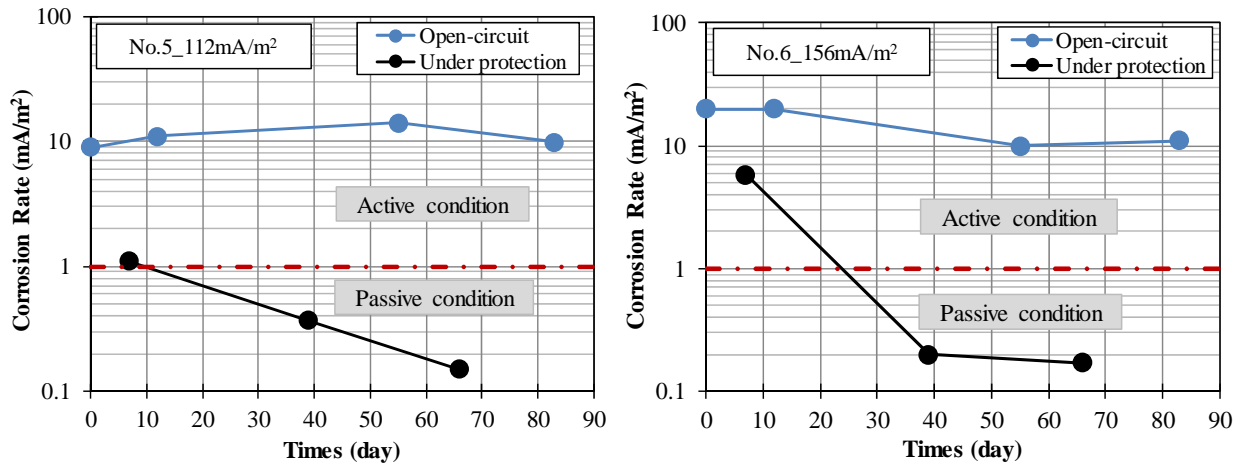


Fig. 6.16 (Continued) Corrosion rate of steel bar with time

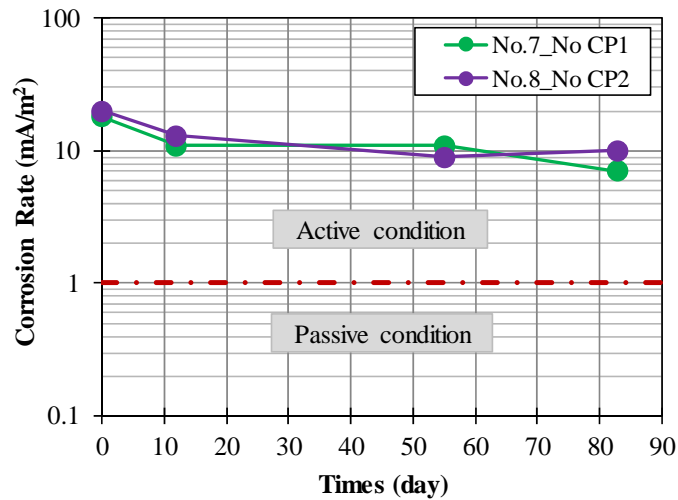


Fig. 6.17 Corrosion rate of steel bar without CP

## 6.3 Constant Potential Shift

### 6.3.1 Method of evaluation

In this test, no additional accelerated corrosion test was performed to the concrete specimen prior CP tests. It means that the initial corrosion rate of steel bar is lower compare to those in the constant CP current method. All specimens were exposed in air curing at constant room temperature of  $20\pm 2^\circ\text{C}$  and relative humidity of 60% during CP test. Exposure period was around 130 days. In total, four concrete specimens were examined as listed in **Table 6.3**.

Similar electrochemical tests were performed in the constant CP current and just different in the method of apply protection. For this, the  $E_{\text{off}}$  of steel bar was shifted 25 mV, 50 mV and 100 mV. Current density was adjusted to achieve these values and repeated after

depolarization test. After 24 hours connected to the CP, the  $E_{i0}$  of steel bar was adjusted again to achieve the actual potential shift of 25 mV, 50 mV and 100 mV. **Figure 6.18** illustrated the CP method used in this experiment. Furthermore, all electrochemical tests were performed using similar procedures and testing equipment from those used in constant CP current.

Table 6.3 Summary of specimen tests (constant potential shift)

No	Series	Potential shift (mV)
1	No CP	0
2	25 mV	25
3	50 mV	50
4	100 mV	100

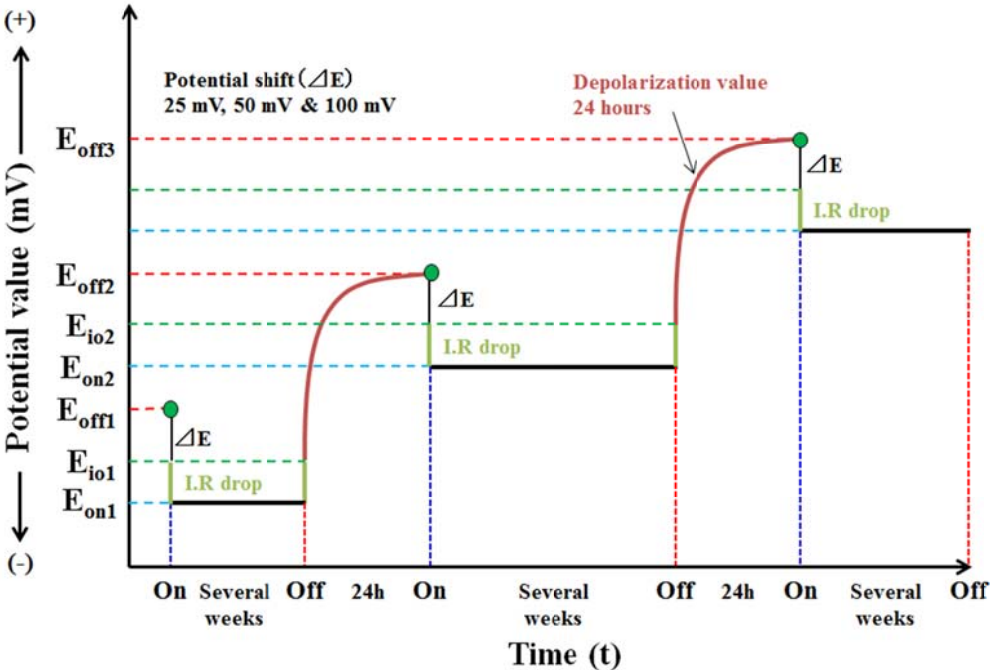


Fig. 6.18 CP method with constant potential shift

**6.3.2 Results and discussion**

**a. Instant-off potential ( $E_{i0}$ ) of steel bars**

**Figure 6.19** shows the instant-off potential ( $E_{i0}$ ) of steel bars versus time for all potential shift. It can be observed that 25 mV and 50 mV of potential shift provide a constant  $E_{i0}$  respect with time. By potential shifting of 100 mV, the  $E_{i0}$  moved significantly to noble

value at 60 days. However, the  $E_{i0}$  becomes stable after 60 days exposure, which represents unchanged condition of the steel bar <sup>(6.1)</sup>.

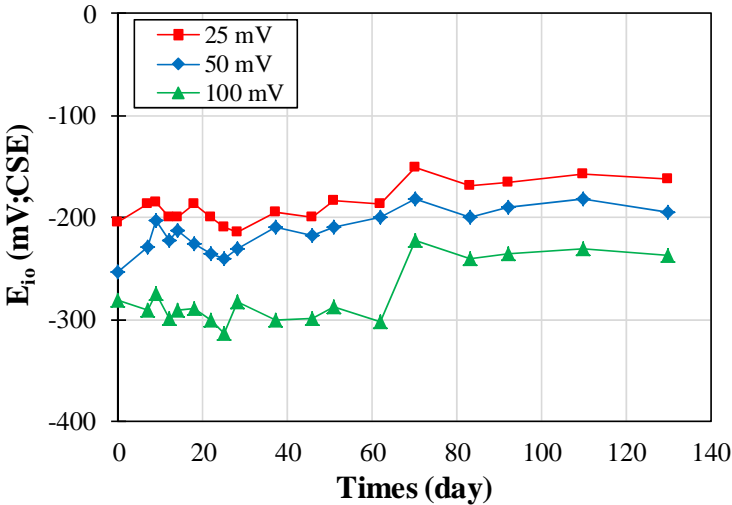


Fig. 6.19 The instant-off potential ( $E_{i0}$ ) of steel bars versus time

**b. Protective current (I)**

From **Fig. 6.20**, the initial protective current is less than 3.5 mA/m of length anode in all potential shifts. It is observed that the protective current of steel decreased with increasing exposure time. After 60 days, no significant changes in protective current were observed. By comparing the protective current required for the specimens with 10 kg/m<sup>3</sup> of chloride in **Chapter 5**, it is found that the protective current is large due to the effect of surface condition of steel bars. It can be said that the protective current require depends on the worse condition of steel bars.

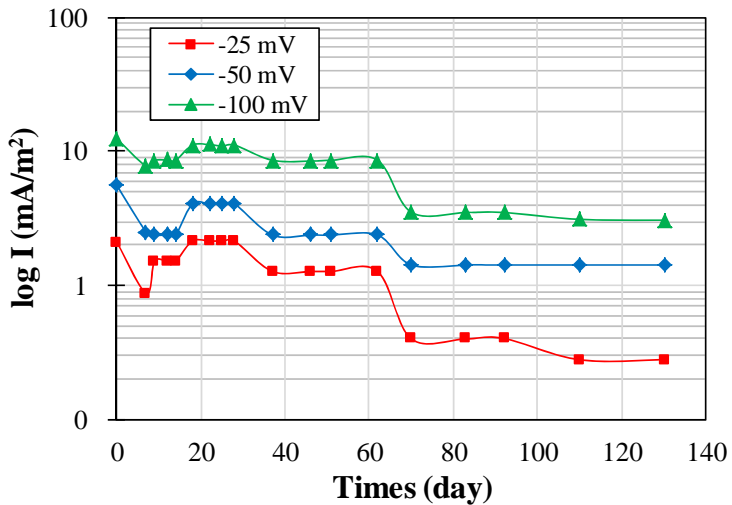


Fig. 6.20 Protective current (I) of steel bars with time

### c. Depolarization tests

Figure 6.21 shows the depolarization values each of steel bar respect with time. The depolarization value increased up to 56 days. The 100 mV depolarization value was achieved at 14 and 28 days for potential shift of 100 mV and 50 mV respectively. Afterwards, the depolarization value tends to decrease in all potential shifts. Possible reasons for these due to the removal of oxygen from the steel bar due to the anodic reaction or insufficient of protective current. Therefore, by shifting 100 mV the depolarization value is still higher than 100 mV. This result suggests that the possibility of decreasing the protective current of steel bar.

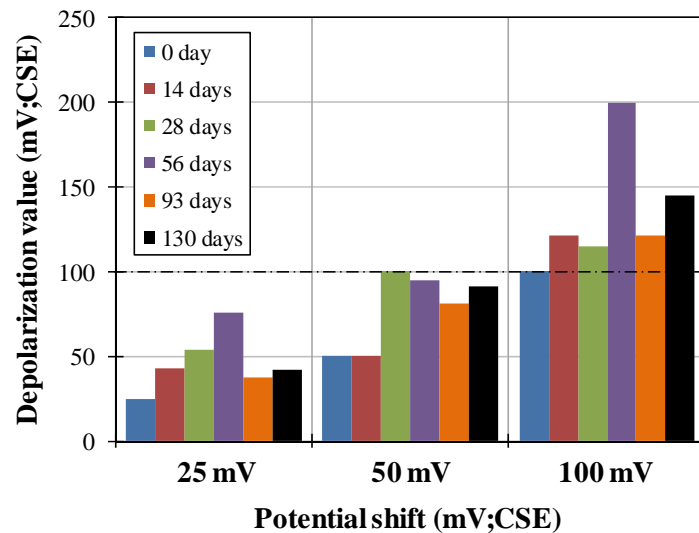


Fig. 6.21 Depolarization value of steel bars versus time

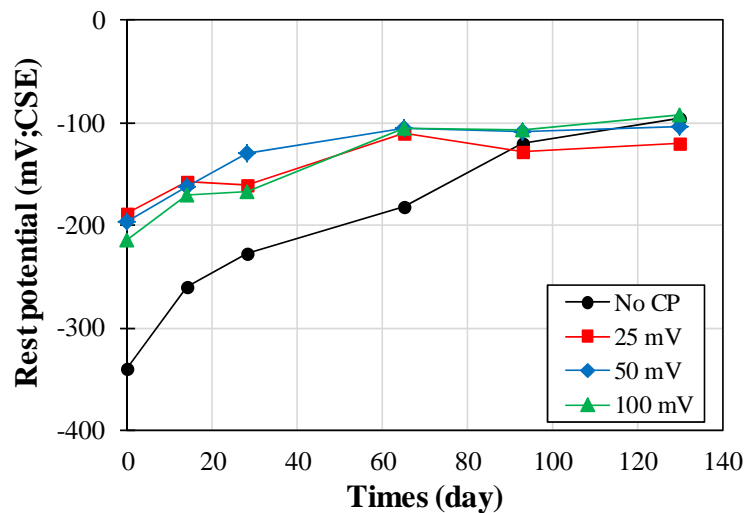


Fig. 6.22 Rest potential ( $E_{off}$ ) of steel bars with time

Figure 6.22 represents the time-dependent change in the rest potential ( $E_{off}$ ) of steel bars after 24 hours disconnecting from anode. It is clearly seen that the  $E_{off}$  was increased substantially until 60 days even in the small potential shift, which indicates improvement of

passivity condition of steel bars due to CP current. Also, the steel bars is categorized as 90% no probability of corrosion <sup>(6.6)</sup>.

**d. Corrosion rate and polarization resistance of steel bars ( $R_p$ )**

The corrosion rates of steel bars both open-circuit and under protection is presented in **Fig. 6.23**. Corrosion rate of steel bars under protection is lower than the open-circuit condition. Also, the specimen without protection (No CP) showed the corrosion rate more than  $1 \text{ mA/m}^2$  at the end of test periods.

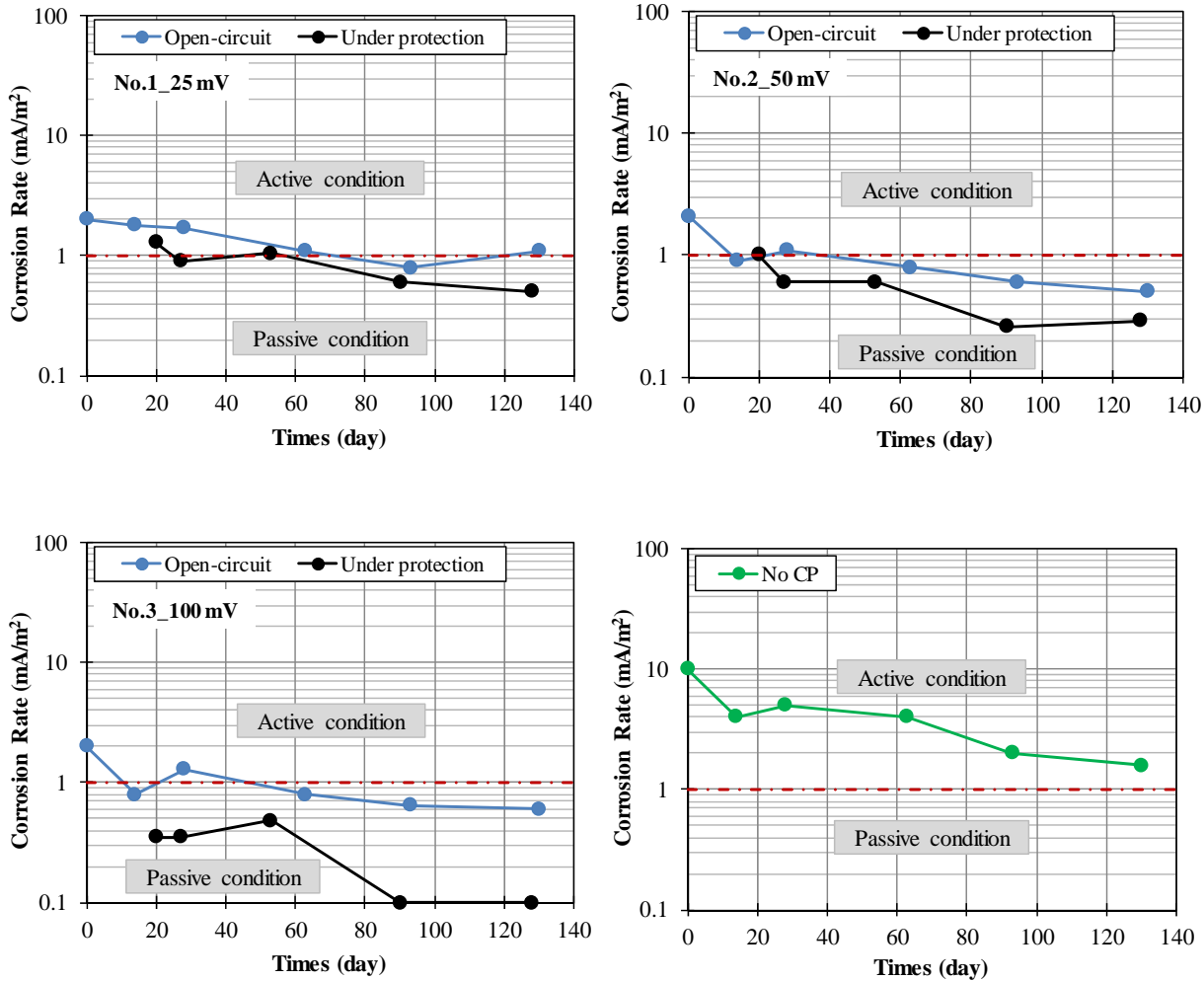


Fig. 6.23 Corrosion rate of steel bars both open-circuit and under protection condition

In the view point of polarization resistance (**Fig. 6.22**), it is observed that the  $R_p$  decreased after 60 days exposure. The  $R_p$  value around  $25 \text{ k}\Omega\cdot\text{cm}^2$ ,  $50 \text{ k}\Omega\cdot\text{cm}^2$ ,  $55 \text{ k}\Omega\cdot\text{cm}^2$  for specimens with 25 mV, 50 mV and 100 mV of potential shift respectively and  $15 \text{ k}\Omega\cdot\text{cm}^2$  without CP. Although the  $R_p$  value of specimens with protection is decreased, the  $R_p$  value with CP still higher than without CP.



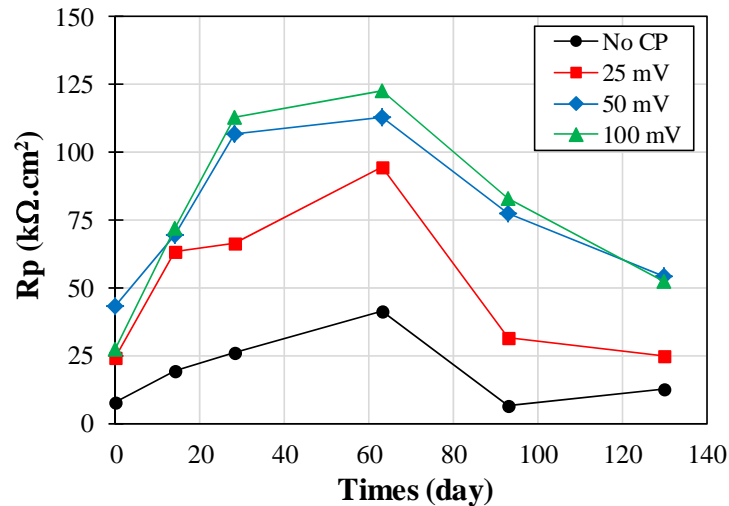


Fig. 6.22 Polarization resistance ( $R_p$ ) of steel bars respect with time

#### 6.4 Summary and Conclusions

When the CP is applied to steel in concrete, it is commonly considered as effective if the 24 hours depolarization value is more than 100 mV. In the case of constant CP current, the small current density could satisfy the 100 mV depolarization value after certain periods. This is due to the environment improvement effects which decrease the aggressive ions and increasing the pH around the steel bar. In this case the protection of steel bar is a gradual process that may take several periods. Also, a larger protective current does not required at early time to satisfy the 100 mV, which leads to the earlier deterioration of anode.

Therefore, reduction of current density is necessary after achieving the 100 mV criterion to reduce the negative effects of large CP current. Although the protective current is decreased, the depolarization value of steel bar is kept higher than 100 mV (constant potential shift of 100 mV). This would indicate that the steel bar can be polarized by decreasing the current density after the 100 mV depolarization value is achieved. In addition, the protective current required is affected by worse condition of steel bar in concrete.

Tests also showed that corrosion rate under protection are lower than the open-circuit condition due to the presence of protective current at surface of steel bar. CP current ensures that supply of electrons at all point of steel inhibits the loss of electrons due to corrosion of the steel surface.

Overall, the test results concluded that the protective current of CP system should be decreased after achievement of specific protection level in order to creates an economic CP

system and reduces secondary deleterious effects such as bond loss steel-concrete, hydrogen evolution and anode deteriorated.

## References

- 6.1 Glass, G. K., et al, "CP Criteria for Reinforced Concrete in Marine Exposure Zones," *Journal of Materials in Civil Engineering*, 12(2), May 2000, pp. 164-171.
- 6.2 Cathodic Protection, "Code of Practice for Land and Marine Application," BS 7361: Part 1, British Standard Institute, London.
- 6.3 Concrete Society, "Model Specification for Cathodic Protection of Reinforced Concrete," Technical Report No. 37, Slough, U.K.
- 6.4 [http://corrpro.com/Resources/~media/Corporate/Files/Corrpro%20Literature/5-29-Lit/Corrpro\\_Mesh%20and%20Ribbon%20Anodes\\_A4.ashx](http://corrpro.com/Resources/~media/Corporate/Files/Corrpro%20Literature/5-29-Lit/Corrpro_Mesh%20and%20Ribbon%20Anodes_A4.ashx)
- 6.5 Rincon, O. T., et al, "Environmental Influence on Point Anode Performance in Reinforced Concrete," *Construction and Building Materials*, 22, 2008, pp. 494-503.
- 6.6 ASTM C 876-95, "Standard Test Method for Half-cell Potentials of Uncoated Reinforcing Steel in Concrete," Philadelphia: American Society of Testing and Materials, 1999.

## **CHAPTER 7. AN APPROPRIATE CATHODIC PROTECTION (CP) DESIGN FOR REINFORCED CONCRETE STRUCTURE**

### **7.1 Introduction**

Corrosion of steel bars in concrete is well known as one of the major factors causes deterioration of reinforced concrete structures. Cathodic protection (CP) method has been introduced to mitigate this problem. CP is achieved by supplying a current from an external source and it causes a change in potential of the steel bar. The -850 mV vs. CSE is most widely used in practical CP design on reinforced concrete structures which was adopted on the protection of underground structures. However, in structures where much of steel bar is naturally cathodic (in a passive state) and the dissolved oxygen available, the application of such criteria has been found to result in very high unneeded current requirements<sup>(7.1)</sup>. This may lead premature deterioration of anode, hydrogen evolution and bond reduction between steel bar and concrete.

Another underground CP criterion is 100 mV decay potential in which commonly use today for evaluating the effectiveness of cathodic protection of reinforced concrete structures. These are the principal criteria currently used to energize CP system for reinforced concrete structures. However, this 100 mV decay potential is not confirmed to be sufficient to ensure the CP of steel in concrete. Some of researchers have suggested that decay potential criterion should be increased to 150 – 200 mV, while other have suggested that it should be reduced depends on the amount of chloride concentration in concrete.

It is extremely important to provide an appropriate CP design for reinforced concrete structures. Based on researches conducted in **Chapter 3, 4, 5** and **6**, the authors attempt to provide recommendation regarding the CP design for reinforced concrete structures.

### **7.2 Review of CP Design in Marine Exposure Zones**

Three areas on concrete structures in marine environments can be divided regarding corrosion namely submerged zone (always below seawater), the splash and tidal zone

(intermittently wet/dry) and the atmospheric zones (well above mean high tide and infrequently wetted). **Figure 7.1** provides a section view of the various corrosion regions in marine environments <sup>(7.2)</sup>.

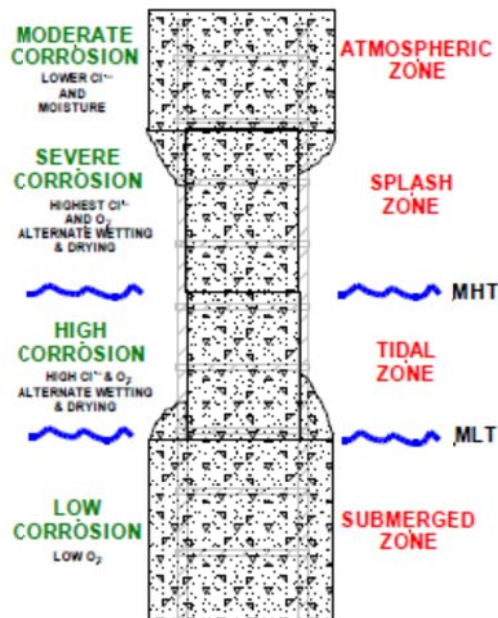


Fig. 7.1 Corrosion regions of concrete structure in marine environments <sup>(7.2)</sup>

Each of above zones has very different corrosion characteristics. For instance, the corrosion rate below water level is limited by low oxygen availability, and conversely lower chloride and moisture content limit the corrosion rate above high tide. Corrosion is found more severe within the splash and tidal zones where alternate wetting and drying result in high chloride and oxygen content. Consequently, the protection criteria applicable to CP in this case may be relative complex.

Glass et al. (2000)<sup>(7.3)</sup> classified the CP criteria for reinforced concrete in marine exposure zones. In the submerged zone, immunity to corrosion is readily achieved by shifting the potential of the steel bar to a sufficiently negative value due to the restricted access of oxygen. In the atmospheric zone, CP induces steel passivity that is indicated by the achievement of 100 mV of a negative potential shift by a relative small applied current density. A major protective effect of CP in this zone is the improvement in the local environment at the steel-concrete interface resulting from the removal of aggressive ions and production of inhibitors. In the splash zone, the type of the CP system may be similar to that installed in the atmospheric zone. The installation of a CP system in the tidal zone is complicated by the

intermittent presence of seawater. The protection criteria applicable to this zone might be a combination of those applied in the atmospheric and submerged zone.

In the present study conducted by the authors, the investigation focused on the CP design in the atmospheric zone. Two CP methods were evaluated in chloride contaminated concrete namely: (1) Constant current density and (2) constant depolarization value. Also, the impacts of the steel bar surface preparation are discussed.

### 7.3 Discussions and Recommendations

#### 7.3.1 Effective CP design for reinforced concrete structures

The 100 mV decay potential (depolarization value) has been used to determine the effectiveness of CP for steel in concrete. The choice of 100 mV is based on the theory that the polarization of corroding steel bar in the cathodic direction will inhibit anodic (corrosion) reactions <sup>(7.4)</sup>. Most disagreement about this criterion is focused on the amount of polarization needed to protect the steel bar against corrosion. For cases of severe corrosion (i.e. very high chloride concentration), the polarization requirement should be higher than 100 mV <sup>(7.1), (7.5), (7.6)</sup>. Based on the results obtained in **Chapter 5**, for concrete contained 2 kg/m<sup>3</sup> and 5 kg/m<sup>3</sup>, the polarization (depolarization value) of 25 – 50 mV and 50 – 100 mV respectively was adequate to reduce corrosion rate of steel bar to acceptable levels less than 1 mA/m<sup>2</sup> (**Fig. 5.9**). However, if the chloride content around 10 kg/m<sup>3</sup>, depolarization value higher than 100 mV is necessary to polarize the steel bar. **Table 7.1** describes the depolarization level requirements based on the chloride concentration in concrete from previous researchers and the present study.

Table 7.1 Summary of the depolarization level requires under various chloride concentration

Source	Exposure condition	Chloride concentration (% wt. of concrete)	Depolarization needed (mV)
Funahashi & Young <sup>(7.5)</sup>	Moisture condition (T: 7°C, 25°C & 25°C)	0.16 – 1	>100
Takewaka <sup>(7.6)</sup>	Dry/wet cycles (T: 40%, RH: 95%)	0.5	150 – 200
Bennett & Turk <sup>(7.4)</sup>	unknown	<0.2	0
		0.2 – 0.3	60
		0.3 – 0.8	80
		0.8 – 1.6	100
		>1.6	150
Present study	Dry condition (T: 20±2°C, RH: 60%)	0.58	25 – 50
		1.45	50 – 100
		2.86	>100

The use of 100 mV depolarization value criterion is reasonable if the chloride concentrations in concrete are not known, as shown in **Table 7.1**. Although it should be increased to 150 – 200 mV if conditions are known to be very corrosive. The depolarization needed not only depend on the chloride content in concrete, but also environmental condition. The presence of moisture and oxygen in concrete could increase the corrosion rate of steel bar. As consequence, the higher protection level is required. An adjustment of depolarization value based on the chloride concentration in concrete, as presented in **Table 7.1**, would have the advantage of reducing the deleterious effects and extending the service life of the CP system.

The protection level was increased with increasing polarization time due to the CP current (higher than 100 mV depolarization value). This can lead in over protection, especially for structures that have been polarized for a long period and in which more passive condition have been achieved as a result of CP current flow <sup>(7.1)</sup>. As shown in **Fig. 4.11 (Chapter 4)**, depolarization value of steel bar was found around 200 – 400 mV after 140 days polarization. In this case, reduction of the protective current is may be necessary in order to obtain an economic CP system. The data from **Fig. 5.5 (Chapter 5)** and **Fig. 6.20 (Chapter 6)** reveal that the protective current can be reduced after achieving depolarization value higher than 100 mV and become stable after certain periods to provide protective current to the steel bar. For example, the initial protective current of 27 mA/m<sup>2</sup> is required to achieve 100 mV depolarization value and it was reduced substantially to 0.7 mA/m<sup>2</sup> after 250 days for similar depolarization value (**Fig. 5.5b, Chapter 5**). From this data, the CP design by decreasing the protective current after achieving depolarization needed is recommended for steel bar in chloride contaminated concrete.

In the viewpoint of corrosion rate, it is found that corrosion rate under protection is smaller than the open-circuit condition due to the presence of current at the surface of steel bar. In **Chapter 4**, the corrosion rate of steel bar under protection is approximately 20, 16 and 100 times lower than the open-circuit condition for potential shifts of 25 mV, 50 mV and 100 mV in concrete with 10 kg/m<sup>3</sup> of chloride.

### **7.3.2 Impact of surface steel condition on corrosion rate**

**Figure 7.2** shows the surface condition of steel bar before embedded in concrete and accelerated corrosion test. The steel bars were covered with protective film, without protective film and pre-corroded without protective film. The results of corrosion rate under protection in concrete with 10 kg/m<sup>3</sup> of chloride at the end of tests are depicted in **Fig. 7.3**. Based on the observation of **Fig. 7.3**, it is clearly seen that the surface condition of steel bar has a significant

impact on the corrosion rate. When the steel bar becomes worse, the higher corrosion rate would result. It is also observed that the corrosion rate in **Chapter 6** around 2 mA/m<sup>2</sup>, 1 mA/m<sup>2</sup> and 0.2 mA/m<sup>2</sup> for potential shift of 25 mV, 50 mV and 100 mV respectively. These values are 10, 5 and 40 times larger than the results in **Chapter 4**.



Fig. 7.2 Surface condition of steel bar prior CP tests

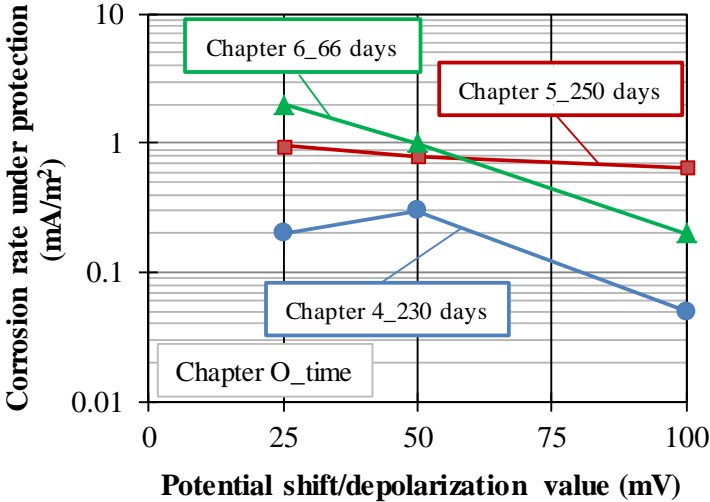


Fig. 7.3 Corrosion rate under protection in concrete with 10 kg/m<sup>3</sup> of chloride at the end of tests

The corrosion process is involving the loss of an electron from the steel surface at the sites of active condition (anode site). CP current is ensuring that a ready supply of electrons to inhibit the loss of the electrons due to the corrosion activity. It means that by applying the similar protection level (i.e. initial potential shift) with different cases of surface steel bar,



reduction of corrosion rate in the worst case may be small due to the CP current have to cover the largest anodic area than other case.

#### **7.4 Conclusions**

Based on the discussions above, an appropriate cathodic protection (CP) design for reinforced concrete structures exposed to the atmospheric zone is recommended as follows:

1. By considering the amount of chloride content in concrete, 50 – 100 mV depolarization value is enough to polarize of steel bar in concrete, with chloride lower than 5 kg/m<sup>3</sup>. However, depolarization value more than 100 mV should be applied if chloride content is more than that value.
2. CP design of decreasing the protective current after achievement of specific protection level is recommended for reinforced concrete structures.
3. An adjustment of the protection level of steel bar in concrete depends on the chloride concentration, corrosion degree and the environmental condition.
4. In the implementation of cathodic protection, many factors are found in adjusting the protection level, such us actual chloride content, corrosion degree of steel bar and non-homogenous environmental condition of structures. An accurate analysis data relating to these factors is needed before installing a CP system.

## References

- 7.1 Bennett, J. and Broomfield, J. P., "An Analysis of Studies Conducted on Criteria for the Cathodic Protection of Steel in Concrete", NACE CORROSION/97, Paper No. 251, 1997.
- 7.2 Daily, S. F., "Using Cathodic Protection to Control Corrosion of Reinforced Concrete Structures in Marine Environments," Corrpro Companies, Inc.
- 7.3 Glass, G. K., "CP Criteria for Reinforced Concrete in Marine Exposure Zones," Journal of Materials in Civil Engineering, Vol. 12 (2), 2000, pp. 164-171.
- 7.4 Bennett, J. and Turk, T., "Criteria for the Cathodic Protection of Reinforced Concrete Bridges Elements," SHRP-S-359, National Research Council, Washington DC, 1994.
- 7.5 Funahashi, M. and Young, W. T., "Investigation of 100 mV Shift Criterion for Reinforcing Steel in Concrete", NACE CORROSION/92, Paper No. 193, 1992.
- 7.6 Takewaka, K., "Cathodic Protection for Reinforced Concrete and Prestressed Concrete Structures", Corrosion Science, Vol. 35, 1993, pp. 1617-1626.

## CHAPTER 8. CONCLUSION AND FUTURE WORK

### 8.1 Conclusions

Evaluation on the effectiveness of Cathodic Protection (CP) system for steel bar in concrete was conducted. Two CP systems were examined in concrete specimens namely Sacrificial Anode Cathodic Protection (SACP) and Impressed Current Cathodic Protection (ICCP). Conclusion for each test is concluded in details as follows:

In **Chapter 3**, the effectiveness of sacrificial point anode for corrosion prevention of steel bars in concrete under various applications was carried out. Also, factor affecting the effectiveness was evaluated. Results showed that the effectiveness sacrificial point anode was affected by the environmental condition of concrete. The presence of gap between sacrificial point anode and steel gave a stable protective current than without gap. In addition, these types of sacrificial point anode can prevent microcell and macrocell corrosion of steel in concrete.

Even though the protective potential of steel bar is changed to noble value in the case of dry condition, the potential of steel bars are in a stable condition which indicates that the steel bar is protected. In the other word, the protective criterion of sacrificial point anode is depending on the environmental condition.

In **Chapter 4**, CP with environment improvement effects of the steel surface was studied. Nine levels of constant current densities were maintained to the concrete specimen in the size of 120 mm x 120 mm x 200 mm with water to cement ratio (W/C) of 55% and contained 2 kg/m<sup>3</sup>, 5 kg/m<sup>3</sup> and 10 kg/m<sup>3</sup> of chloride. Prior to CP tests, accelerated corrosion test were performed to generate initial corrosion on the surface of steel bar. Three levels of current densities were maintained in each of chloride content. The amount of current density was determined according to the initial potential shift value of 100 mV, 50 mV and 25 mV at the first stage (0 days) and kept continuously during CP tests. The results showed that the higher chloride content required a greater current density to protect the steel bar.

The 100 mV decay potential (depolarization value) was achieved even with small protective current after certain periods in all chloride contents due to the “Environment

Improvement” effects. It means that the protection of steel bar is not instantaneous but gradual process to achieve. In addition, depolarization value of steel bar was decreased for the greater potential shift at the end of test periods due to the depletion of oxygen, followed by a breakdown of passivity film of steel bar. Furthermore, the corrosion rate of steel under protection is approximately 20, 16 and 100 times lower than the open-circuit corrosion rate for current densities of 10, 20 and 100 mA/m<sup>2</sup> respectively.

In **Chapter 5**, the CP criterion less than 100 mV for steel bar in chloride contaminated concrete exposed to the atmospheric zone was examined. All the materials, concrete composition and dimension of specimens are similar as in **Chapter 4**. The protective films of steel bar were removed before being embedded in the concrete specimen and then subjected to the accelerated corrosion test with similar technique in **Chapter 4**. Protection level (depolarization value) of 25 mV, 50 mV and 100 mV were kept constant during tests. The current density was adjusted after depolarization test to provide the protection level. The results showed that the depolarization level of 25 mV and 50 mV is sufficient to polarize the steel bar in concrete, with chloride lower than 5 kg/m<sup>3</sup>. However, the depolarization level should be higher than 100 mV when the chloride content in concrete is more than 5 kg/m<sup>3</sup>. In addition, the protective current may be reduced under the CP of stable condition after a certain period.

In **Chapter 6**, the effectiveness of CP design under severe corrosion was investigated. Two CP methods were used: (1) constant current density and (2) constant potential shift from its natural potential of steel bar 24 hours after switch off. Both CP methods were examined in the concrete specimens with corrosive steel bar and high chloride concentration. Concrete with water to cement ratio (W/C) of 60% with initial chloride content of 10 kg/m<sup>3</sup> were prepared. The initial corrosion of steel bars were formed by dry/wet cycles 3% NaCl solution spray (1W:1D) about two weeks before concrete casting. In the case of constant current density, additional accelerated corrosion tests were performed for 15 days prior to CP tests. Protection levels of 25 mV, 50 mV and 100 mV were maintained.

The results showed that a larger protective current was not required at early time to satisfy the 100 mV, which leads to the earlier deterioration of anode. Therefore, reduction of current density is necessary after achieving the 100 mV criterion to reduce the negative effects of large CP current. Although the protective current decreased, the depolarization value of steel bar is kept higher than 100 mV (in the case of the constant potential shift of 100 mV). This would indicate that the steel bar is polarized even the current density is decreased after the 100 mV depolarization value is achieved.

The test results also showed that corrosion rate under protection are lower than the open-circuit condition due to the presence of protective current at the surface of steel bar. CP current ensures that supply of electrons at all point of steel inhibits the loss of electrons due to corrosion of the steel surface.

In **Chapter 7**, discussions and recommendations regarding the CP design for reinforced concrete structures was presented. Also, the impact of the steel bar surface preparation is evaluated. By considering the amount of chloride content in concrete, 50 – 100 mV depolarization value is enough to polarize of steel bar in concrete, with chloride lower than 5 kg/m<sup>3</sup>. However, depolarization value more than 100 mV should be applied if chloride content is larger than that value. In addition, CP design of decreasing the protective current after achievement of specific protection level is recommended for reinforced concrete structures.

The corrosion process is involving the loss of an electron from the steel surface at the sites of active condition (anode site). CP current is ensuring that a ready supply of electrons to inhibit the loss of the electrons due to the corrosion activity. It means that by applying the similar protection level (i.e. initial potential shift) with different cases of surface steel bar, reduction of corrosion rate in the worst case is small due to the CP current have to cover the largest anodic area than other case.

An adjustment of the protection level of steel bar in concrete depends on the chloride concentration, corrosion degree and the environmental condition. In the implementation of cathodic protection, many factors are found in adjusting the protection level, such us actual chloride content, corrosion degree of steel bar and non-homogenous environmental condition of structures. An accurate analysis data relating to these factors is needed before installing a CP system.

## **8.2 Future Work**

In order to develop the CP system, several future works are recommended to establish the CP design applicable for steel bar in concrete as follows.

Sacrificial point anode is effective to prevent microcell and macrocell corrosion of steel in concrete against chloride. Regarding to the criteria and service life design of these systems in the real structures, is still unclear and need to be undertaken. In addition, research on the anode materials is necessary to ensure the service life extend of structures.

Cathodic protection with environment improvement effect can satisfy the 100 mV decay potential even in the small current density after a certain period. It is necessary to

investigate the possibility to reduce the protection current after achieved 100 mV protection criterion. Also, the relationship between dissolved oxygen, protective current and corrosion rate should be pointed out.